UNIVERSITÀ POLITECNICA DELLE MARCHE

FACOLTÀ DI INGEGNERIA

PhD Program:

Civil, Environmental and Building Engineering and Architecture (ICAEA)

PhD Curriculum:

Civil, Environmental and Building Engineering and Architecture
XXXII Cycle (2016-2019)

PhD Thesis tile:

Landslide hazard assessment in structurally complex soils

PhD Candidate:
Antonio Ferretti

Advisor:
Prof. Ing. Giuseppe Scarpelli

Curriculum Coordinator:
Prof. Ing. Francesco Fatone

Department of Materials, Environmantal Sciences and Urban Planning (SIMAU)
Via Brecce Bianche 12, 60131, Ancona (Italy)

TABLE OF CONTENTS

ABSTRACT

In the European context, Italy is the most landslide prone country where landslides are the most frequent and disperse natural hazards. Therefore, the landslide hazard assessment, especially in terms of quantity, is a relevant and current problem and plays a central role within the risk assessment and management framework, allowing to find the best remedial measures and strategies to cope with such phenomena.

In this context, this work has focused on the analysis and understanding of the most relevant slope factors and processes that contribute to the stability of natural slopes. In fact, a proper diagnosis of the landslide mechanism is of primary importance to the quantitative definition of the hazard posed by a given landslide.

In particular, a stepwise diagnosis of a real landslide, which interacts with a segment of an important highway in central Italy, has been developed. Such landslide has been properly chosen since well representative of a class of slope failures so widespread in the national territory, generally referred to as "active slow moving landslides". These large-scale slope movements take place in gentle slopes made of stiff clayey deposits, very often tectonically disturbed, that exhibit periodically reactivations related to the rainfall regime of the area. Since low entity velocities characterize these landslides, they are not hazardous for human lives but they have an important economic impact on society, being responsible for extensive damage to urban settlements and infrastructures.

In the developed diagnostic process, monitoring turned out to be a precious instrument that allowed depicting clearly the actual response of the system to the external actions affecting its stability, i.e. rainfalls and seismic shakings. This aspect highlights the central role played by a good quality monitoring as a part of the investigation of slope stability.

With regard to the rainfall-induced effects, transient hydraulic analyses have been carried out by means of finite element method modelling that tried to account for the most relevant aspects that govern the infiltration process. A good agreement between the simulated groundwater fluctuations and the monitored ones has been obtained, demonstrating that the numerical model is able to reproduce realistically the hydraulic response of the slope as a function of the rainfall regime. Subsequently, limit equilibrium stability analyses have been conducted by considering the simulated groundwater fluctuations in order to quantify their effect on the slope stability. The general low values of the factor of safety, obtained considering that the residual shear strength is fully

attained along the entire slip surface, confirmed the precarious stability of the landslide, as highlighted by inclinometer monitoring. Therefore, such modelling provided a further interpretation of the analysed landslide mechanism.

Moreover, the stability of the slope has been also evaluated under earthquake loadings. Thanks to the very rare availability of both monitored seismic displacements and accelerometric records, it has been possible to estimate the critical acceleration of the system based on real data. To do so, a back-analysis procedure has been carried out by the well-known Newmark's method. The obtained values are in good agreement with other estimates reported in literature and with the ones calculated by the pseudostatic method. As a result, it has been possible to give a reliable estimate of the critical acceleration of the slope, which is an essential parameter in evaluating its performance under earthquake loadings.

In conclusion, even though this work has been focused on a specific case study, most of the findings are relevant to deepen the knowledge of such complex natural phenomena and the interpretative process adopted can be applied to other similar situations.

SOMMARIO

Nel contesto europeo, l'Italia è il paese più incline al dissesto da frana, dove i fenomeni franosi sono i più frequenti e diffusi tra i pericoli naturali. Una stima quantitativa del pericolo da frana è perciò un importante e attuale problema e riveste un ruolo centrale nella valutazione e gestione del rischio, permettendo di individuare i migliori interventi e strategie per fronteggiare tali fenomeni.

In tale contesto, questo lavoro si è concentrato sull'analisi e la comprensione dei più rilevanti fattori e processi che, alla scale del versante, regolano la stabilità dei pendii naturali. Una corretta diagnosi del meccanismo di instabilità, infatti, è di primaria importanza al fine di quantificarne il pericolo associato.

Nello specifico, è stato sviluppato un processo diagnostico di una frana esistente, la quale interagisce con un tratto di un'importante arteria stradale situata in Italia centrale. Tale frana è stata opportunamente selezionata dal momento che è ben rappresentativa di una tipologia di frane ampiamente diffusa nel territorio nazionale, generalmente identificate come "frane attive a cinematica lenta". Tali movimenti di vaste proporzioni si sviluppano in pendii dolci costituiti da depositi argillosi consistenti, molto spesso tettonizzati, che manifestano riattivazioni periodiche in relazione al regime piovoso dell'area. Dato che tali frane sono caratterizzate da velocità contenute, esse non costituiscono un pericolo diretto per le persone ma hanno un importante impatto economico sulla società, danneggiando insediamenti urbani e infrastrutture.

All'interno del processo di diagnosi, il monitoraggio si è rivelato essere un prezioso strumento che ha permesso di evidenziare in maniera chiara la risposta del sistema alle azioni esterne che ne compromettono la stabilità, ossia le piogge e gli scuotimenti sismici. Per quanto riguarda lo studio degli effetti pluvioindotti, sono state condotte delle analisi idrauliche in regime transitorio attraverso una modellazione numerica agli elementi finiti che ha cercato di tener conto degli elementi più significativi che governano il processo di infiltrazione. È stato riscontrato un soddisfacente accordo tra le oscillazioni della falda simulate e quelle monitorate, evidenziando che il modello numerico è capace di riprodurre in maniera realistica la risposta idraulica del pendio in funzione del regime piovoso. Successivamente, sono state effettuate delle analisi di stabilità all'equilibrio limite considerando le oscillazioni di falda simulate in modo da quantificare il loro effetto sulla stabilità del pendio. I valori del fattore di sicurezza, ottenuti considerando che la

resistenza a taglio residua sia pienamente sviluppata lungo la superficie di scorrimento, sono risultati essere generalmente bassi, confermando la condizione di precaria stabilità della frana messa in luce dal monitoraggio inclinometrico. Perciò tale modellazione ha effettivamente permesso di approfondire il meccanismo di instabilità considerato.

La stabilità del pendio, inoltre, è stata valutata anche nei confronti delle azioni sismiche. Grazie alla rara disponibilità sia degli spostamenti sismici monitorati che delle registrazioni accelerometriche, è stato possibile stimare l'accelerazione critica del sistema sulla base di dati reali. A tal fine, è stata eseguita una procedura di back-analysis impiegando il ben noto metodo di Newmark. I valori così ottenuti trovano un buono accordo con altre stime riportate in letteratura e con i valori calcolati attraverso il metodo pseudostatico. Di conseguenza, è stato possibile fornire una stima attendibile dell'accelerazione critica del pendio, che è un parametro fondamentale per la valutazione della risposta del pendio alle azioni sismiche.

In conclusione, sebbene questo lavoro si sia focalizzato sullo studio di uno specifico caso, la maggior parte dei risultati è di rilevante importanza per approfondire la conoscenza di così complessi fenomeni naturali e il processo interpretativo adottato può essere applicato ad altre situazioni simili.

ACKNOLEDGMENTS

LIST OF FIGURES

LIST OF TABLES

1 CHAPTER – Introduction

1.1 Problem statement and work objective

Landslides are well-known and widespread geohazards that affect many hilly and mountainous regions all over the world, causing damage to man-made works and several fatalities every year (PETLEY 2012).

According to a recent study published by HERRERA et AL. (2018), within the European context Italy is the most landslide prone country where landslides are the most frequent and disperse natural hazards. This is essentially due to the peculiar orographic and geological setting of the national territory that predisposes it to instability phenomena under both natural and anthropogenic influences.
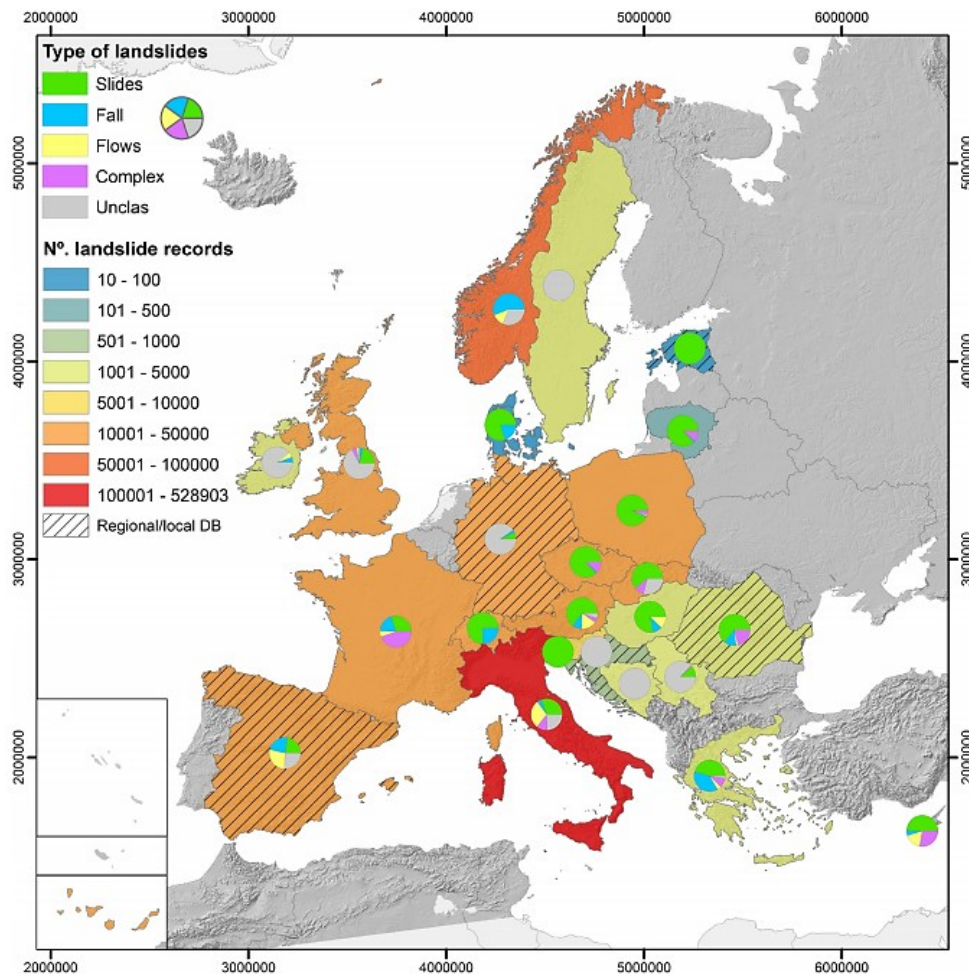
Figure 1-1: Number of landslide records gathered by Geological Surveys of Europe (from HERRERA et AL. 2018).

With the increase of population, a consequent growing need of new areas to be urbanized and infrastructures to be constructed or enhanced occurs. Consequently, the interaction between landslides and assets of any kind is becoming more and more frequent and inevitable.

Therefore, the ability of quantifying the landslide risk (risk assessment) of an exposed element is a relevant and current problem to cope with. Once such estimate is achieved with a satisfactory degree of confidence, considerations about how to deal with the risk (risk management) can be developed and, eventually, the best remedial strategies can be undertaken by land owners and decision makers to lower the risk to an acceptable level (risk mitigation).

According to Varnes (1984), the landslide risk (R) can be expressed by the following equation:

$$R = H \times E \times V \qquad\qquad (1\text{-}1)$$

where H is the hazard, E is the element(s) at risk and V is its vulnerability. This is a simple but very powerful equation that identifies separately the principal factors contributing to risk. These include the occurrence likelihood of a damaging landslide of a given magnitude (hazard), the valued attributes at risk (elements at risks) and the amount of damage expected from the specified landslide (vulnerability). How is it possible to guess, the landslide risk assessment is a complex task and a multidisciplinary approach involving different professional figures (e.g. engineers, geologists, environmental experts, economists and sociologists) is highly recommended in order to obtain a reliable estimate. Within the geotechnical field, the attention is mainly focused on the hazard analysis since this component is the one related to the peculiarities and mechanisms of the considered slope failure. According to CROIZER & GLADE (2005), in fact, the landslide hazard is defined as "*the physical potential of the process to produce damage because of its particular impact characteristics and the magnitude with which it occurs (or is encountered)*". Following this definition, it is evident that the hazard assessment cannot disregard from the landslide type, generally identified by the type of movement of the unstable mass and by the material involved (CRUDEN & VARNES 1996), and from the considered movement stage of the sliding process as pointed out by LEROUEIL et AL. (1996), i.e. first-time landslides or existing landslides. Within the hazard assessment

framework, these are important ingredients in defining the most relevant features (e.g. the volume of the unstable mass, its characteristic velocity, the occurrence time of the event with respect to the possible triggering factors) to estimate the destructiveness of the landslide and the related possible consequences.

In literature several methods and approaches have been proposed (GUZZETTI et AL. 1999, PARDESHI et AL. 2013) to assess the landslide hazard at different scales (e.g. national, regional, local and slope scale), both in qualitative and quantitative terms. Over large areas, landslide hazard zoning maps are often developed by means of heuristic or statistical methods while process-based, or physically-based, methods are more suitable and adopted with regard to areas of limited extension (COTECCHIA et AL. 2019). Based on specific studies such as site investigations, field surveys and monitoring data, these latter methods try to provide for the most relevant slope factors and the physical processes contributing to the stability by means of analytical and numerical tools. In such a way, it is possible to interpret rationally the landslide mechanism and to quantitative evaluate the level of safety of the slope and its evolution with respect to the different triggering factors, e.g. rainfalls and earthquakes.

Among the wide spectrum of landslide phenomena, this work has focused on a class of slope failures so widespread in the national territory that are generally identified as active slow moving landslides (GLASTONBURY & FELL 2008).

Such large-scale movements usually take place in gentle slopes made of marine turbiditic deposits that have experienced a more or less important tectonic disturbance. As a result, these "structurally complex formations" (ESU 1977) are characterized by a marked heterogeneity and pervaded by discontinuities that constitute surfaces of weakness, strongly influencing the hydro-mechanical behaviour of the slope.

As it is well demonstrated in literature (ALONSO et AL. 2003, CALVELLO et AL. 2008, TOMMASI et AL. 2013, VASSALLO et AL. 2015 among many others), active landslides can be considered climate driven phenomena since they show an intermittent kinematics being related to the rainfall regime of the area, which is the main factor affecting their stability. In fact, the sliding mass exhibits seasonal reactivations because of the groundwater level fluctuations occurring within the slope. Understanding such slope-atmosphere interaction (COTECCHIA et AL. 2014) and its mechanical effect on the slope stability is a complex problem and many aspects (e.g. geo-structural set up of the slope,

hydro-mechanical properties of the soil, evapotranspiration rate, etc…) should be taken into account to understand properly the landsliding mechanism. In this context, monitoring is a key element in the diagnosis process since it allows detecting the actual response of the system to external inputs. A combination between such phenomenological interpretation and hydro-mechanical numerical analyses (ELIA et AL. 2017), which are able to reproduce the most relevant factors contributing to the stability, seems to be a valid approach to quantify the hazard posed by these natural phenomena.

Under climatic inputs, seasonal accelerations are of low entity and typical velocities of these landslides range from few millimeters to some centimeters per year. Thus, even though they are not hazardous for human lives, they have an important economic impact on the civil society, being responsible for extensive damage to urban communities and infrastructures (MANSOUR et AL. 2011). Moreover, it is important to underline that these landslides are very often located in high seismicity area and earthquake, therefore, is another triggering factor to be considered. Regarding this aspect, the evaluation of slope stability under earthquake loadings is of primary importance as long as seismic induced effects can be catastrophic and severe consequences to both people and manufacts can be encountered.

Within this context, this work is aimed at deepening the physical processes occurring at slope scale and the most relevant factors that contribute and govern the stability of natural slopes. In particular, a deterministic methodology to assess the landslide hazard has been developed based on a critical analysis of monitoring data in combination with numerical and analytical instruments. Such methodology has been applied to a real case study, properly chosen as well representative of the type of slope failures described above, i.e. active slow moving landslides. Therefore, the findings gathered from the analysis of this specific case can contribute to deepen the knowledge of such complex natural hazards and can be extended to other similar situations.

1.2 "Innovative monitoring and sustainable strategies for landslide risk mitigation" research project

This work is set within a national research project (PRIN2015) entitled "*Innovative monitoring and sustainable strategies for landslide risk mitigation*". It has been founded

by the Italian Ministry of Instruction, University and Research (MIUR) and many Italian Universities are involved in.

Figure 1-2: Universities involved in the PRIN2015 research project.

"The project is entirely devoted to support the solution of the major civil problem manifested by the injuries to society generated by landslides in regions intensely urbanized and/or location of infrastructures and service networks. The relevance of the scientific contribution of the project stems from the innovative methodologies that the several research units intend to promote when dealing with the different aspects of landslide risk mitigation: the monitoring of the slope processes, the landslide mechanism interpretation and the devising of countermeasures. The up to date methods, whose application is promoted, invoke the use of the most advanced scientific inter-disciplinary Knowledge to accomplish safer life conditions…"

With regard to active slow moving landslide, this scientific contribution has focused on the cause-effect interpretation of landslide processes and mechanisms by means of monitoring evidences and numerical/analytical instruments.
The research project abstract is reported below.

"Landslide risk mitigation is of importance in countries of severe landslide susceptibility, especially where there is an intense urbanization. This requires a coherent scientific programme of characterization of the mitigation strategies in relation to the phenomena, to identify the most sustainable design. This research project is framed within such a

programme and is intended to contribute to three essential actions for the landslide risk mitigation: 1) the monitoring of the landslide processes, 2) modelling the processes to identify the most appropriate remedial measures, and 3) the development of innovative design strategies. This research intends to devise a strategy for the diagnosis of landslide processes and their causes, both on the basis of the wide and diverse experience of the scientists involved in studying landslide phenomena in geologically complex conditions and through the combined use of the advanced slope modelling and innovative monitoring technologies. The diagnoses will be trained on soil/rock slope case histories for which both field and laboratory data are available and representative of recurrent slope processes of important social impact. For soil slopes, the research will require coupled hydro-mechanical numerical modelling, including the geo-hydro-mechanical complexity typical of the most unstable natural slopes in mountain chain areas. For rock-falls, the research will address both the probabilistic calculation of the rock block dimensions and the longevity of the mitigation measures, which is still a major challenge of risk mitigation.

Unconventional monitoring tools, making use of advanced technologies, will be developed and applied. Prototypes of fibre optic sensors will monitor straining either landslide bodies or interacting structures. A sensor system will be tested for real time in-situ monitoring of the most relevant soil state variables. Also, advanced satellite techniques to monitor surface displacements (DInSAR) will be validated as an indicator of landslide activity, by comparing satellite data with ground measurements. Through the integration of the new and traditional monitoring data with the modelling results, the research will deliver advanced design of early warning systems. For climate driven landslides, the effectiveness of innovative drainage diaphragms and the use of high transpiration vegetation will be also tested. Based on chemo-mechanical coupled modelling, a chemical soil strength improvement respecting ecosystems will be tested as a stabilizing measure for clayey slopes. The products of this research will give not only an immediate benefit in the cost-effectiveness of stabilization works, but also will prompt the economies of landslide prone areas. There will also be benefit to industry of rational and safe design, the methodologies of which could be exported to countries of similar landslide hazard."

2 CHAPTER – Main features of active slow moving landslides

2.1 Evolution stages of a landslide process

Following the scheme previously proposed by VAUNAT et AL. (1994), LEROUEIL et AL. (1996) and LEROUEIL (2001) schematized a landslide process into four main stages. These stages are characterized by different displacement rates and summarize the phases that a landslide undergoes during its life. In particular, they identified: the pre-failure stage, the onset of failure, the post-failure stage and the reactivation stage (see **Figure 2-1**).
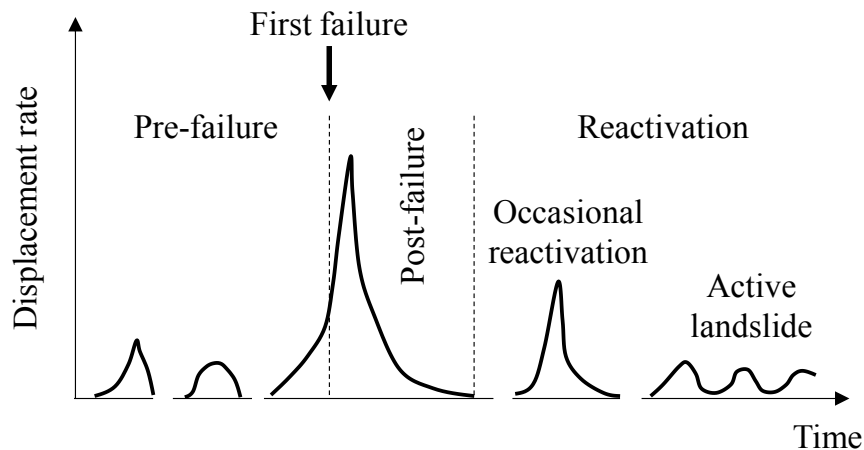
Figure 2-1: Different stages of slope movements (redrawn from LEROUEIL 2001).

The first stage could be identified as a progressive failure process. Because of changes in boundary conditions, the stress field within the slope, which is generally non-uniform, changes and locally the shear stress can match the maximum shear strength of the soil and thus local failure occurs. If soil presents a strain-softening behaviour (e.g. overconsolidated clays), the failed soil elements will support a decreasing shear stress as strain increases. The part of the shear stress that is no longer supported by the failed elements is then transferred to the neighbouring soil elements, which can fail in turn. The process continues until an equilibrium has been reached. At that time, along a potential failure surface, part of it can exceed the peak, with possibly some elements at large deformation or residual strength, whereas another part of the potential surface has not reached the peak.

If such equilibrium cannot be obtained, the process will continue until failure conditions extend along the entire failure surface, leading to a general collapse of the slope (URCIOLI et AL. 2007): this is the second stage mentioned above.

While the pre-failure stage is characterised by small displacements, during the onset of failure and at the beginning of the post-failure stage the displacement rate increases abruptly and the soil mass involved in the landslide experiences very large displacements. After this, the diaplacement rate tends to decrease until the system finds a new equilibrium configuration and thus it stops. It is worth noting that the actual configuration of the slope could be sensibly different from the starting one.
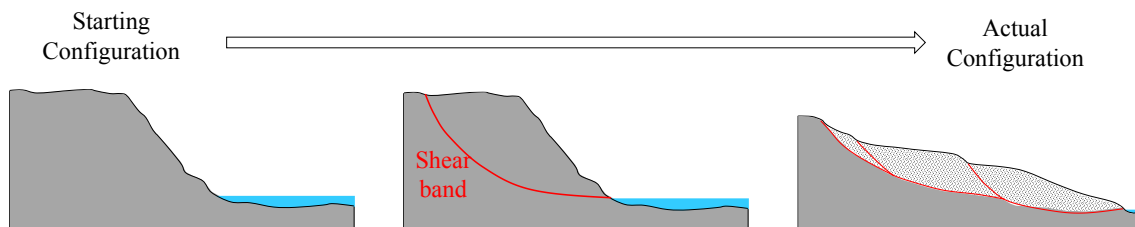
Figure 2-2: Schematic representation of morphological evolution of the slope through the different stages.

Now, if the changes in boundary conditions are able to mobilize the shear stregth along the one or more slip surfaces developed in the previous stage, the landslide may undergo a reactivation stage. This reactivation could be occasional or more or less continous: this latter is the case of active landslides. Their rate of movement is dependant on the seasonal variations of the hydraulic conditions of the slope induced by the alternation of wet and dry periods.

The knowledge of the movement phase is the basis of the geotechnical characterization of landslides according to VAUNAT & LEROUEIL (2002) together with the type of movement and material involved. These ingredients are relevant to understand the controlling laws, parameters and causes (all aspects that could be sensitively different from one stage to another) governing the phenomenon of interest within the framework of hazard and risk analysis.
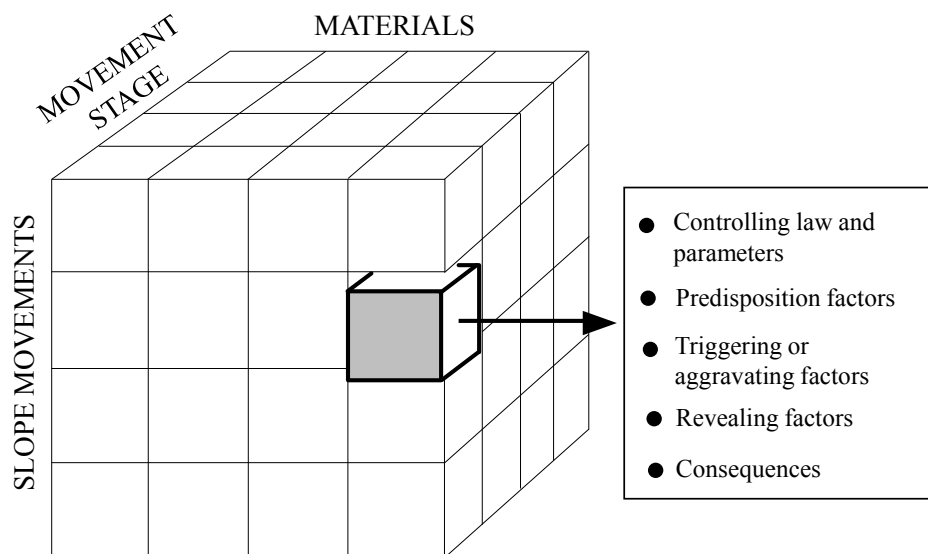
Figure 2-3: Scheme of the 3-D matrix for the geotechnical characterization of a landslide (redrawn from VAUNAT & LEROUEIL 2002).

2.2   Types of movement and material

When we deal with slope stability problems, the classification of the type of movement is a crucial aspect since the type of landslide is related to the main aspects of the phenomenon such as the speed of movement, the volume involved, the distance of run-out and so on.

It should be stated that a landslide is a natural dynamic process whose behaviour results from the combination of several factors, so giving a unique and exhaustive classification it has always been a difficult task.

Through the years, many Authors have proposed several classifications (SHARPE 1938, SKEMPTON & HUTCHINSON 1969, VARNES 1978, HUTCHINSON 1988, CRUDEN & VARNES 1996, HUNGR et al. 2014 among many others) based essentially on geomorphological features and type of material.

The most widely used classification is the one proposed by CRUDEN & VARNES (1996), considered in this work and illustrated in **Figure 2-4**.
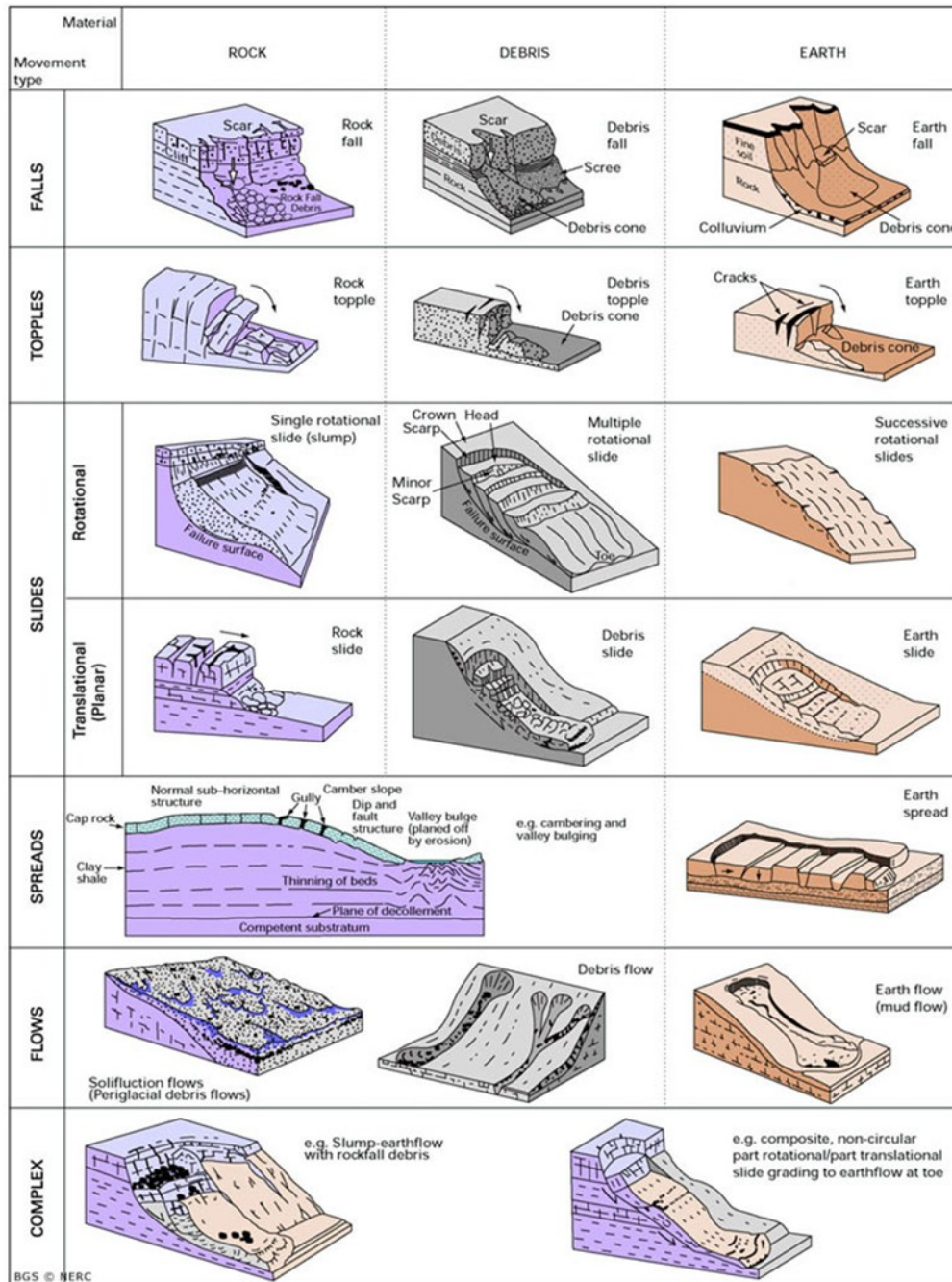
Figure 2-4: Landslide classification proposed by CRUDEN & VARNES (1996).

Within this framework, landslides are classified according to the type of movement and the type of material. The type of movement describes the actual way of how the landslide mass is displaced. The five "basic" types of movement are: *fall*, *topple*, *slide* (*rotational* or *translational*), *spread* and *flow*.

A sixth class, named *complex* or *composite*, has been introduced in order to take into account intermediate situations deriving from the combination (both in time and/or in

space) of two or more basic types: roto-translational landslides (also called *compound* slides), falls or slides wich turn into flows, etc…

Concerning the type of material, the landslide mass can be constituted either by rock or soil, defined *bedrock* and *engeneering soils* by the Authors, respectively. The term bedrock stands for "hard or firm rock that was intact and in its natural place before the initiation of movement" while eneginering soils are clssified as *earth* if mainly composed of sand-sized or finer particles and as *debris* if composed of coarser ones.

Thus, landslides are decribed using two terms that refer to material and movement: rock fall, earth slide, debris flow and so on.

In this work will be analyzed those mass movements that move along a well-defined shear surface and are not characterized by rapid collapse.

Therefore, falls, topples and rapid flow-type landslides (e.g. debris flow) will be not treated. The spread-type mass movements, although characterized by low velocity, will be not considered as well, since they took place in specific stratigraphic conditions and their mechanics is sensibly different from that of the other types (governed by liquefaction or consolidation of the lower more deformable stratum).

The attention will be focused on translational slides or compound slides where the translational component is generally prevailing: the sliding surface(s), in fact, shows a circular shape in the upper part of the slope (next to the scarp) which becomes flatter in the accumulation zone. The maximum depth of such movements generally reaches several tens of meters and the adjective deep-seated, thus, is often used in contrast to shallow. These landslides, moreover, have a considerable areal extension and consequently the volume involved could reach millions of cubic meters.

Description	Volume [m^3]
Extremely large	$>5x10^6$
Very large	$>1x10^6$, $<5x10^6$
Medium-Large	$>2.5x10^5$, $<1x10^6$
Medium	$>5x10^4$, $<2.5x10^5$
Small	$>5x10^3$, $<5x10^4$
Very small	$>5x10^2$, $<5x10^3$
Extremely small	$<5x10^2$

Table 2-1: Indicative size of landslides in term of volume involved (from FELL 1994).

In this class can also be incorporated mudslides in the sense described by PICARELLI (2007), which are essentially earth flows that have been evolved into earth slides. The typical flow-like style of mudslides is revealed just at failure, when the landslide body displays a high mobility. Subsequently, the soil mass decelerates assuming the characteristic of a slide with the formation of a clear basal slip surface. The occurrence of previous flow-like mechanisms can be still recognized from the assumed morphology of the landslide body, characterised by an hourglass shape where an alimentation zone, a track and a fan-shaped accumulation zone are recognisable. A well-documented case history of such a type of landslide is the Costa della Gaveta landslide in southern Italy (DI MAIO et AL. 2010, VASSALLO et AL. 2013, 2015).

The materials involved is a crucial aspect since the class of landslides described above takes place in a peculiar typology of fine-grain formations whose behaviour is something in between soils and rocks. For this reason, the types of material proposed by CRUDEN & VARNES (1996) do not seem representative for the purpose.

As far as the materials involved are concerned, here is reported the classification proposed by VAUNAT & LEROUEIL (2002) in **Figure 2-5**.
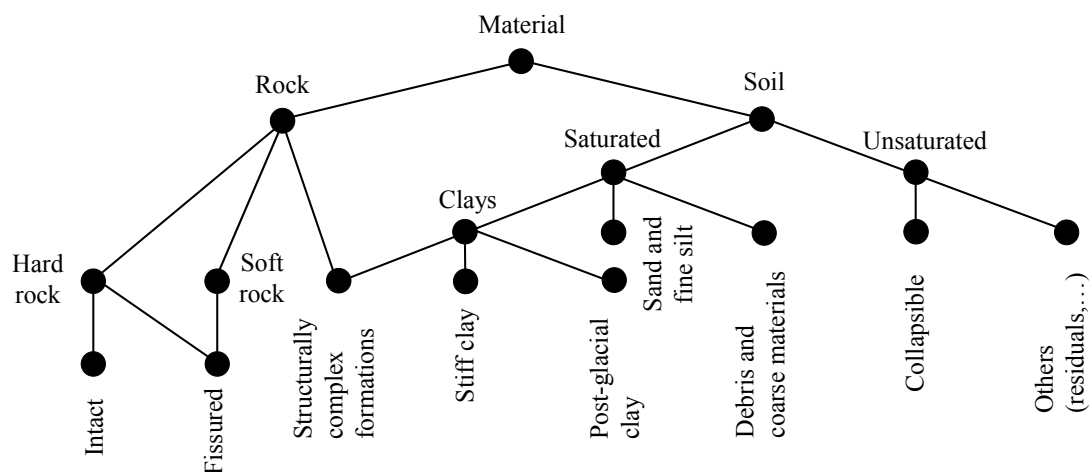
Figure 2-5: Classification of materials involved in landslides according to VAUNAT & LEROUEIL (2002).

This classification is interesting because it comprises several typologies of soils and rocks among which a "special" class is enclosed: this is the case of the so-called "structurally complex formations". This class, which is located between soft-rocks and stiff clays, will be treated in detail in the next paragraph. It is appropriate to state that these formations

are widespread in the Italian territory, especially along the Apennines chain and in Sicily (MANFREDINI et AL. 1985), and the relation between these deposits and large-scale slope movements is well known (D'ELIA et AL. 1998).
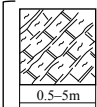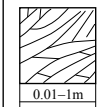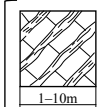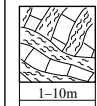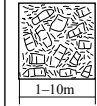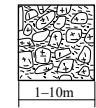
2.2.1 Structurally complex formations

Geotechnically complex materials are those whose geotechnical properties vary rapidly across a wide range within an engineering site (MORGENSTERN & CRUDEN 1977).

In the class of "structurally complex formations" are generally included those deposits that cannot be confidently studied and modelled with the classical approaches of soil mechanics or rock mechanics as a consequence of their lithological heterogeneity and complex structural features.

D'ELIA et AL. (1998) underlined that the main causes of complexity may be found in the heterogeneous and discontinuous nature of deposits at laboratory samples (mesostructure) and at the scale of engineering problems (macrostructure).

With the aim of describing the main features of these type of materials, ESU (1977) proposed the classification reported in **Figure 2-6**.

	Description	Types of complexities
A₁ 0.5–5m	Layered clay shales and shales (with or without fissility) more or less fissured and/or jointed	Geotechnical complexity depending upon mineralogy and stress history (mainly vertical loading)
A₂ 0.01–1m	Sheared clay shales and shales	Geotechnical complexity depending upon mineralogy and stress history (mainly shearing)
B₁ 1–10m	Ordered sequences of more or less fissured and jointed layers of rock and clay or shale	Geotechnical complexity depending upon heterogeneity, mineralogy and stress history (mainly vertical loading)
B₂ 1–10m	Disarranged layers of rock and from highly fissured and jointed to sheared clay or clay shale	Geotechnical complexity depending upon heterogeneity, mineralogy and stress history (flexural, torsional and shearing loads)
B₃ 1–10m	As B₂ with a chaotic structure	Geotechnical complexity depending upon heterogeneity, mineralogy and stress history (repeated cycles of flexural, torsional and shearing loads with large displacements)
C 1–10m	Blocks or fragments of more or less weathered rocks in a clayey matrix of various origin	Complexity depending upon heterogeneity and mineralogy (residual and colluvial soils)

Figure 2-6: Classification of structurally complex formations (redrawn from ESU 1977).

The first group (A) encloses homogeneous clayey materials having syngenetic or superimposed structures. Formations where at least two constituents with marked differences in their mechanical properties are present constitute the second group (B): these constituents can form separate domains with an ordered and clearly recognizable arrangement (B1), or can randomly assembled (B2, B3).

The third group (C), finally, includes detrital, colluvial or residual materials consisting of a clayey matrix whit rocky fragments.

The second group can be identify with the term *flysch*, introduced in the geological terminology by B. Studer in 1827. Flysch is a deep marine sedimentary sequence deposited contemporaneously with mountain building (syn-orogenic deposit) consisting of a rhythmic alternation of weak layers and strong layers with a variable proportion.

Shales (more or less marly) generally constitute the weak component while the strong layers are generally constituted by sandstones or limestones. These latter components often present a set of joints (of brittle nature) perpendicular to the bedding planes. The structure of the mass, however, can be sensitively dislocated and made chaotic as a function of tectonic disturbance (MARINOS & HOEK 2001).

Figure 2-7: An example of flysch constituted by shales (of grey colour) and sandstones (of brownish colour) (Image taken from MARINOS & HOEK 2001).

In the Italian context, these formations involve all the marine turbiditic deposits that have experienced a more or less important tectonic disturbance and environmental changes, that is geomorphological and climatic.

As pointed out by MORGENSTERN and CRUDEN (1977), the complexity of these formations arises from three classes of process:

− *genetic* processes associated with the formation of the material (also called *syngenetic*);
− *epigenetic* processes associated with its subsequent modification by deformation (e.g. tectonic) and diagenesis;
− *weathering* processes (both physical and chemical) associated with alteration at the earth surface.

Such processes have given rise to complex geotechnical settings characterized by heterogeneity and pervaded by weakness horizons constituted by "discontinuities".

This is why slopes located in structurally complex formations are prone to landslide or have already experienced instability phenomena that can be still in act or occasionally reactivated.

2.2.2   Discontinuities in clayey materials

Already some decades ago, SKEMPTON & PETELY (1967) highlighted the importance of discontinuities in clayey soils since they represent surfaces of weakness that can reduce the strength of the clay mass, at least in certain directions, to values much below the strength of the "intact" clay. Therefore, in many geotechnical problems such discontinuities govern in large part of even entirely the behaviour of the whole system.

The Authors furnished a "partial" classification of these discontinuities reported in **Table 2-2**.

Group	Type	Occurence	Relative movement
Depositional or Diagenetic	BEDDING SURFACES	Bedding planes Laminations Partings	Zero
Structural	JOINTS "Brittle fracture" surface	Systematic joints "Fissures"	Pratically zero
	MINOR SHEARS Non-planar, slikensided	Small displacement shears Riedel and thrust shears	Less than 1 cm
	PRINCIPAL DISPLACEMENT SHEARS Subplanar, polished	Principal slip surfaces in: Landslides Faults Bedding plane slips	More than 10 cm

Table 2-2: Classification of discontinuities in stiff clays according to SKEMPTON & PETELY (1967).

Landslides occurring in clayey deposits are characterized by the presence of a principal shear discontinuity as consequence of large displacement: this is the so-called shear zone or shear band. This zone separates the sliding mass above it from the underlying stable formation and its thickness, which depends on the soil nature, on its consistency and on the confining pressures, can be of the order of few millimetres (SKEMPTON et AL. 1967) until a couple of meters (GLASTONBURY & FELL 2008).

A schematic representation of a shear zone in a landslide is reported in **Figure 2-7**.
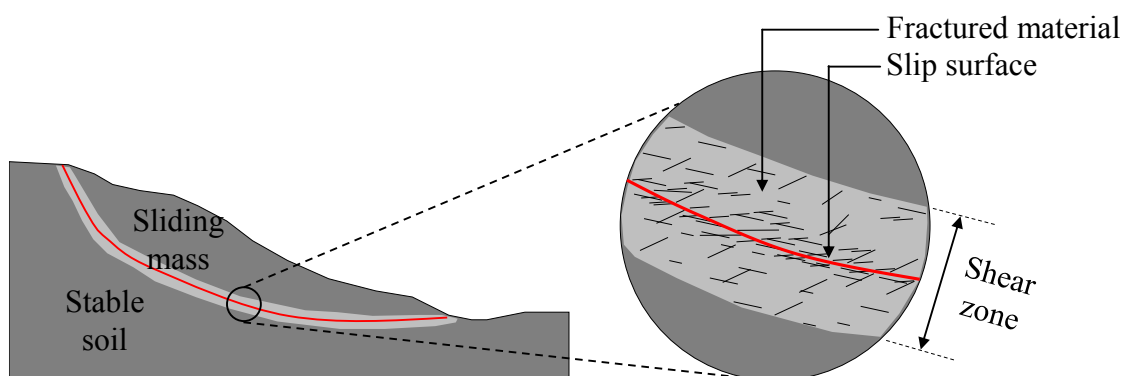
Figure 2-8: Schematic representation of a shear zone in a landslide.

The mechanical process which leads to the formation of a shear zone is caused by stress changes and associated shear (and/or volumetric) plastic starins which sensibly destructure the fabric of the material.

Typically, shear zones present a set of short fissures (minor shears) gently inclined to the direction of movement and one (or more) slip surface (principal shear) oriented with the movement direction, as shown in **Figure 2-9**.
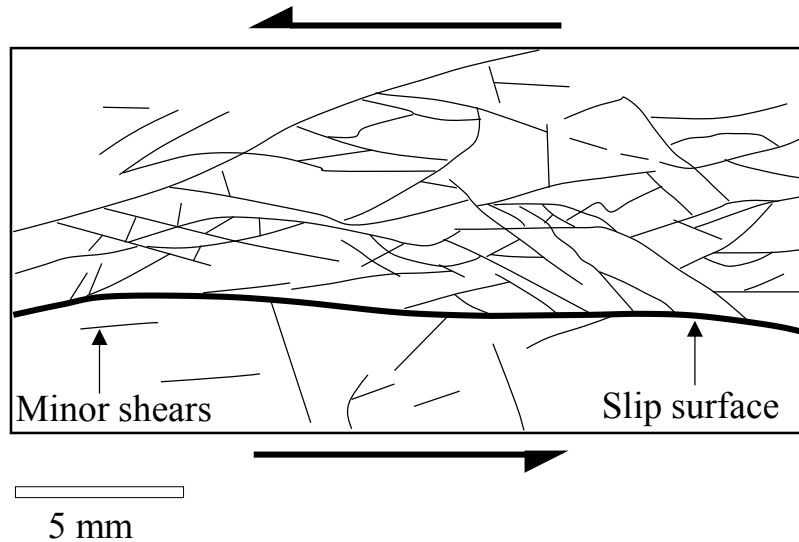
Figure 2-9: Fabric of a shear zone (redrawn from SKEMPTON & PETELY 1967).

With the increase of the displacement along the slip surface, typically some tens of microns wide (MORGENSTERN & TCHALENKO 1967), an orientation of the clay particles in the direction of movement occurs and the shear strength undergoes a progressive reduction. This orientation generally creates planar and polish surfaces often observed in clayey soils.

Figure 2-10: Typical slickensided slip surface in fissured shales (image taken from COROMINAS et AL. 2005).

When this "flattening" process makes the clay particles reach the maximum degree of orientation, along the slip surface the so-called "residual" strength is attained.

The associate Mohr-Coulomb failure envelope is generally linear in a wide range of effective normal stress with a negligible cohesion and an inclination characterized by friction angles that can be very small (COROMINAS et AL. 2005, RUGGERI et AL. 2016, ASSEFA et AL. 2015, among many others).
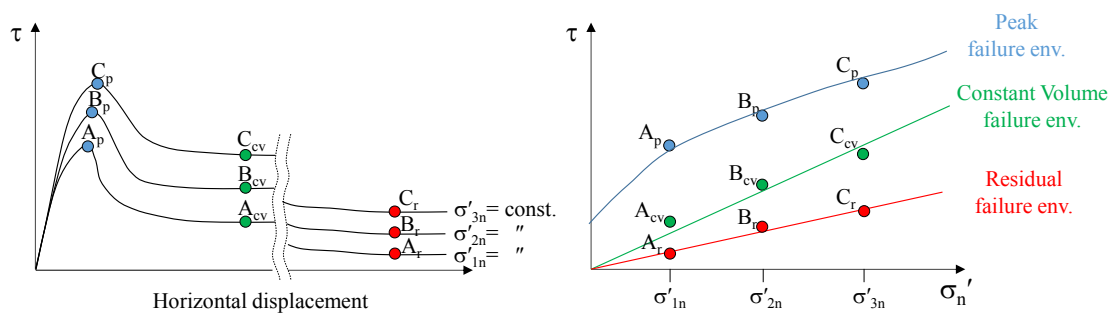
Figure 2-11: Typical failure envelopes of an overconsolidated clay evaluated from a shear test.

Althogh it is well-known that the value of the residual friction angle is a function of the amount of the clay fraction and on its mineralogical composition, some Authors highlighted that the hydrochemical effects of fresh water on some types of soil can play an importat role.

BOTTINO et AL. (2011) studied the influence of the calcite content ($CaCO_3$) of a marly arenaceous formation in northen Italy on the residual shear strength. They found that the residual friction angle obtained after a total decalcification of the material taken on site decresed from 18.5° to 14.8° in one case and from 21.5° to 12° in another, strarting from an initial calcite content of 16% and 34% respectively. Thus the decalcification of the material caused by rainfall water (rich in CO_2) flowing through structural discontinuities can reduce considerably their shear resistance. This aspect had been already pointed out by HAWKINS & McDONALD (1992) for the Fuller's Earth clay in UK.
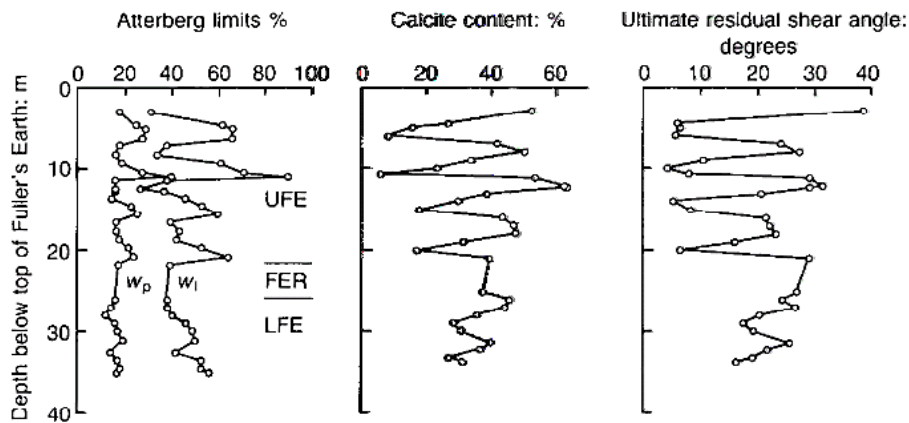
Figure 2-12: Relationship among calcite content, Atterberg limits and residual shear angle in calcareous mudrocks (from HAWKINS & McDONALD 1992).

DI MAIO et AL. (2014) analyzed the influence of the chemical composition of the pore-water on the residual shear strength of clay shales of marine origin in southern Italy. They demonstrated that the shear resistance of these materials decreases as the salt concentration in interstizial water decreases. Also in this case it is evident the hydrochemical deleterious effect of rainfall-water infiltration on these kind of materials (see **Figure 2-13**).
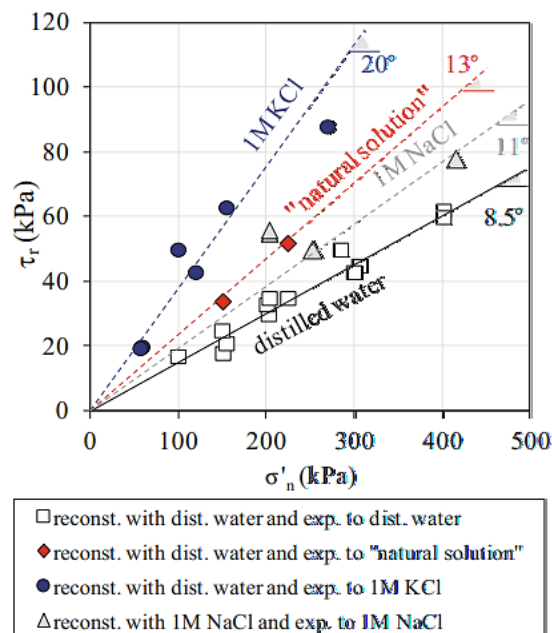
Figure 2-13: Residual shear resistance of clay shales of marine origin as a function of the chemical composition of the pore-water (from DI MAIO et AL. 2014).

These latter effects, which can be classified as wethering processes of chemical nature, in combination with the mechanical destructuration, contibute to the creation of a zone of weakness (PICARELLI & DI MAIO 2010) charactherized by a marked anisotropy, both mechanical and hydraulic (COMEGNA & PICARELLI 2008).

As far as slope stability is concerned, the detection of discontinuites (e.g. shear bands) and the knowledge of the processes that lead to their creation are imporant aspects to be taken into account.

Since shear bands exhibit different properties from the underlying parent formation as well as from the overlying sliding mass, the geotechnical characterization should be based on specific investigations of these relative small zones (respect to the unstable volume involved) which govern the behaviour of the whole system.

2.3   Rate of movement

In the previous paragraphs the adjectives "rapid" and "slow" have been using regarding the kinematics of landslides: but, from a quantitative perspective, when does a landslide can be defined rapid or slow? The answer to this question can be found in the velocity classification of landslides proposed by CRUDEN & VARNES (1996), which is the universally recognised scale adopted to identify the representative rate of movement of landslides.

Modifying the velocity thresholds formerly proposed by VARNES (1978), the Authors defined seven classes, summarised in **Table 2-3**: the scale factor between one velocity limit and another is equal to 100.

Class	Description	Velocity [mm/sec]	Typical Velocity
7	Extremely Rapid		
		5×10^{3}	5 m/s
6	Very Rapid		
		5×10^{1}	3 m/min
5	Rapid		
		5×10^{-1}	1.8 m/hour
4	Moderate		
		5×10^{-3}	13 m/month
3	Slow		
		5×10^{-5}	1.6 m/year
2	Very Slow		
		5×10^{-7}	16 mm/year
1	Extremely Slow		

Table 2-3: Landslide velocity classes proposed by CRUDEN & VARNES (1996)

The fastest class, defined as "extremely rapid", includes all the landslides whose typical velocity is higher than 5 m/s (which is approximately the speed of a person running). The lowest one, defined as "extremely slow", includes all the landslides characterized by an annual velocity less than 16 mm/year.

The Authors analyzed several case histories in which the effects of landslides on humans and their activities had been well described and the corresponding velocities had been known. Within this framework, they considered the velocity of a landslide as a parameter related (independently from other features of the considered phenomenon) to a certain destructive significance. To every class, therefore, they associated a probable destructive significance, as reported in **Table 2-4**. In brief, the higher the velocity class, the higher the damages to structures and people.

LANDSLIDE VELOCITY CLASS	PROBABLE DESTRUCTIVE SIGNIFICANCE
7	Catastrophe of major violence; buildings destroyed by impact of displaced material; many deaths; escape unlikely
6	Some lives lost; velocity too grat to permit all persons to escape
5	Escape evacuation possible; structures, possessions and equipment destroyed
4	Some temporary and insensitive structures can be temporarily maintained
3	Remedial construction can be undertaken during movement; insensitive structures can be maintained with frequent maintainance
2	Some permanent structures undamaged by movement
1	Imperceptible without instruments; construction possible with precautions

Table 2-4: Definition of probable destructive significance of landslides for different velocity classes (from CRUDEN & VARNES 1996).

From now on, the term "slow moving" will be used to identify those landslides characterized by a measurable rate of movement falling into the first three classes (class 1, 2 and 3 in **Table 2-4**) and the adverbs "extremely" and "very" will not be specified.

These landslides are not hazardous for human lives since their velocity is low enough to permit the evacuation of the structures that can be rebuilt or subjected to maintenance works.

It is worth noting that the rate of movement can differ within the displaced mass of the landslide with position, time and the period over which the velocity is estimated. A landslide, for instance, can fall into a velocity class if the movement rate over a long period is considered. However, if it shows higher velocities during limited periods, the velocity class to be considered should be another (e.g. an "extremely-slow" landslide may become "very slow" or a "slow" one can become "moderate"). This concept is well summarized by the graph reported in **Figure 2-14**.

When good quality long-term monitoring data are available, it is appropriate to describe the kinematic behaviour of the sliding mass with both the average velocity (over the entire period) and the maximum velocity recorded.
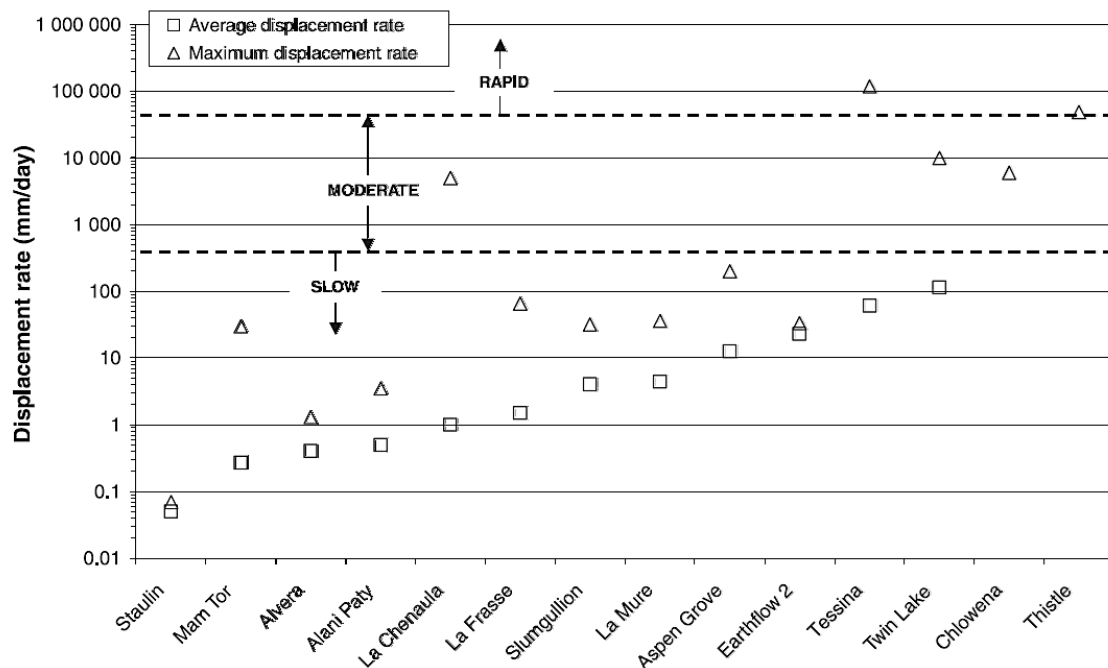
Figure 2-14: Average and maximum displacement rate of some mudslides (form GLASTONBURY & FELL 2008).

2.4   State of activity

After the onset of the general failure, as described in the first paragraph of this chapter, the displaced mass can exhibit some different state of activity. CRUDEN & VARNES (1996) defined the following states:

- **active**: the landslide is currently moving;
- **suspended**: the landslide has moved within the last annual cycle of seasons but it is not moving at present;
- **inactive**: the landslide last moved than one annual cycle of seasons ago;

This last state can be subdivided in:
- **dormant**: inactive landslide that can be reactivated by its original causes or other causes;
- **abandoned**: inactive landslide that is no longer affected by its original causes;
- **relict**: inactive landslide that developed under geomorphological or climatic conditions considerably different from those at present;
- **stabilized**: inactive landslide that has been protected from its original causes by artificial measures.

They also used the adjective **reactivated** for a landslide that is again active after being inactive. A graphic representation of some states mentioned above is reported in **Figure 2-15**.
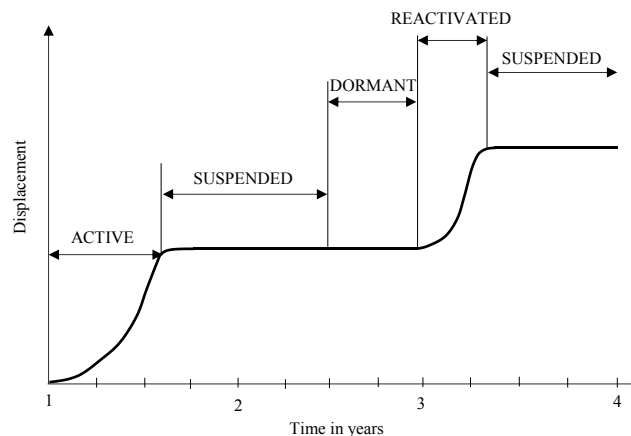
Figure 2-15: State of activity of a landslide (CRUDEN & VARNES 1996).

FLAGEOLLET (1996) summarized the state of activity of a landslide as reported in **Table 2-5**. He considered three states (active, dormant and stabilized) characterized by a certain type of activity. In particular, an active landslide can exhibit a displacement rate continuous or intermittent, while a dormant soil mass can undergo episodic reactivations with a certain frequency. It is interesting to note that the Author also introduced a quantitative time scale in term of return period.

State of activity	Type of activity	Return period
Active	Continuous	<1 day
	Intermittent	<1 year
Dormant	Episodic high frequency	1-10 years
	Episodic medium frequency	10-100 years
	Episodic low frequency	100-1000 years
Stabilized	None	>1000 years

Table 2-5: State of activity of landslides (modified from FLAGEOLLET 1996).

Without being too bound to the terms and definitions just mentioned above, it is relevant to understand the main aspects characterising the kinematics. To do so, in **Figure 2-16** a typical displacement series (both in term of rate of movement and cumulative displacement) is schematized.
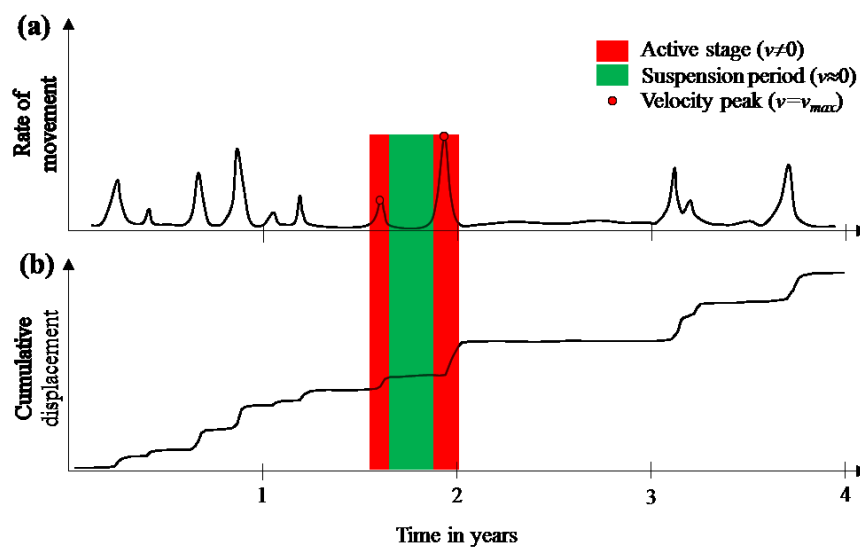
Figure 2-16: Schematic representation of displacement series of an active landslide in terms of (a) rate of movement and (b) cumulative displacement.

We can define a landslide "active" if there has been at least one movement during a seasonal cycle; a movement is identified as period during which the velocity increases. After that, the soil mass experiences a suspension period until a new active stage occurs: this is the typical intermittent kinematics of slow moving landslides. The time interval between one active stage and another (which can be identified as the return period according to FLAGEOLLET 1996) can be equal to some days, some months or even one year depending on the frequency of the changes in boundary conditions and how the system reacts to them.

If the instable mass does not show any movement for some years or more, the landslide can be classified as "dormant" and it generally undergoes a reactivation stage because of the occurrence of unusual natural event (such as an extreme rainfall or an earthquake) or because of a geometry change induced by human activity.

2.4.1 Displacement trends of slow moving landslides

With the aim of characterizing the active stages just mentioned above, CASCINI et AL. (2014) have analysed some case studies reported in the scientific literature for which a consistent dataset of good-quality displacement measures were available.

To do so, they have introduced two dimensionless variables characterising each landslide activity stage, which are $D_i(t_j)$ and $T_i(t_j)$, defined as:

$$D_i(t_j) = \frac{d(t_j) - d_{min,i}}{d_{max,i} - d_{min,i}} \tag{2-1}$$

$$T_i(t_j) = \frac{t_j - t_{min,i}}{t_{max,i} - t_{min,i}} \tag{2-2}$$

where $d(t_j)$ is the monitored cumulated displacement at time t_j; $d_{min,i}$ and $d_{max,i}$ are the cumulated displacements at the beginning and at the end of active stage i, respectively; $t_{min,i}$ and $t_{max,i}$ are the instants at the beginning and at the end of active stage i, respectively. After plotting these values in a T-D plane, it has been possible identifying three distinct common trends of movements, which can be described using just one exponential equation of the type:

$$D_i\left(t_j\right) = T_i\left(t_j\right)^x$$ (2-3)

where x=1 for **trend-type I**, x<1 for **trend-type II** and x>1 for **trend-type III**. In **Figure 2-17**, a graphic representation of the equation (2-3) is reported.
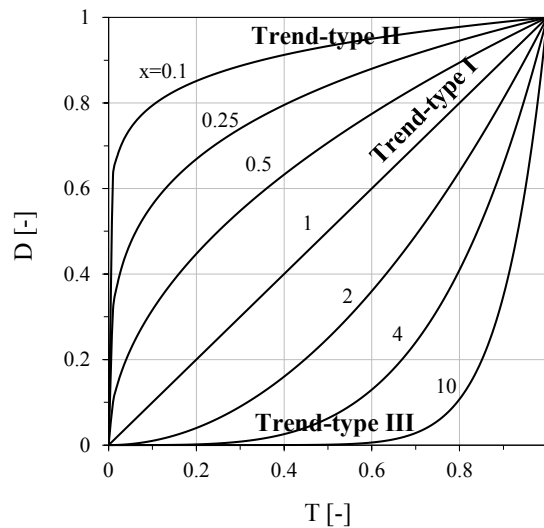
Figure 2-17: Analytical description of displacement trends of slow moving landslides according to CASCINI et AL. (2014).

It is worth noting that each type of trend is related to a specific mobility condition of the landslide considered.

The **trend-type I** describes a stage during which the velocity is constant over the period considered and it indicates, according to the Authors, that the landslide is "stationary" in the sense of a creep-type behaviour. This phase can be representative of a period (e.g. prolonged dry period) where no groundwater level changes occur and thus the effective shear stresses along the slip surface remain almost constant.

The **trend-type II**, instead, shows a rate of displacement that tends to decrease over time after an initial (more or less accentuated) acceleration. This trend is essentially representative of the rainfall-induced activity stages. After a rainfall event, in fact, the pore water pressure along the slip surface increases, causing a reduction of the shear strength mobilized. After that, the dissipation process of the excess pore-water pressure takes place and the slip surface experiences a general shear strength regain that leads to a deceleration of the landslide.

The **trend-type III**, finally, is a non-stationary process that, in contrast to the previous one, is not due to the repetitive seasonal variations of the groundwater level but to other

boundary conditions acting on the system (such as applied loads, excavation or river erosion).

Although all of the three trends has been detected by the Authors among the selected case histories, most of them owned to the trend-type II category and their analytical description indicated that the values of parameter x were not lower than 0.25.

This is an interesting aspect concerning slow moving landslides because it underlines that the main cause of their mobility is due to the rising and lowering of pore-water pressure caused by rainfalls.

2.5   Landslides causes

"The processes involved in slope movements comprise a continuous series of events from cause to effect" (VARNES 1978). Until now, it has been talking about only the kinematics of slow moving landslides, so only the effect in term of displacement rate has been analysed. Now it is right and proper to discuss about the causes, previously described with the general term "boundary conditions".

The aim of this paragraph is not to make a list of all the possible landslide causes but rather to underline differences among some causes and the role they play in the process.

In every slope, there are forces that tend to promote downslope movement and opposing forces that tend to resist movement: the slope level of safety results from comparing the downslope shear stress with the shear strength of the soil along an assumed or known rupture surface. The ratio between resisting and driving forces is the well-known factor of safety (FS).

TERZAGHI (1950) divided landslide causes into external causes, which result in an increase of the shear stress, and internal ones, which result in a decrease of the shear strength. This distinction can be misleading because there are a number of external or internal causes that may be operating either to reduce the shearing resistance or to increase the shearing stress, affecting simultaneously both terms of the FS. The shaking motion produced by an earthquake, for example, generate inertial forces proportional to the weight of the sliding mass (increase of the shear stress) but can also generate excess pore pressure (decrease of the shear resistance).

According to POPESCU (2002), it is more appropriate to discuss "causal factors", including both "conditions" and "processes", than "causes" per se alone.

A causal process, which can be natural or anthropogenic, encloses all the factors that lead the slope system to fail. In **Table 2-6** is reported a list of landslides causal factors grouped in four classes according to their origin.

1. GROUND CONDITIONS
(1) Plastic weak material
(2) Sensitive material
(3) Collapsible material
(4) Weathered material
(5) Sheared material
(6) Jointed or fissured material
(7) Adversely oriented mass discontinuities (including bedding, schistosity, cleavage)
(8) Adversely oriented structural discontinuities (including faults, unconformities, flexural shears, sedimentary contacts)
(9) Contrast in permeability and its effects on ground water contrast in stiffness (stiff, dense material over plastic material)
2. GEOMORPHOLOGICAL PROCESSES
(1) Tectonic uplift
(2) Volcanic uplift
(3) Glacial rebound
(4) Fluvial erosion of the slope toe
(5) Wave erosion of the slope toe
(6) Glacial erosion of the slope toe
(7) Erosion of the lateral margins
(8) Subterranean erosion (solution, piping)
(9) Deposition loading of the slope or its crest
(10) Vegetation removal (by erosion, forest fire, drought)
3. PHYSICAL PROCESSES
(1) Intense, short period rainfall
(2) Rapid melt of deep snow
(3) Prolonged high precipitation
(4) Rapid drawdown following floods, high tides or breaching of natural dams
(5) Earthquake
(6) Volcanic eruption
(7) Breaching of crater lakes
(8) Thawing of permafrost
(9) Freeze and thaw weathering
(10) Shrink and swell weathering of expansive soils
4. MAN-MADE PROCESSES
(1) Excavation of the slope or its toe
(2) Loading of the slope or its crest
(3) Drawdown (of reservoirs)
(4) Irrigation
(5) Defective maintenance of drainage systems
(6) Water leakage from services (water supplies, sewers, stormwater drains)
(7) Vegetation removal (deforestation)
(8) Mining and quarrying (open pits or underground galleries)
(9) Creation of dumps of very loose waste
(10) Artificial vibration (including traffic, pile driving, heavy machinery)

Table 2-6: List of some causal factors.

Causal factors are divided in two groups according to their effects:

- **preparatory causal factors**: which make the slope susceptible to movement without actually initiating it;
- **triggering causal factors**: which initiate movement.

Ground conditions, for instance, such as low-strength soil, degree of weathering and fracturing influence the stability of the slope but they are not causes in the strict sense. They are part of the conditions necessary for an unstable slope to develop, to which must be added other environmental factors: it does not matter if the ground is weak as such, failure will only occur as a result if there is an effective causal process that acts as well.

It is possible to interpret this process with a progressive decrease of the *FS* over time. Although the formulation of the *FS* makes a "rigid" distinction between stability (*FS>1*) and instability (*FS=1*) of the slope, it is better to consider slopes existing in one of the following three stages (CROIZER 1986): *stable*, *marginally stable* and *actively unstable*. *Stable* slopes are those where the margin of stability is sufficiently high to withstand all destabilizing forces. *Marginally stable* slopes are those that fail at some time in response to the destabilizing forces attaining a certain level of activity. *Actively unstable* slopes are those in which destabilizing forces produce continuous or intermittent movement.

The three stability stages must be seen to be a part of a continuum as a result of a causal process. It is worth noting that a particular causal factor may perform either or both functions (preparatory or triggering) depending on its degree of activity and the margin of stability.

Another classification of the factors associated with landsides mobility is the one proposed by VAUNAT et AL. (1992, 1994). The Authors individuated three main classes of factors: **predisposition** factors, **triggering** or **aggravating** factors and the **revealing** factors.

Predisposition factors are essentially those site characteristics that make the slope susceptible to fail: these characteristics are essentially related to the nature of the materials, to the geological history and to the geomorphological context of the site.

Triggering factors are those that lead to failure, while **aggravating** factors produce a significant modification of stability conditions or of the rate of movement. They can be temporary (e.g. heavy rainfall, earthquake) or progressive (e.g. erosion).

Revealing factors provide (past or actual) evidence of slope movement but generally do not participate to the process. In this class can be incorporate not only characteristic landscape forms but also cracks in buildings and facilities (the activity of a landslide, thus, can be detected by the observation of its consequences on human-made works). Considering the four stages (pre-failure, failure, post-failure and reactivation), the authors pointed out that these factors can be sensitively different from one stage to another.

2.5.1 Stability of active landslides and their causes

Considering the specific case of active landslides, they can be defined "actively unstable": their precarious stability is characterized by a general low value of the factor of safety, which is next to one. Consequently, the system is very sensitive to destabilising forces that cause intermittent movements of the sliding mass (due to a temporary drop of the *FS* over time).

Excluding some causes such as erosion of the toe or any geometric change of the slope caused by human activity, the main factor affecting the stability and in turn, the mobility of active landslides is the rainfall. The amount of water that infiltrates through the soil causes a rising of the groundwater pressure along the slip surface and, thus, its shearing resistance decreases.

In this perspective, rainfall (and/or snowmelt) can be defined the main "aggravating" factor of active landslides. It can be noticed that, in this case, "triggering" factor in not appropriate since it is correlate to a general collapse or, in other words, to a first time failure. Concerning active landslides, this is not the case since they are characterized by a more or less pronounced changing in the rate of movement due to a temporary modification of the stability conditions.

If the landslide is situated in a seismic area, as the most part of the Italian territory is, earthquake can represent another aggravating factor. Considering the precarious stability of active landslides under "static" conditions, even a low-magnitude earthquake is theoretically able to induce effects to the sliding mass in terms of permanent

displacements. Even more so, the occurrence of a strong earthquake could lead to severe consequences.

With regard to active landslides, we can incorporate in the class of "predisposition" factors all the factors that facilitate the water infiltration into the soil. The rate of infiltration, for instance, is higher if the soil constituting the sliding mass is highly permeable (this mechanism can be favoured by the presence of cracks of any kind at the surface). The presence of vegetation favours the evapotranspiration, reducing the available amount of water that can recharge the aquifer: barrenness, thus, can be considered a predisposition factor. Gentle slope is another predisposition factor since the lower the angle of slope the lower the amount of water that can run off. The climate of the area in general can be incorporated in this class of factors (humid regions vs. arid regions).

Another important predisposition factor of such slope movements is the presence of a well-defined shear surface with poor mechanical properties that constitutes a weakness for the system.

To conclude with this class of factors, the seismic activity of the site can be considered a predisposition factor as well.

As far as active landslides are concerned, the "revealing" factor par excellence is the monitoring. Since the general low-entity of the rate of movement exhibited by the unstable mass, specific devices are required in order to directly quantify the entity of the displacements over time and in different points within the volume involved.

2.6 Consequences

The knowledge of the potential effects of slope movements on human lives and properties is a major issue in risk assessment. In the last decades landslide risk has experienced an important increase in many parts of the world because of the growth of population with the associate need of new areas to be urbanized and of infrastructures to be constructed or upgraded. Therefore, this interaction is becoming more and more inevitable and represents a current problem to cope with.

As pointed out by CRUDEN and VARNES (1996), the intensity of a landslide, which quantifies its effect on the exposed element, depends on the rate of movement: in the

specific case of slow moving landslides, the main consequence concerns serviceability problems to structures and infrastructures, while loss of lives can be avoided.

According to URCIOLI & PICARELLI (2008), the interaction between landslides and man-made works mainly depends on the velocity and the mass of landslides. They divided landslides into fast and slow movements: the first are extremely hazardous for human lives and for all structures located along the run-out of the landslide while the latter cause damage to structures and infrastructures built on the slope because of differential soil movements.

A very comprehensive scientific work about this topic is the one published by MANSOUR et AL. (2011). The Authors collected and analysed several cases reported in literature of slow moving landslides where monitored movements were available as well as their effects on facilities.

They divided the considered typologies of infrastructure in four categories: *urban communities*, *highways*, *bridges* and *dams*. For each one of them, they furnished the expected extent of damage in relation to a certain range of the movement rate, as reported in **Figure 2-18**. In **Figure 2-19**, instead, a synoptic graph of the degree of damage against the movement rate for the considered classes is shown.
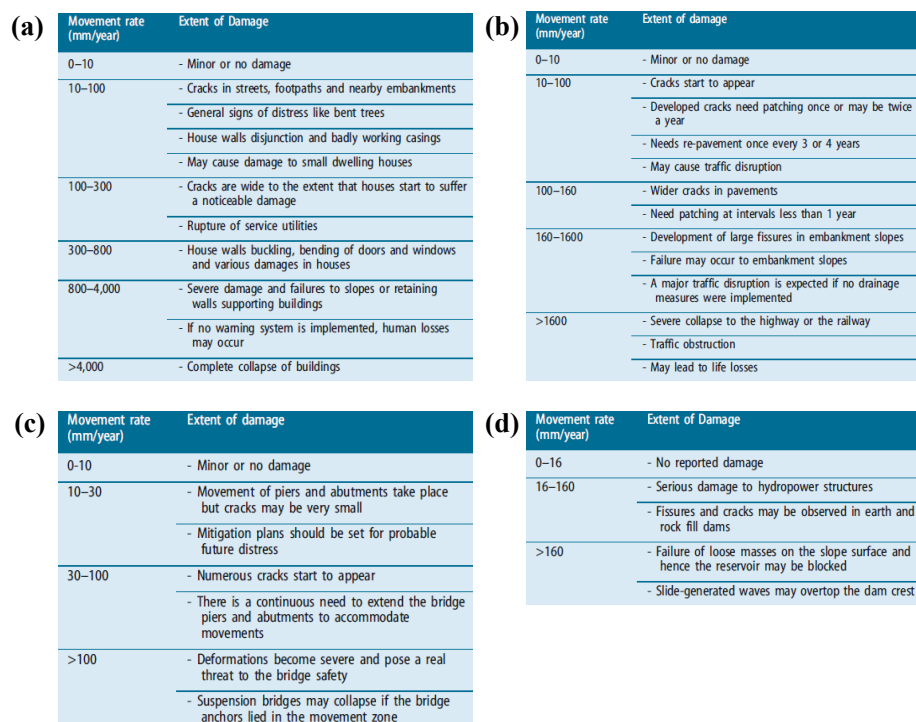
Figure 2-18: Damage expected from slow moving landslides to (a) urban communities, (b) highways, (c) bridges, (d) dams as a function of movement rate (from MANSOUR et AL. 2011).
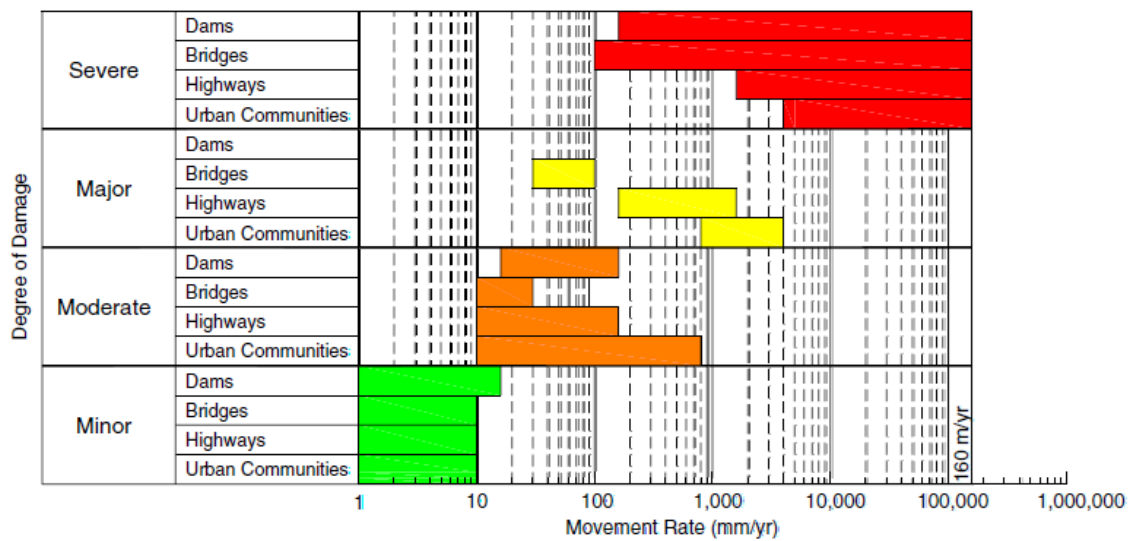
Figure 2-19: Schematic representation of the expected extent of damage versus movement rate for various forms of infrastructure (from MANSOUR et AL. 2011).

As pointed out by the same Authors, the damage description corresponding to every movement rate range is based only on the shown range. The extent of damage will become more severe if proper mitigation measures are not applied promptly to prevent the effect of movement accumulation. This movement magnitude will bring the resulting damage to a higher level, which may be destructive in some cases. Therefore, the cumulative displacement ultimately controls the extent of damage rather than the annual movement rate (PICARELLI 2011).

Another interesting aspect regards the thresholds of the movement rate is that they differ from one class to another. This is due to the "vulnerability" of the facility considered, intending with this term the predisposition of a structure to suffer damages (the same movement rate can be harmful for a bridge but not for a highway).

Although the framework proposed by the Authors takes into account the concept of vulnerability by considering different classes of facilities, the problem is more complex. For a given facility class, the vulnerability depends on other aspects such as the structural typology (e.g. masonry building vs. reinforced concrete building) and the degree of redundancy (a statically indeterminate structure is more sensitive to differential displacements than a statically determinate one).

Another aspect that plays an important role is the position of the element with respect to the movement direction of the landslide. RAJANI et AL. (1995) outlined this aspect concerning pipeline-landslide interaction and they showed that pipelines crossing a

landslide in the direction normal to the movement could safely experience very large displacements, while pipelines laid in the same direction could be subjected to large axial stresses because of smaller displacements.

After this brief discussion, it is evident the relevant economic consequences of slow moving landslides and how much complex their interaction with structures and infrastructures is as well as the evaluation of the associated risk.

3 CHAPTER – The case history of "La Sorbella" landslide

3.1 Introduction of the case history

The case history analysed in these work concerns a large deep-seated landslide (named "La Sorbella" landslide) affecting a segment of a new national road in Umbria region (central Italy). The "Strada Statale 318" (SS 318) owns to a major infrastructure network ("Umbria-Marche Quadrilatero") of economic relevance since it connects important urban communities located along the Adriatic coast with equally important centres located in the inner part of the national territory (see **Figure 3-1**).

Figure 3-1: Location of the site of interest and layout of the "Umbria-Marche Quadrilatero" road network.

Construction works, started at the end of 2014, ended in the mid of 2016 and the infrastructure was open to traffic in July 2016.

During and after the construction works, inclinometer monitoring highlighted the activity of the landslide that shows the typical features of slow moving landslides discussed in the 2 CHAPTER.

Although the phenomenon is still under investigation, the main aspects in terms of cause-effect have been recognized. In particular, thanks to high frequency readings of a fixed-

in-place inclinometer probe, a clear correlation between rainfall and displacement rate has been detected, as will be discussed in detail in the following.

Moreover, the monitoring system also recorded the effects on the landslide induced by the 2016 seismic sequence that struck central Italy. The availability of these "precious" data underlines the important role played by a good quality monitoring, which is the base for a rational understanding of the mechanisms governing any landslide.

It is appropriate to underline that "La Sorbella" landslide is representative of a typology of slope failure mechanisms so widespread in hilly areas of central Italy, affecting urban communities and compromising the serviceability of many facilities.

1) "La Sorbella" landslide (this study)

2) "Casanuova dam" landslide (Assefa et al. 2015)

3) "Ivancich" landslide (Calò et al. 2014)

4) "Montemartano" landslide (Grana & Tommasi 2013)

5) "Acqualoreto" landslide (Faralli et al. 2004)

6) "Porta Cassia" landslide (Tommasi et al. 1997)
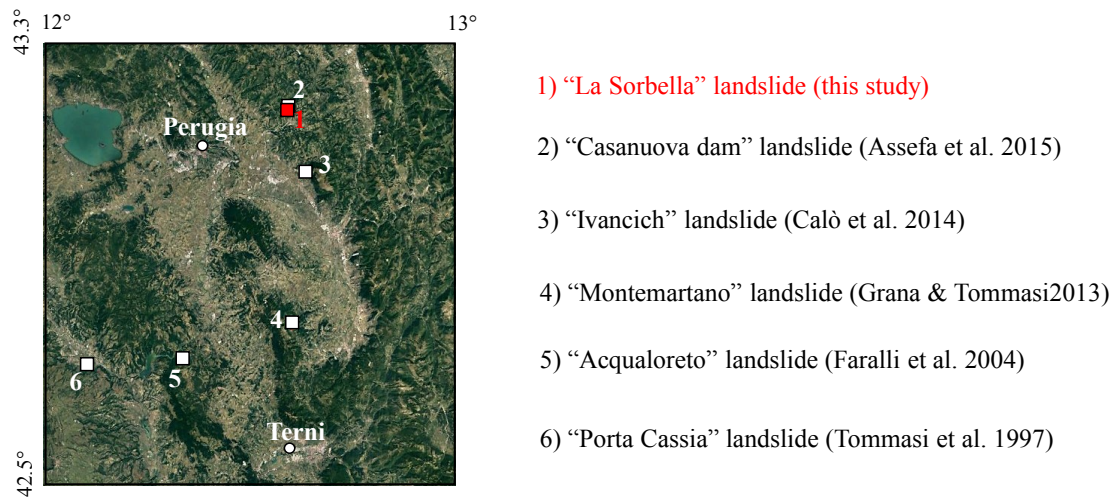
Figure 3-2: Some well-documented slow moving landslides in Umbria region.

In this context, a reasonable "diagnosis" of each single case study can contribute to deepen the knowledge of such complex natural hazards and in turn to individuate the best remedial measures to adopt.

3.2 Structural and geological settings of Umbria-Marche Apennines

Before analysing in detail the geological and structural features at the slope scale, it is important to give an overview at a regional scale. In **Figure 3-3**, the location of the site of interest is reported within a sketch map of the Umbria-Marche territory, where the main structural settings and geological formations are illustrated.
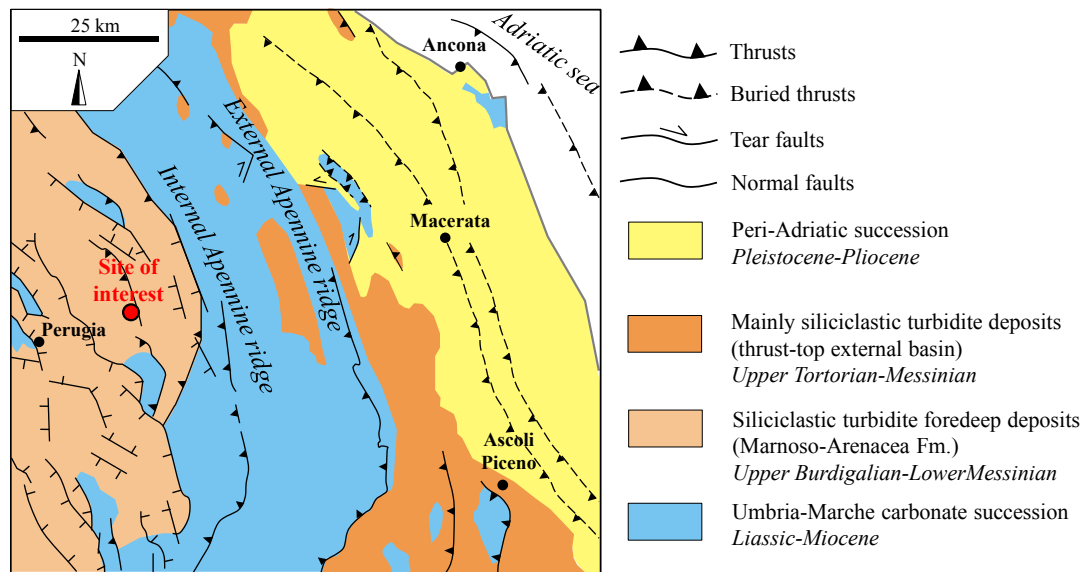
Figure 3-3: Geo-structural sketch map of Umbria-Marche Apennines (modified from GUERRERA et AL. 2015).

The Umbria–Marche Apennines are a typical arc-shaped fold-and-thrust belt verging towards E-NE. The compressional tectonics started in middle Miocene in western Umbria and migrated eastwards towards the Adriatic coast, deforming the Umbria-Marche Meso-Cenozoic carbonate succession; this latter constitutes the mountain ridge, formed by two main groups of anticlines (one inner and one outer).

From the internal Apennine sectors (Umbria-Romagna domain) to the external Adriatic margin (Marche domain), the siliciclastic successions were deposited during the orogenic process. The whole depositional area can be considered as a singlewide basin with depocentres or main sedimentation areas progressively migrating eastwards (GUERRERA et AL. 2012).

The Marnoso-Arenacea Formation (MAF) is one of these sin-orogenic turbidites that was deposited in the inner foredeep basin (NW-SE oriented) bounded to west by the Tuscan Nappe (Cervarola, Falterona and Trasimeno units) and by the Umbria-Marche carbonate succession to est.

The MAF (Langhian-Tortorian) is constituted by an alternation of sandstones and marls and it is characterized by some facies markedly different from one area to another, as it can be observed from several exposed outcrops (an example is shown in **Figure 3-4**).

Figure 3-4: One of the most famous outcrop of the Marnoso-Arenacea Formation in the municipality of Galeata (Emilia-Romagna region).

This is consistent with the "complex" nature of the MAF foredeep (as meant by RICCI LUCCHI 1986) characterized by sin-sedimentary structural highs and depocentres related to the main thrust fronts within the foredeep basin, which significantly control the lateral and vertical distribution of turbidite facies (TINTERRI et AL. 2011).

As far as the tectonic history is concerned, the area of interest underwent an extensional phase starting from late Pliocene–lower Pleistocene (BROZZETTI & LAVECCHIA 1994) that is still in act. As a result, the former compressional structures have been dissected by NW-SE trending normal faults, giving rise to a complex geological environment.

This ongoing extensional regime is confirmed by the velocity field resulting from the analysis of GPS data as reported in MANTOVANI et AL. (2015) who highlighted that the outer sector of the Apennines moves significantly faster and with a greater eastward component with respect to the inner part of the belt. This evidence (consistent with the geological long-term extensional kinematics) justifies the high seismic activity of central Italy. The epicentres of the strongest historical and more recent earthquakes, in fact, took place along extensional fault systems periodically activated by this peculiar kinematics.

3.3 Geo-structural and morphological features of the slope

The site of interest is located next to Valfabbrica, a medieval town in the district of Perugia (central Italy).

The main characteristic element is the Chiascio River that progressively craved and modelled the rock base formation outcropping in the area, which is the Miocene Marnoso-Arenacea Formation (MAF).

The resulting morphological context, representative of many Preappenine hilly territories, is constituted by a quite narrow alluvial plain bounded on both sides by slopes of relative gentle inclinations. These latter are very often constituted by colluvial covers and/or by landslide deposits resulting from earlier slope failures.

This is exactly the situation observed for the slope of interest whose geological settings are reported in **Figure3-5**, where it is also possible to see the location of the infrastructure.
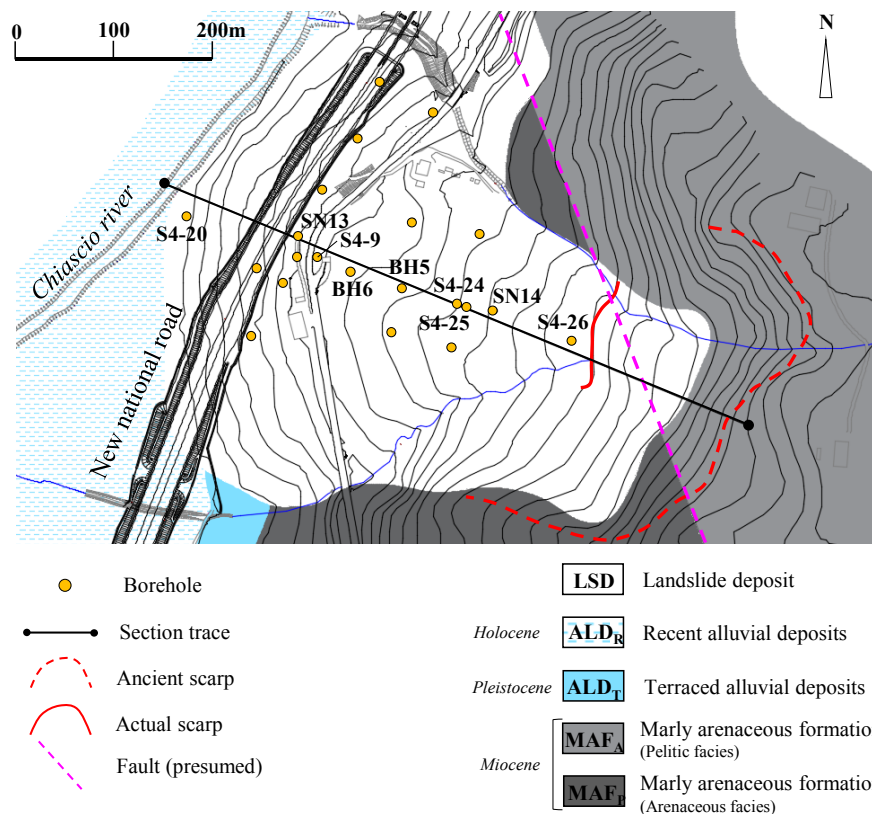
Figure 3-5: Geological map and morphological features of the slope. Continuously cored boreholes are also reported (the ones named are those considered for the reconstruction of a representative longitudinal section).

Before the starting of the construction works, several continuous logging drillings have been made. Therefore, it has been possible to know the stratigraphy of the site and to reconstruct a representative longitudinal section, shown in **Figure 3-6**.

The slope is characterized by an average inclination equal to 8° and is constituted by a chaotic material (landslide deposit-LSD) overlying the parent base formation that outcrops in the upper part. Although this latter is not directly observable because of the presence of a weathered cover, its more competent nature is justified by the higher slope angle reaching the value of 25°.
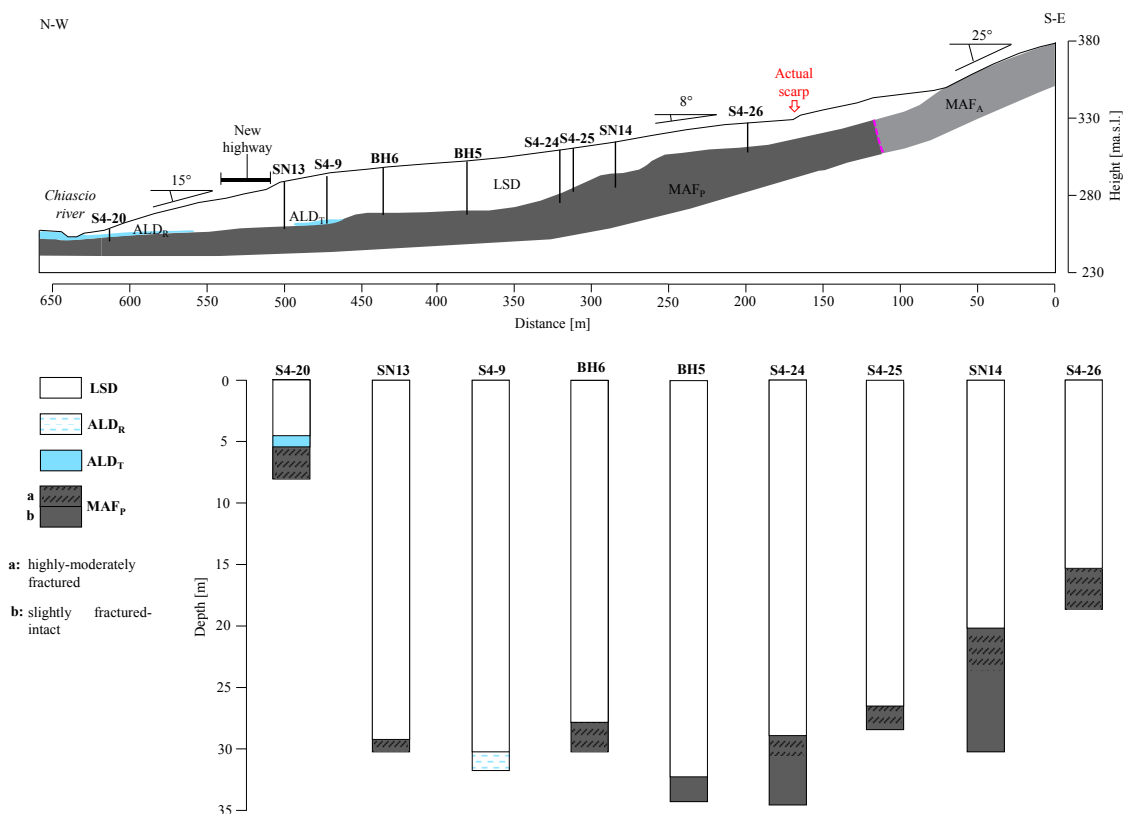
Figure 3-6: Longitudinal section of the slope and detail of boreholes stratigraphy.

The occurrence of a previous landslide event is confirmed by the typical fan-shaped configuration that the chaotic material exhibits in the lowermost part of the slope, which constitutes the accumulation zone of the old landslide.

In this zone, the displaced mass reaches the Chiascio River and overlies the alluvial deposits, both recent (ALD_R) and terraced (ALD_T). Since the recent alluvial deposits have been supposed to be of Holocene age, the landslide certainly occurred after that period.

Regarding the base formation, two main facies have been recognized: the first one (MAF_P) consists of marls and siltstones with thin layer of sandstones, while the second one (MAF_A) is constituted mainly by sandstones with thin layer of marls and siltstones, although their thickness can sometimes reach some meters. In a zone next to the site of interest, it has been possible to observe directly the stratigraphy from an outcrop, as shown in **Figure 3-7**.

Arenaceous layer (A)
Sandstones

Pelitic layer (P)
Marls and Siltones

MAF_A : Predominately arenaceous facies
A/P = 3/1 ÷ 4/1

10m

5

0

MAF_P : Predominately pelitic facies
A/P = 1/7 ÷ 1/8
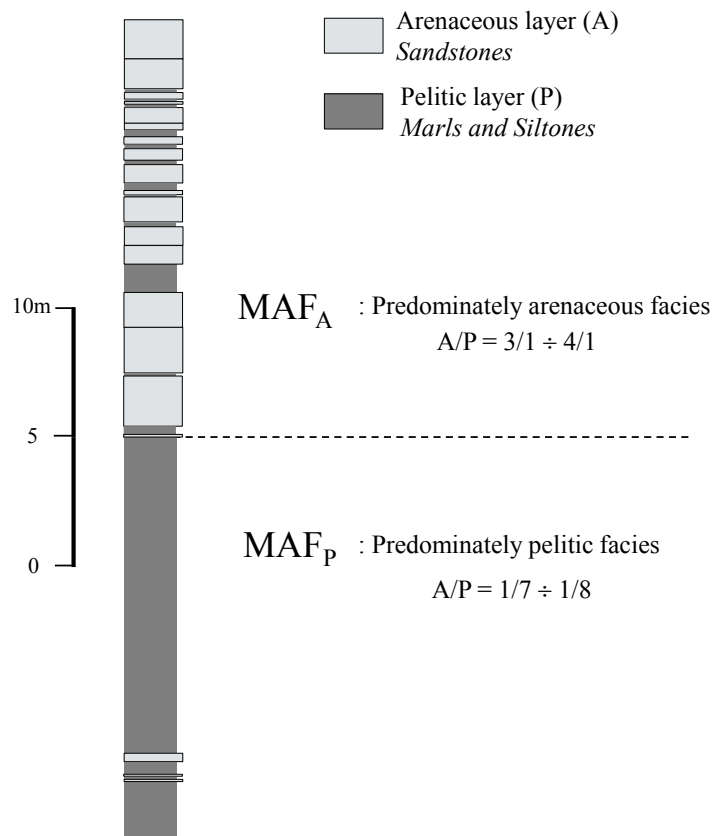
Figure 3-7: Main facies of the Marnoso-Arenacea Formation observed from an outcrop next to the site.

A main tectonic discontinuity, of normal attitude, has been hypotized by means of interpretation of aerial images and sudden variations of the facies. Its location and orientation can be seen in **Figure 3-5**, while the dip angle has been supposed to be higher than 80°.

3.4 Rainfall regime

Thanks to the presence of a weather station next to the site of interest, it has been possible to know the main climatic variables in terms of rainfall and temperature. Since the station is located approximately 2 kilometres far from the slope (see **Figure 3-8**) and at the same elevation above the sea level (335 m a.s.l.), the recorded data can be considered representative for the investigated site.
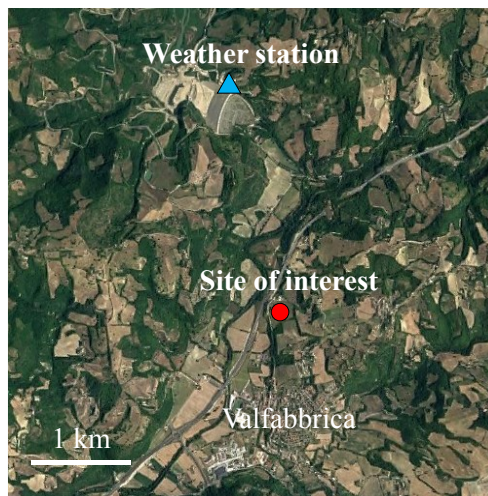
Figure 3-8: Location of the weather station close to the site of interest.

Unfortunately, the station was installed in 2008, thus only ten years of registrations are available, covering the period from 2009 to 2018. Despite this fact, these values are in good agreement with statistical data evaluated over longer periods for neighbouring areas of similar geographical context. Monthly rainfalls and temperatures are reported in **Figure 3-9**.

Regarding the rainfalls, the annual amount rages from 517 mm to 1154 mm, with an average value equal to 924 mm over the entire period.

Analysing the trend of the monthly rainfall, a clear peak is registered in November while August is the driest month of the year. Furthermore, abundant rainfalls generally characterize the period from January to May.

In the area of interest, finally, snowfalls sometimes occur during the winter season, but the intensity of such events is generally low (few centimetres of cumulated height).
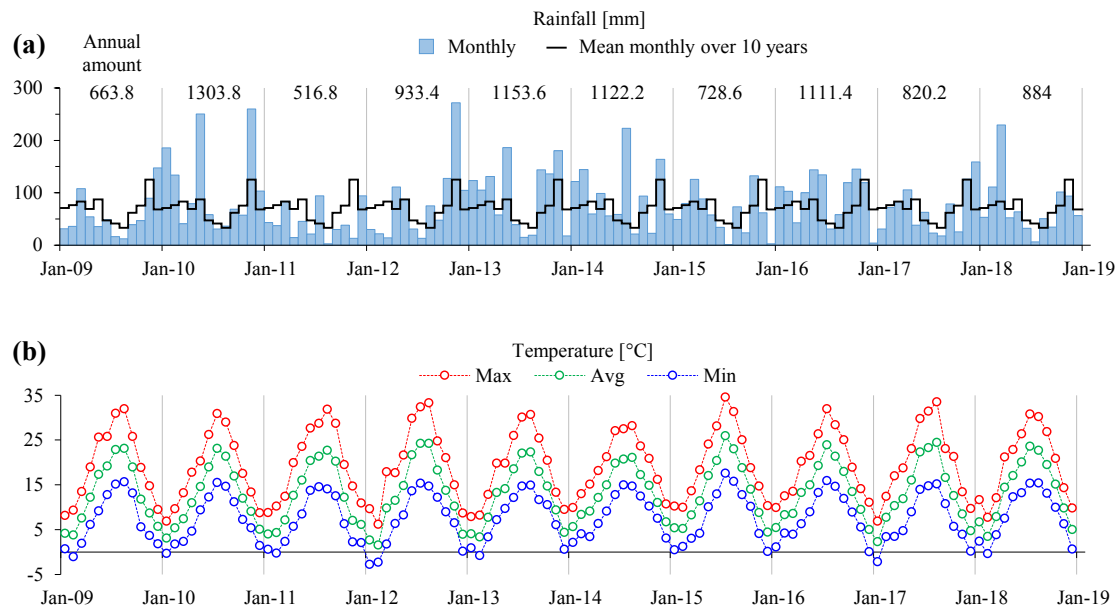
Figure 3-9: Monthly (a) rainfall and (b) temperature data recorded from 2009 to 2018.

3.5 Monitoring activities

In order to investigate the state of activity of the landslide, inclinometer casings have been installed along the slope through the years and periodically manual readings have been carried out. Moreover, the sub-surface monitoring system has been enhanced by conditioning two casings with fixed-in-place inclinometer probes with a daily automatic acquisition (which is still in act).

The inclinometer monitoring considered and analysed in this works cover more than five years, from April 2014 to July 2019; some available previous readings are also reported. It is worth noting that inclinometers highlighted the activity of the landslide and allowed to define a representative longitudinal section of the unstable mass whose thickness exceeds 40m of depth. At the current level of knowledge, unfortunately, the number of the "control verticals" and their location are inadequate to define a reliable boundary of the landslide.

Piezometers of different types have been also installed with the aim of detecting the position of the water table along the slope and monitoring its seasonal fluctuations. These data cover the period from April 2014 to November 2016.

The position of monitoring verticals are reported in **Figure 3-10**.
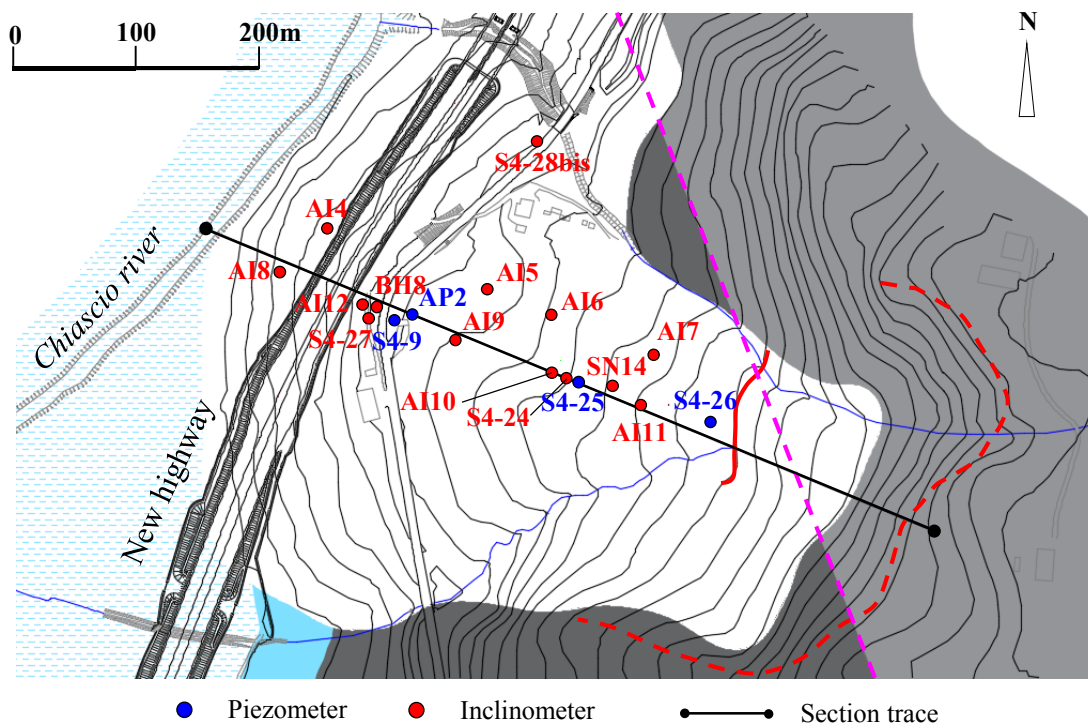
Figure 3-10: Position of inclinometer and piezometer verticals installed in the slope.

3.5.1 Manual inclinometer monitoring

All the inclinometer readings, which have been installed along two main parallel alignments, are coherent in detecting a slope movement whose direction is approximately W-NW oriented. In **Figure 3-11**, the displacement profiles of the alignment, where a major number of instruments are available, is reported.
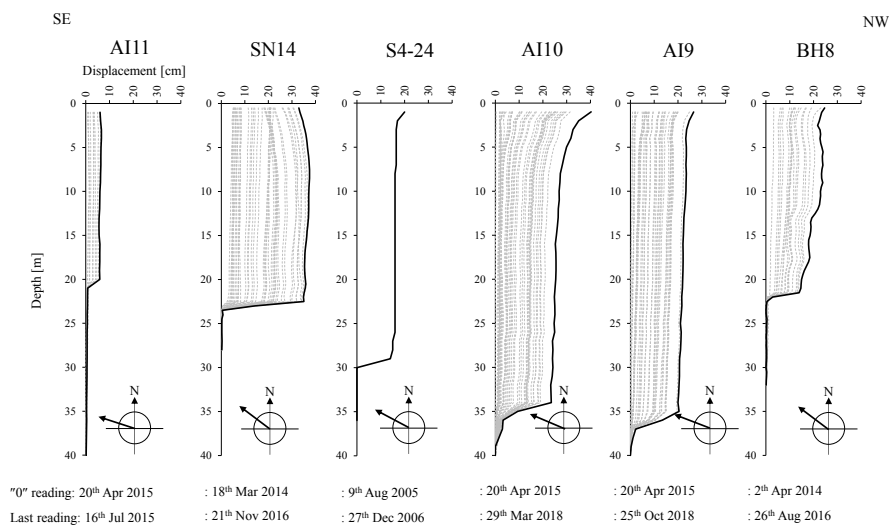
Figure 3-11: Deformation profiles of some inclinometers installed in the slope.

All the verticals highlighted a typical "block-type" deformation profile consisting of a soil mass that slides almost rigidly along a basal shear band where displacements take place. This shear band, whose thickness ranges from 0.5 to 2 m, reaches its maximum depth in the middle of the slope and tents to become thinner moving towards the upper and lower part of the slope. It is worth noting that the AI5 inclinometer (see **Figure 3-10**) has not detected any slip surface in a zone where its presence is confirmed by nearby instruments. This is probably due to the fact that the casing (40 meters long) is too short. It can be deducted, thus, that the maximum thickness of the landslide body is equal to 40 metres or more. Moreover, the inclinometer profiles AI4 and AI8 are not reported because they have not shown any appreciable movement, indicating that the zone seems to be stable.

In **Figure 3-12** are reported those inclinometer verticals for which the associate stratigraphy is available. It is interesting to note that the shear band develops along the roof of the base formation in the upper and middle part of the slope, while it intercepts the landslide deposit in the lowermost part (in the proximity of the infrastructure).
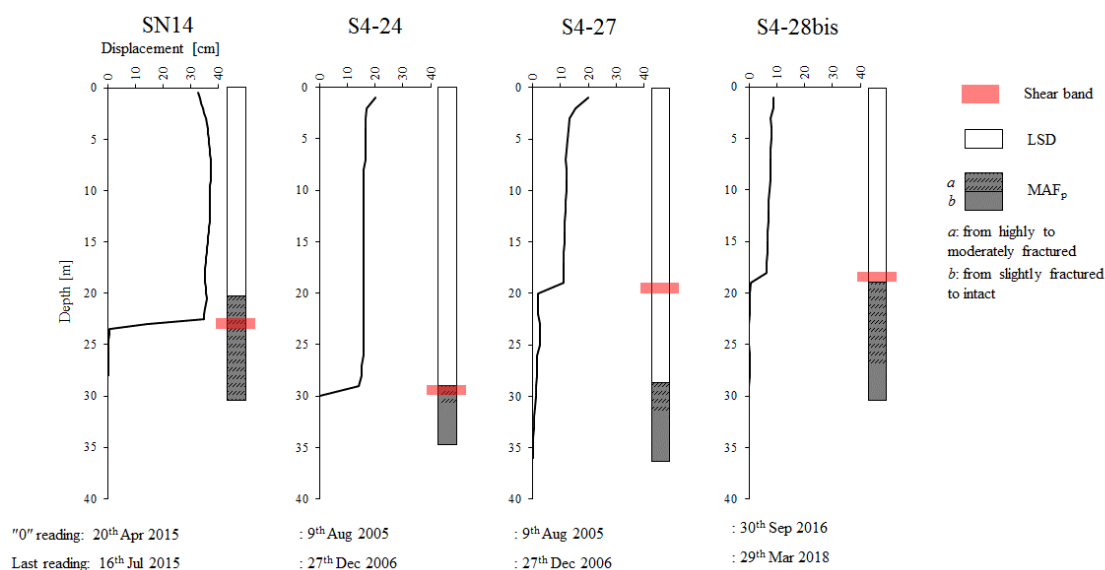
Figure 3-12: Position of the shear band along the stratigraphy.

Overlapping inclinometer profiles with the slope stratigraphy, a representative longitudinal section of the landslide body has been reconstructed, as shown in **Figure 3-13**.
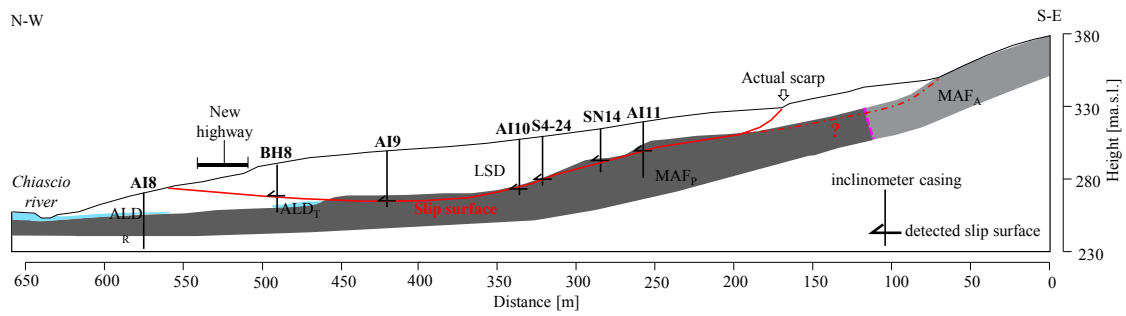
Figure 3-13: Longitudinal section of the landslide body.

In **Table 3-1** are summarized the main information gathered from manual inclinometer readings in terms of shear band depth, cumulative displacement and average velocity evaluated over the entire monitoring period. Cumulative displacement time series are illustrated in **Figure 3-14**.

Instrument	Readings		Shear band depth [m]		Tot. displ. [mm]	Velocity [mm/y]
	"0"	Last	min	max		
S4-24	Aug-2005	Dec-2006	29	30	14	10
S4-27	Aug-2005	Dec-2006	19	20	11	8
SN14	Mar-2014	Nov-2016	22.5	23.5	35.1	13
BH8	Apr-2014	Aug-2015	21.5	22	14	10
AI10	Apr-2015	Mar-2018	34	36	23.5	8
AI9	Apr-2015	Oct-2018	35	37	20.4	6
AI7	Apr-2015	Mar-2018	28	30	27.7	9
AI6	Apr-2015	Mar-2018	35	37	21.4	7
S4-28bis	Sep-2016	Mar-2018	18	19	6.2	4

Table 3-1: Summary of manual monitoring readings.
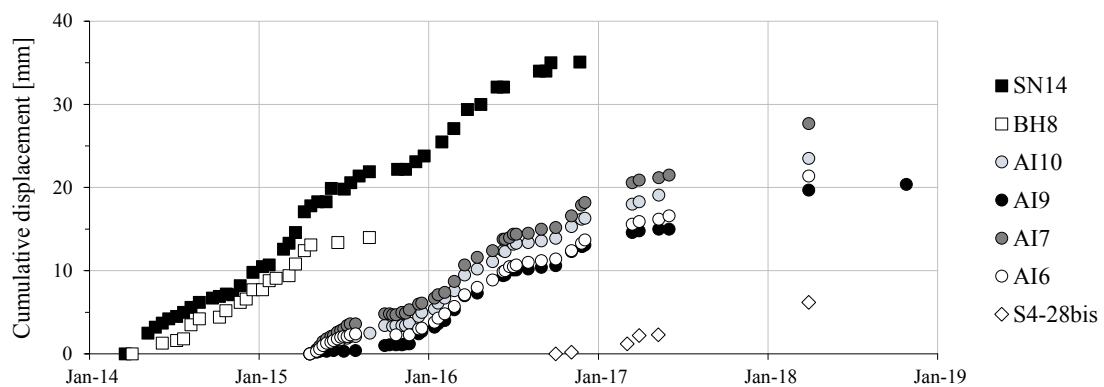
Figure 3-14: Cumulative displacement series of inclinometer manual readings.

The landslide can be defined as "extremely slow" according to the kinematic classification proposed by CRUDEN & VARNES (1996) since its average rate of movement ranges from 13 to 4 mm/year. It can be noted that slightly higher velocities are recorded in the upper part of the landslide and they tend to decrease moving downward. Despite this aspect, the sliding mass exhibits a "synchronous" behaviour in terms of displacement: the trend of each series, in fact, it is almost the same for all the verticals. Furthermore, this latter seems to be related to the climate regime of the area: higher velocities are recorded during rainy periods (winter-spring) while lower movement rates occur during dry ones (summer-autumn).

3.5.2 Automatic inclinometer monitoring

In order to monitor the evolution of the phenomenon more systematically, two verticals with fixed-in-place inclinometer probes have been installed. In particular, the first one was located in the uppermost part of the slope next to the existing AI11 vertical, where manual readings had been carried out before, while the second one (AI12) was located in the lower part of the slope. Four probes were installed in both casings: two in correspondence of the shear band, one some few meters below the ground surface and the lowest one in the stable formation.

Unfortunately, none of the AI12 probes have recorded movement evidences although, in that zone, other inclinometers (e.g. S4-27 and BH8) clearly highlighted the presence of the slip surface: it is very likely that this finding is related to a wrong positioning of the probes. In the following, thus, only monitoring data coming from the AI11 vertical will be presented and analysed in detail. The location of the AI11 fixed-in-place probes along the vertical is reported in **Figure 3-15**, where the main components of the monitoring station are also shown.
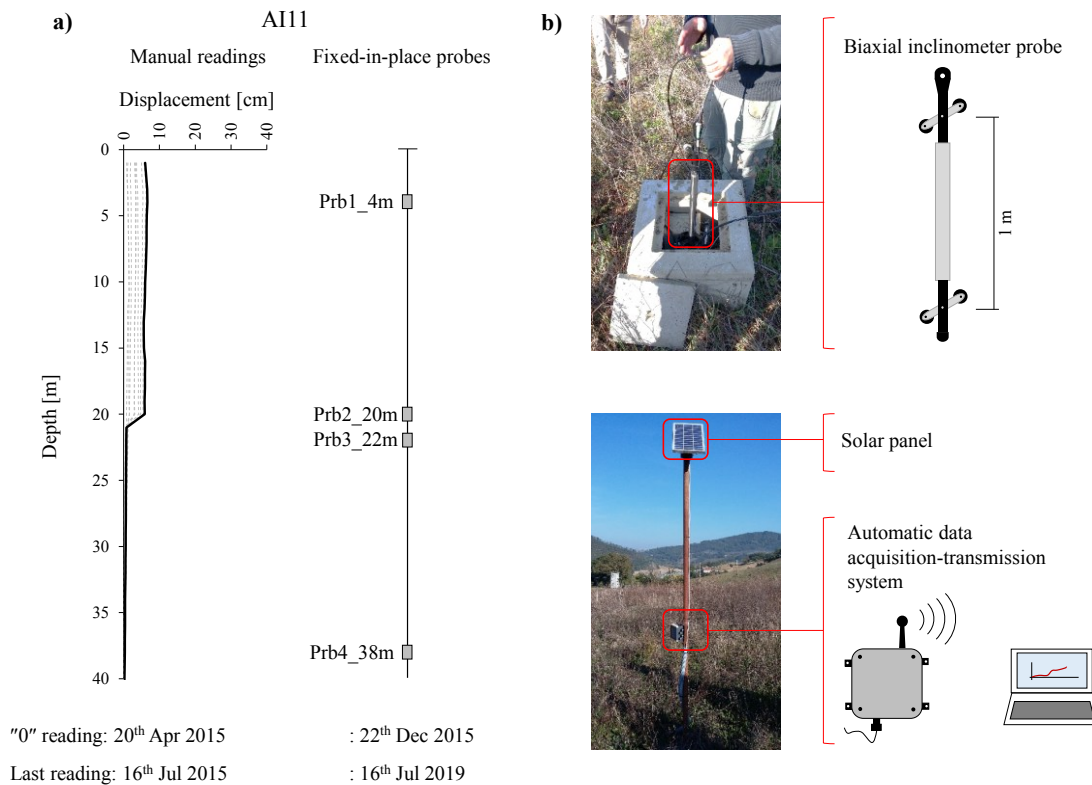
Figure 3-15: AI11 inclinometer monitoring station: a) location of the probes along the vertical and b) main components of the system.

On a daily basis, monitoring data are automatically acquired and sent in order to be visualized and handled remotely. The analysis of more than three and a half years of high frequency readings (covering the period from December 2015 to July 2019) have been carried out and are discussed in the following.

The most superficial probe and the deepest one (Pbr1 and Prb4 respectively) have not detected any movement while the probe located at 20m of depth (Prb2) clearly registered an ongoing movement as it might be expected since, at that depth, the presence of the shear surface had been already detected. Moreover, also the probe positioned at 22m of depth (Prb3) monitored an unexpected displacement. The representativeness of such evidence was put in doubt not only because it was not congruent with the displacement profile depicted by former manual readings, but also because its orientation was unrealistic (indicating an upslope-oriented movement!). To a better understanding, the cumulative displacement of the two probes and their polar representation are reported in **Figure 3-16**.
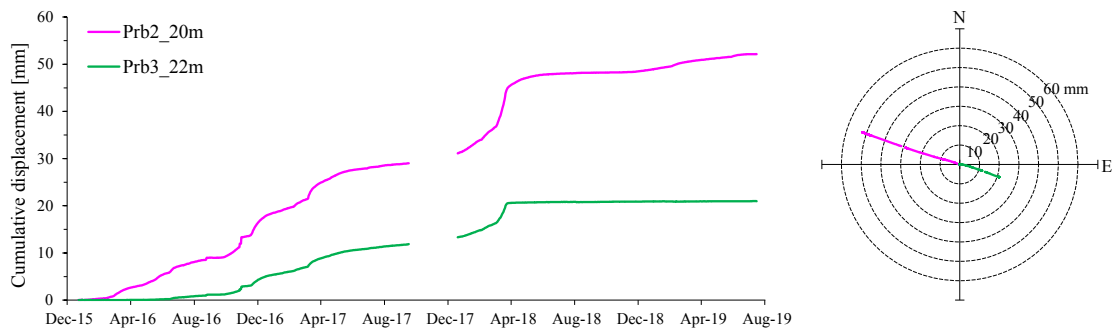
Figure 3-16: Prb2 and Prb3 displacement series and their polar representation.

Analysing the polar graph of the cumulative displacements, it is evident that Prb3 recorded a movement whose direction is rotated exactly 180° respect to the one of the Prb2, which is the actual movement direction of the landslide (coherent with the overall direction detected by other inclinometers). Moreover, the rate of movement detected by Prb2 was more than twice the average velocity of the landslide.

With the aim of clarifying these inconsistencies, at the end of October 2018 the probes were removed and a manual reading of the casing was carried out. The local displacement profile and its integration along the vertical (from the bottom) are reported in **Figure 3-17**. Readings along the E-W and N-S planes are kept separated.
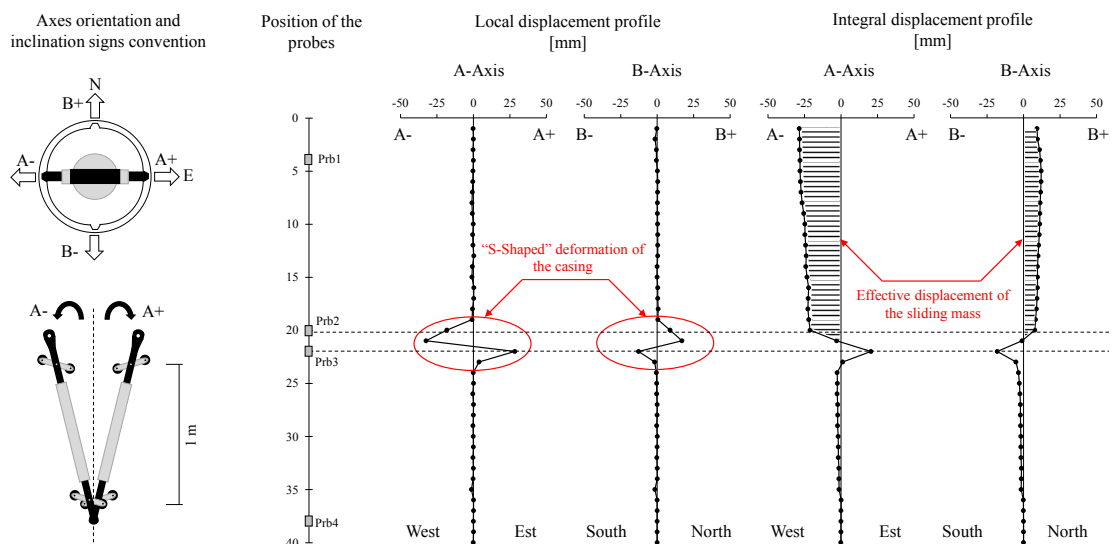
Figure 3-17: Manual reading of the AI11 casing.

After the removal of the probes, it has been possible to prove that the Prb3 was correctly installed in the sense that its measuring axis was oriented in the same direction of the other probes, as illustrated in **Figure 3-17**. The recorded displacement, thus, was

effectively upslope-oriented. Despite this fact, this monitoring evidence was not due to a real ongoing mass movement but to a peculiar deformation of the casing in correspondence of the shear zone. In particular, the manual reading highlighted an "S-shaped" deformation probably caused by vertical compression stresses related to a downward component of the displacement occurring in the upper part of the landslide. This finding is consistent with the evidences reported by JENG et AL. (2017).

Consequently, the effective horizontal displacement of the landslide is the resultant obtained from the difference between the displacement of the Prb2 and the one of the Prb3.

Making this correction, the displacement entity of Prb2 becomes representative and consistent with the ones coming from manual readings, as shown in **Figure 3-18**. The effective displacement rate and the cumulative displacement of Prb2 are reported in detail in **Figure 3-19**.
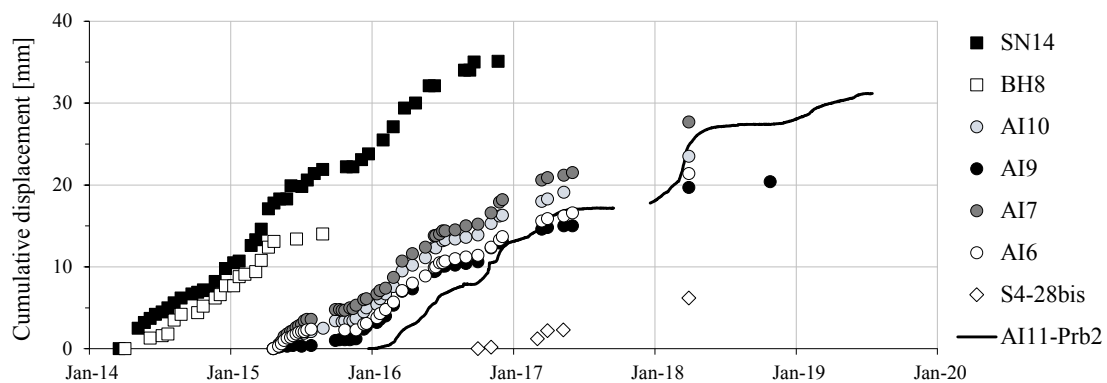
Figure 3-18: Comparison between manual and corrected automatic inclinometer readings in terms of cumulative displacement.
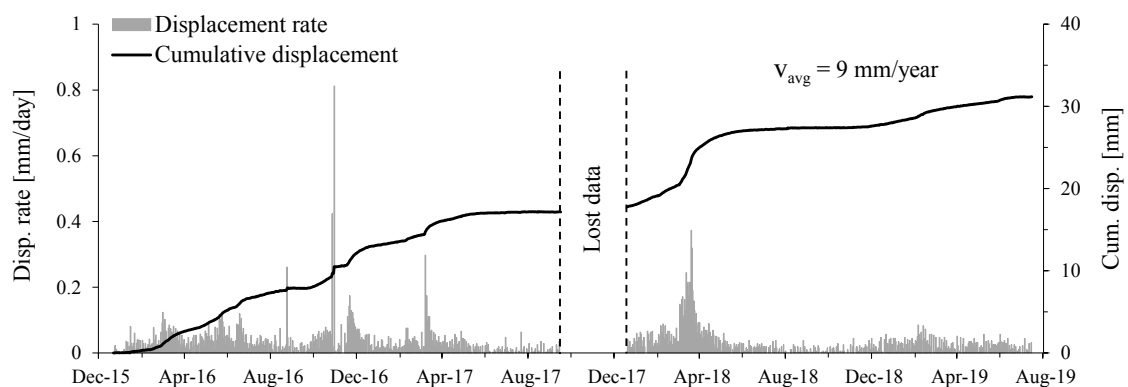
Figure 3-19: Effective displacement rate and cumulative displacement of the AI11 probe located at a depth of 20m.

The high frequency readings allowed identifying the typical intermittent kinematics of active landslides: during a seasonal cycle, in fact, an alternation of activity stages and periods of suspension are clearly recorded.

3.5.3 Groundwater monitoring

Different types of piezometers have been installed along the slope to detect the water level position and its seasonal fluctuations. Monitoring data, covering the period 2011-2016, are reported in **Figure 3-20** and compared with monthly rainfalls recorded by a weather station next to the site.
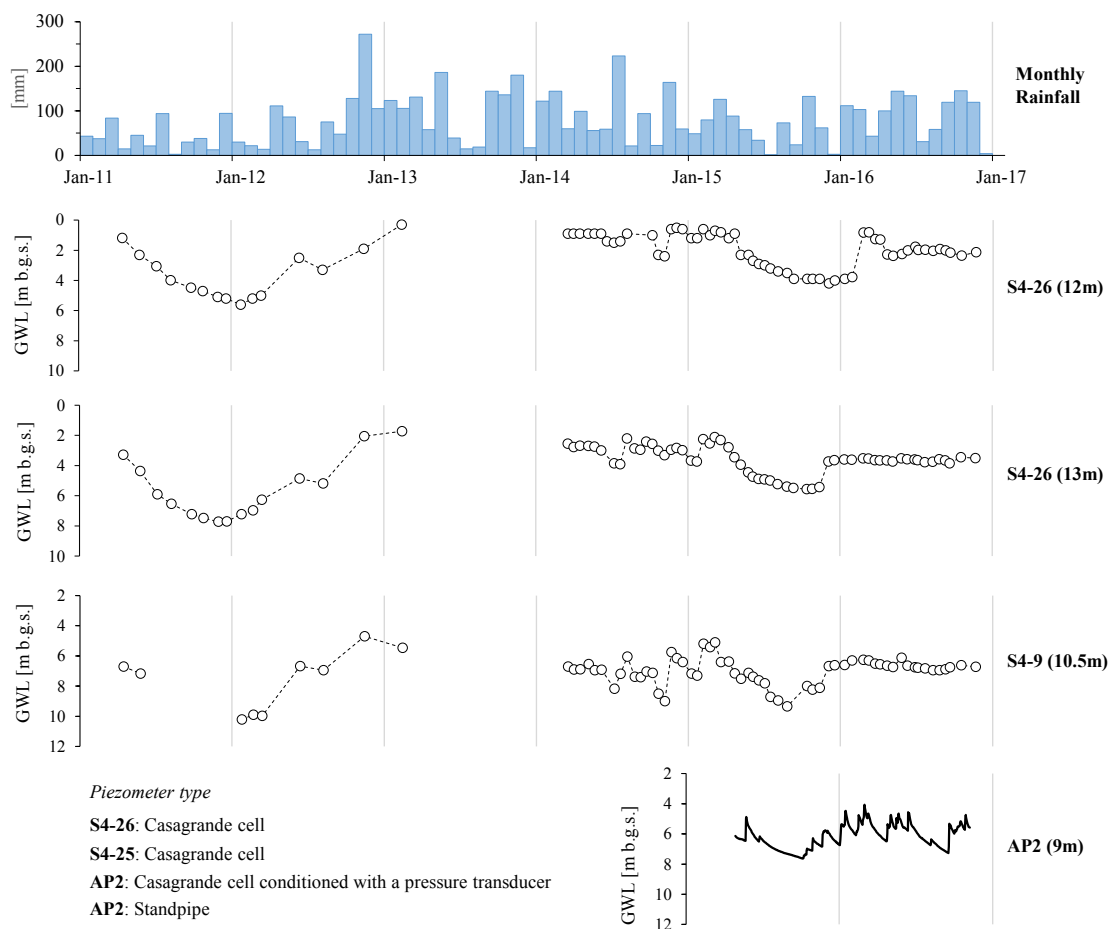
Figure 3-20: Monthly rainfalls and groundwater regime within the slope.

All the verticals highlighted a synchronous fluctuation of the groundwater that is related to the rainfall regime. In fact, higher levels are recorded during autumn and winter while

lower values are measured during dry months (especially between the end of summer and the beginning of autumn). The lowest levels were recorded at the end of 2011 that was characterized by an annual amount of rainfall well below the average of the area.

It is worth noting that the stratigraphy and the morphology of the slope strongly influence the hydraulic regime within the slope. In fact, high piezometric levels next to the ground surface are recorded in the upper part of the slope where the base formation (less permeable than the overlaying deposit) is closer to the surface. A general lowering of the groundwater level, instead, is encountered moving towards the foot of the slope, where the Chiascio River and its alluvial deposits are located.

Although the available groundwater monitoring allowed depicting the hydraulic regime within the slope, this does not seem to be appropriate in relation to the nature of the landslide. In fact, the location of the measuring points is superficial and thus the pore-water pressures entity next to the sliding surface is unknown. Moreover, the frequency reading of the piezometer monitoring is not congruent with the response of the landslide to rainfalls, which seems to be quite fast (as highlighted by automatic inclinometer monitoring). Less than two years of daily automatic acquisitions are available and were recorded by the AP9 piezometer, but, also in this case, the piezometer is located well above the sliding surface.

3.6 Material characterization

The characterization of the materials within the slope was based on the available results coming from laboratory and in situ tests carried out before the construction of the infrastructure. These were conducted almost entirely in the landslide deposit material.

The attention has been focused on those parameters that play a crucial role in the analysis of pre-existing landslides, that are the residual shear resistance and the permeability of the materials involved in the process. Index, physical and compressibility properties are also reported.

The base formation was considered as a rock-like material and some uniaxial compression and point load tests were conducted. The unconfined compressive strength (UCS) was found to be in the range of 1-5 MPa (very weak rock).

It is worth mentioning that the geotechnical characterization of structurally complex formations is not an easy task and many uncertainties are related to the variegated feature of these materials. In this context, the representativeness of each single result has to be always evaluated.

3.6.1   Index, physical and compressibility properties

Most of the landslide body is constituted by a chaotic mixture of materials (landslide deposit-LSD) derived from the parent base formation. This deposit is markedly heterogeneous and any kind of its original structure has been obliterated by the disturbance induced by large displacements. According to the classification proposed by ESU (1977), this material can be identified as a "C-type" structurally complex soil: in fact, more or less weathered rock blocks and fragments are present floating in a soil-like matrix. This latter can be mostly fine-grained as well as mostly coarse-grained, as it can be seen in **Figure 3-21**.
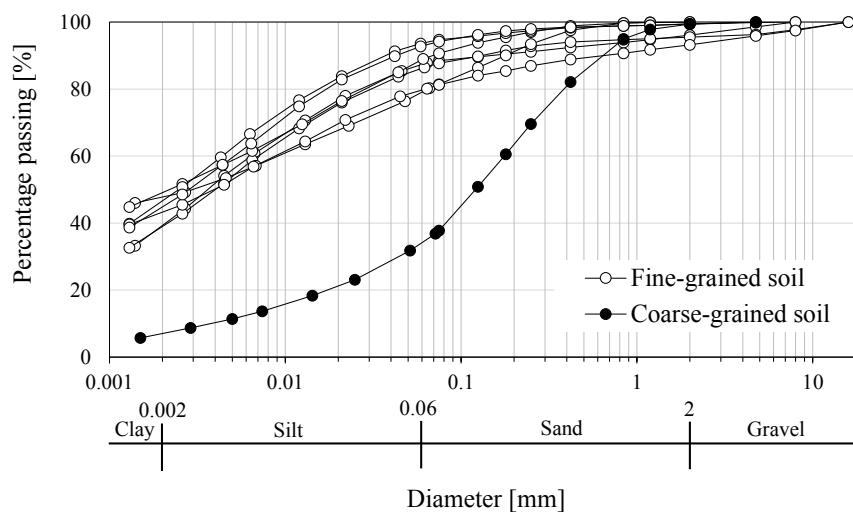
Figure 3-21: Grain size distribution of samples taken from the landslide body.

It is worth noting that, despite only one silty-sand sample is available, layers of coarse-grained soil were frequently observed in the borehole logs. Regarding the finer component of the matrix, this is mainly composed by clay and silt in equal proportion (C+S ranging from 95 to 80%) with a certain sand percentage ranging from 5 to 20%.

In **Table 3-2**, some physical properties of the finer material constituting the landslide deposit are reported.

Natural unit weight γ	19.2 - 20.7	[kN/m³]
Specific gravity G_s	2.5 - 2.6	[kN/m³]
Natural water content w	14.7 - 24.6	[%]
Void ratio e	0.44 - 0.60	[-]
Degree of saturation S	84 - 100	[%]

Table 3-2: Ranges of some physical characteristics of the finer soil matrix.

Atterberg limits were also determined (for both the landslide deposit and the base formation): the liquid limit w_L and the plasticity index I_P vary in the range 34-56 and 11-25, respectively. Plotting these values in the Casagrande plasticity chart (see **Figure 3-22**), the material can be classified as clay and silt of low plasticity (CL-ML). Only two samples resulted to be silt of high plasticity (MH).
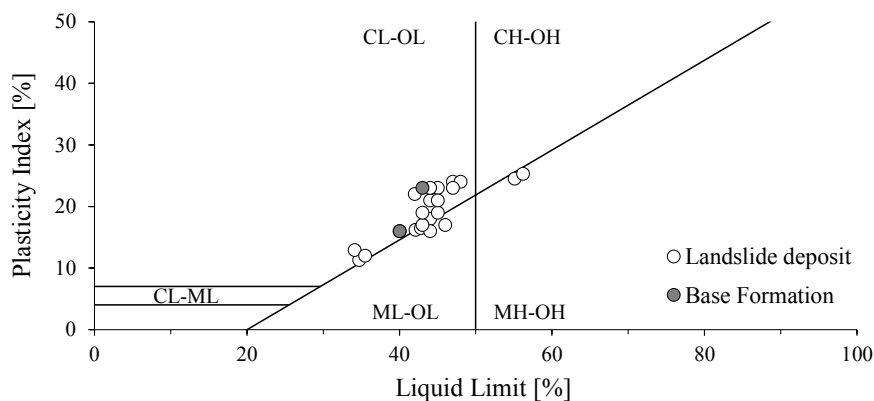
Figure 3-22: Plasticity of samples coming from the landslide deposit and the base formation.

Some oedometer tests were conducted on undisturbed samples coming from the landslide deposit and the resulting compressibility curves are summarized in **Figure 3-23**.
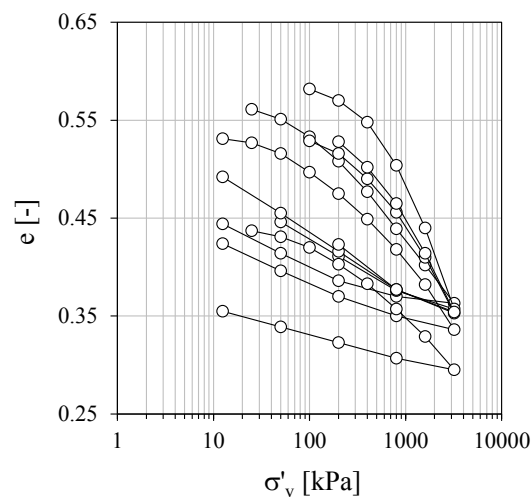
Figure 3-23: Results of oedometer tests conducted on undisturbed samples coming from the landslide deposit.

These tests have been analysed with the aim of evaluating a representative value of the compressibility coefficient m_v, defined as the reciprocal of the oedometeric modulus E_{ed}. As pointed out by some Authors (COTECCHIA et AL. 2014, STARK et AL. 2015, VASSALLO et AL. 2015), this is an important parameter when hydraulic analyses in transient conditions are carried out since it governs the pore-water pressure response in saturated conditions. For the range of vertical stress between 100-200kPa, a representative oedometeric modulus equal to $8x10^3$kPa was estimated to which corresponds a compressibility coefficient equal to $1.25x10^{-4}$kPa^{-1}.

3.6.2   Effective shear strength parameters

Some direct shear tests have been carried out on undisturbed samples taken from the landslide body. Results in terms of effective shear strength parameters are quite dispersive and they reflect the heterogeneous nature of the deposit. In particular, some samples exhibited an effective cohesion ranging from 35 to 50kPa and friction angles between 20° and 28°; some others, instead, showed a ductile behaviour with shear strength envelopes characterized by higher friction angles that are in the 28-34° range. Even considering the highest monitored groundwater level, these parameters do not justify the activity of the landslide that takes place on a gentle slope whose average inclination is equal to 8°. As far as active landslides in fine-grained soils are concerned, the shear strength to consider is the one at residual, developed along the shear band after long-lasting movements.

Two direct shear tests and two ring shear tests have been made on samples coming from the landslide body. The former furnished residual friction angles of 19° and 18°, while lower values equal to 15° and 14° were provided by the latter. This difference can be due to the fact that the repeated direct shear method of testing can overestimate the residual strength relative to ring shear tests. Values obtained from ring shear tests, thus, would be expected to provide the most reasonable estimate of the residual shear strength and consequently have been assumed for stability analyses. Moreover, the representativeness of such values has been tested by stability analyses conducted for the landslide of interest, presented and discussed in the following chapters.

At present more tests seems to be necessary to define properly the failure envelope at residual. These tests should be carried out on samples taken from the slip surface in order to investigate the material that is directly involved in the sliding process whose parameters can differ considerably from the ones of the overlying soil and the underneath formation. Regarding this aspect, ASSEFA et AL. (2015) carried out some tests on a slip surface of a deep-seated landslide affecting the right bank of the Casanuova dam, located less than 2 kilometres far from "La Sorbella" landslide. The material coming from the shear zone, consisting of a 0.15-0.20m thick band of clay gouge entrapping rock fragments, possesses high plasticity (PI= 32.4%) and its grain size composition is dominated by a high silt-clay proportion (S+C= 91%). Direct shear tests highlighted a very low value of the residual friction angle, equal to 7.9°.

Despite this evidence, this value does not seem representative for the "La Sorbella" landside. Stability analyses carried out considering such value along the slip surface, in fact, furnished a factor of safety well below the unit even considering the lowest monitored groundwater level.

3.6.3   In situ hydraulic conductivity

Inside a borehole located within the unstable mass, three Lefranc falling-head tests (LFT) were conducted in order to evaluate the hydraulic conductivity of the landslide deposit. As far as heterogeneous deposits are concerned, in-situ tests give more reliable estimations than laboratory ones since the former investigate a larger volume and thus are able to take into account the presence of meso and macro structures at site scale.

In **Figure 3-24** a scheme of the Lefranc method, the stratigraphy of the borehole and the location of the tested sections are reported.
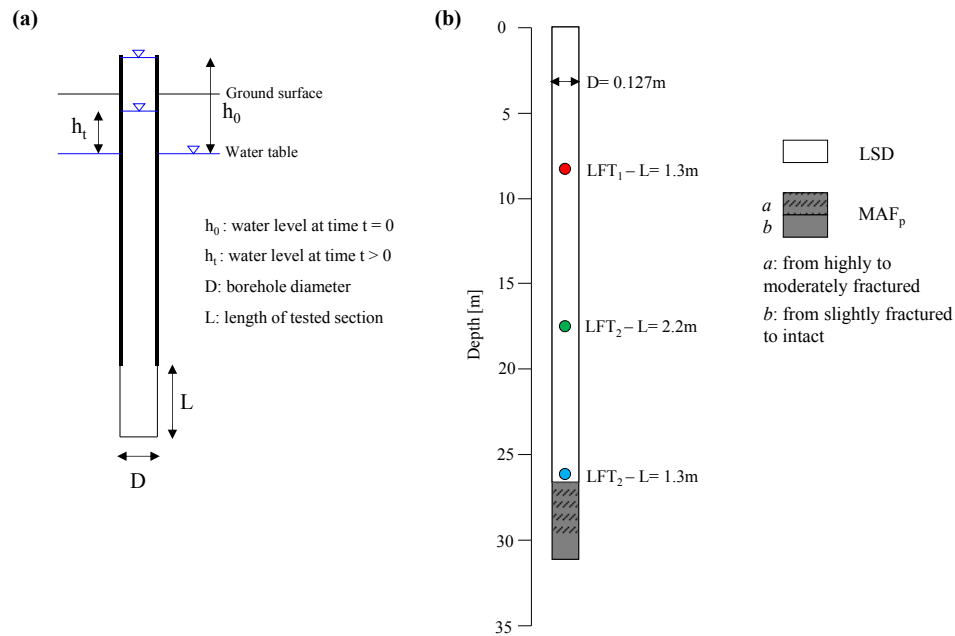
Figure 3-24: (a) Scheme of falling-head test and (b) location of the tested sections along the borehole.
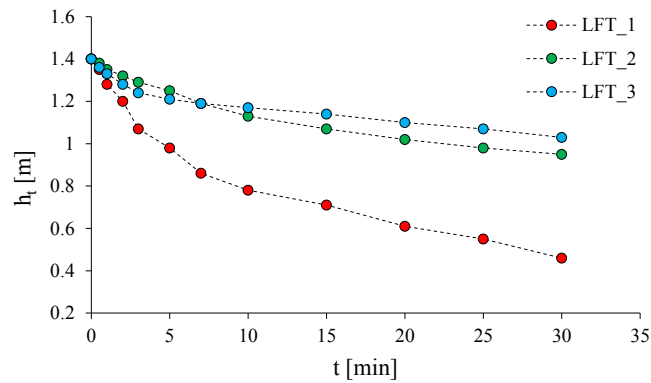
Figure 3-25: Heights of water measured inside the borehole.

Following the recommendations of the Italian Geotechnical Association (AGI 1977), the permeability coefficient can be estimated through the following formula:

$$k = \frac{A}{C_L(t_2 - t_1)} \ln\left(\frac{h_1}{h_2}\right) \tag{3-1}$$

where

k [m/s] = permeability coefficient

A [m^2] = area of the borehole cross-section

h_1, h_2 [m] = heights of water inside the borehole measured with respect to the in situ water table

t_1, t_2 [s] = times at which h_1 and h_2 are measured

C_L [m] = shape factor depending on D and L.

In this case, *h_1* and *h_2* were assumed as the initial and final heights of water that delimit the linear trend of the curves reported in **Figure 3-25**. When *L>>D*, the shape factor *C_L* can be assumed equal to the length of the tested section. Under these assumptions, values equal to $4.4X10^{-6}$, $9.4X120^{-7}$ and $1.1X10^{-6}$ m/s were obtained for the LFT$_1$, LFT$_2$ and LFT$_3$ respectively. Thus, a representative hydraulic conductivity in the range of $1-5x10^{-6}$ m/s can be assumed for the landslide deposit.

Regarding the base formation, no direct measurements of permeability are available. GRANA & TOMMASI (2014) reported some results about in-situ permeability tests conducted in two marly units of the Umbria-Marche sequence, which are the *Schlier* formation (alternating layers of marly limestones and clayey marls) and the *Bisciaro* formation (alternating layers of grey limestones and marls with thick clayey interbeds). Values equal to $1x10^{-7}$m/s and $5x10^{-7}$m/s were found, respectively.

ASSEFA et AL. (2017) carried out some Lugeon tests in the same base formation of "La Sorbella" landslide and they found hydraulic permeability values ranging from $1x10^{-7}$ to $3x10^{-7}$m/s. Similar values (in the $1-4x10^{-7}$m/s range) were found by OBERTI et AL. (1986) based on several Lugeon tests carried out in a marl-sandstone formation for the construction of the Ridracoli dam (Emilia Romagna region).

3.7 Mobility of the landslide and its causes from monitoring evidences

Thanks to the high-frequency readings (on a daily basis) acquired by the AI11 inclinometer, it has been possible to obtain a detailed description of the mobility of "La Sorbella" landslide and to understand the main causes that govern its mechanics.

As mentioned above, the typical intermittent behaviour of active landslides is clearly detectable by the occurrence of displacement rate peaks, indicating a pronounced mobility of the sliding mass during certain periods. A careful analysis of such events allowed

individuating two main different types of peak (named "R-type" and "S-type" respectively) that take place in a different way, as it can be observed in **Figure 3-26**.
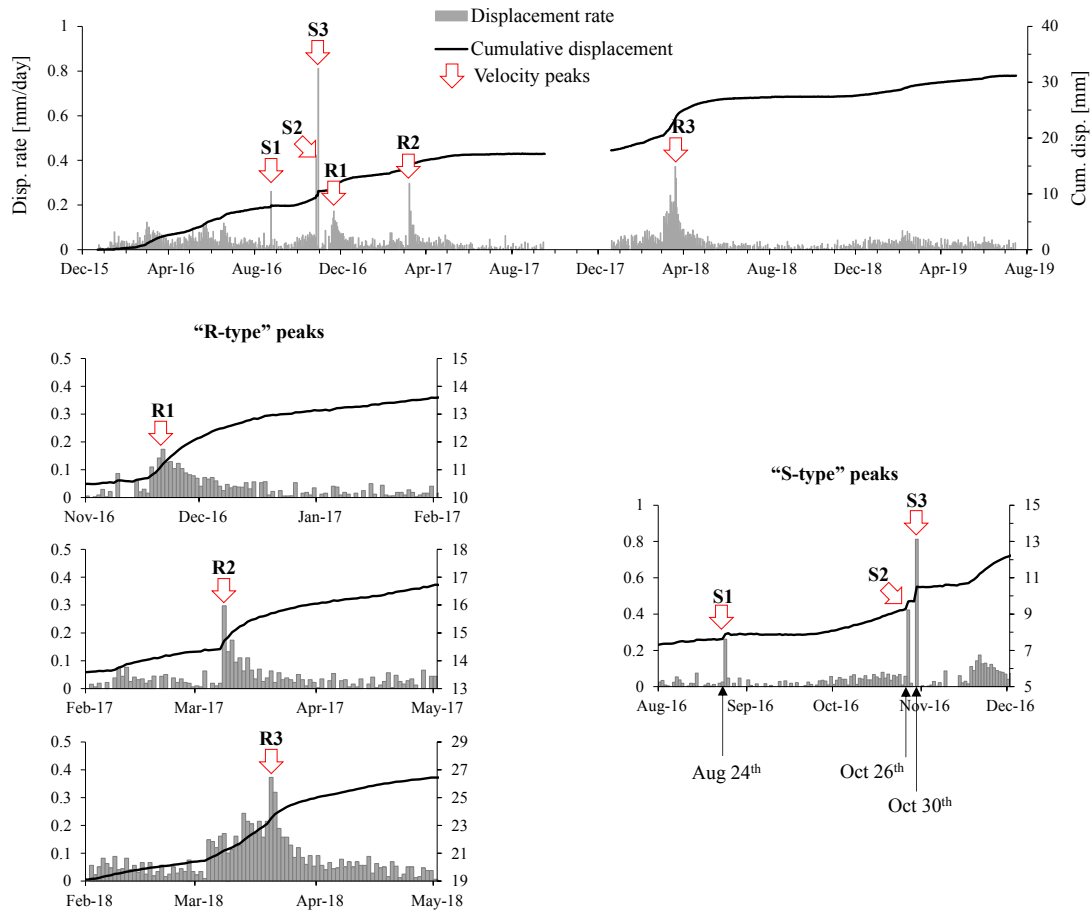
Figure 3-26: Main active stages of the landslide highlighted by increase of the displacement rate of different nature.

The main interesting aspect of such evidence is that the different nature of these accelerations is related to the different nature of the causes that produced them.

Focusing on the "R-type" peaks, these are characterized by an increase of the displacement rate that, after reaching a maximum value, progressively slows down and are representative of the landslide response to rainfalls. This is a well-known behaviour regarding landslides in clayey deposits that undergo seasonal re-activations because of groundwater level fluctuations connected to the rainfall regime. It is worth noting that the trend of the displacement rate and the associate cumulative displacement clearly reflect the mechanical effect produced by rainfall-water infiltration. After rainfall events of a certain intensity, the rising of the pore-water pressures along the shear surface takes place

with a consequent reduction of the shear strength: this leads to an increase of the displacement rate. Later, the progressive lowering of the water level is accompanied by a regain of the shear resistance and thus the landslide gradually decelerates. This behaviour is described by a "non-linear" trend of both the displacement rate and the cumulative displacement, as pointed out by GRIMALDI (2008) and CASCINI et AL. (2014).

The "S-type" peaks of the displacement rate, instead, depict a different behaviour of the landslide. These latter, in fact, take place in a very rapid way without any effects in the following days and are representative of a stick-slip motion caused by earthquakes.

Their repeated occurrence exactly on the dates of the three mainshocks of the 2016 central Italy seismic sequence is a first confirmation of their representativeness. A detailed analysis of these data will be developed in the 5 CHAPTER but it is appropriate to stress that, at present, no data like these are reported in the scientific literature and therefore cannot be compared with similar evidences. This aspect underlines the importance of these monitoring evidences that represent a very rare instrumental measurement of seismic-induced effects of an active landslide.

3.7.1   Comparison between rainfalls and automatic inclinometer data

With the aim of investigating the dependency of the landslide kinematics on the rainfall regime, a comparison between daily rainfalls and AI11 displacement time series has been made, as reported in **Figure 3-27**. Unfortunately, the hydraulic response could not be directly evaluated since the location and depth of the installed piezometers were not adequate to evaluate the pore-water pressure changes next to the sliding zone. Despite this fact, some interesting considerations regarding the stability of the landslide as a function of rainfall regime can be made.
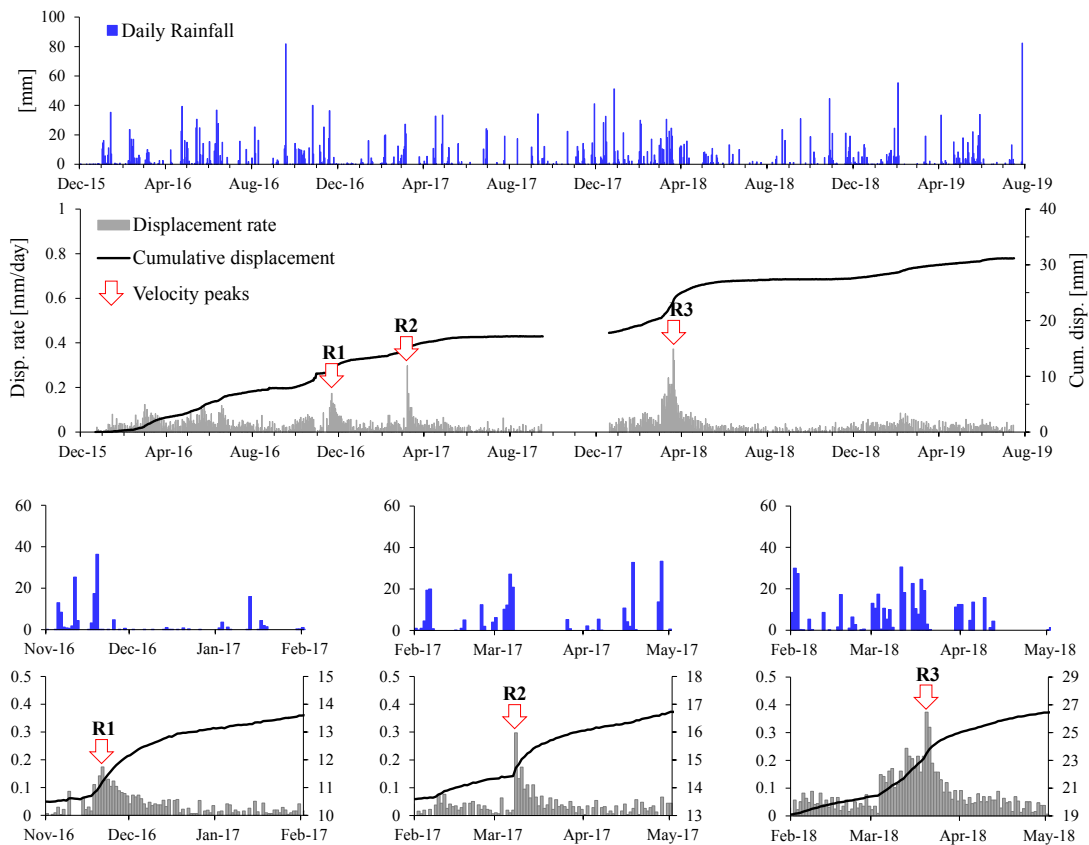
Figure 3-27: Comparison between daily rainfalls and displacement time series recorded by the AI11 fixed-in-place inclinometer probe.

Analysing the three most evident peaks of the displacement rate (see **Figure 3-27**), it was recognised that these took place just one or two days after the end of the rainfall event considered. A similar evidence was observed by LOLLINO et AL. (2006) regarding a deep-seated landslide located in North-Western Italy that involves a debris deposits overlaying a marly-calcareous substratum ("Antola" formation). In that case, a time lag of 9 days was identified.

Such very small time lag is not usual where it comes to deep-seated landslides that generally are not sensitive to a single rainfall event but rather to a certain amount of precipitation cumulated over some months (TOMMASI et AL. 1997, TAGARELLI & COTECCHIA 2018). This is essentially related to the considerable depth of the sliding surface and the low permeability of the materials involved.

This peculiar behaviour of "La Sorbella" landslide can be justified by the quite high permeability of the landslide deposit that accelerates the infiltration process and, in turn, the rising of the pore pressures along the slip surface.

61

With the aim of finding a reference amount of rainfall able to produce significant accelerations, the three main velocity peaks have been considered and cumulative rainfalls over certain periods before their occurrence have been evaluated, as reported in **Table 3-3**.

Event	Displacement rate		Rainfall			
	Date	v_p [mm/day]	Date[*]	Cum_10[**] [mm]	Cum_20[**] [mm]	Cum_30[**] [mm]
R1	21/11/2016	0.2	19/11/2016	87	113	161
R2	08/03/2017	0.3	07/03/2016	81	101	122
R3	20/03/2018	0.4	19/03/2018	133	202	231

[*]End date of the rainfall event considered

[**]Cumulative rainfall over the 10, 20 and 30 days before the occurence of the velocity peak

Table 3-3: Main rainfall-induced peaks and cumulative rainfalls registered before their occurrence.

It was not possible to define such reference amount since it has been observed that similar rainfalls occurred during other periods, particularly in dry periods (e.g. summer), do not produce appreciable displacements such as those reported in **Table 3-3**. It should be noted that these latter occurred in November and March that are the rainiest periods of the year and therefore a certain seasonality of the landslide mobility can be recognized. As pointed out by PICARELLI et AL. (2004), in Italy, pore pressures reach their maximum between the end of winter and the beginning of spring. During this period, the groundwater reacts to rainfall with a pore pressure that develops within a short time. The lower pore pressures, instead, are attained during the fall, after a long period of slow decline. During the dry season, rainfall does not have a significant effect on the pore pressure regime because of prevailing evapotranspiration.

In this context, some aspects such as the evapotranspiration rate, antecedent rainfalls over longer periods and rainfall patterns can play an important role. A procedure (e.g. numerical modelling) able to take into account all the aspects just mentioned above, seems to be the more appropriate tool to deepen the mechanism governing the stability of the slope.

As far as the entity of the velocity peaks are concerned, these are of small entity and the highest value, recorded in March 2018 after a period of particularly intense rainfalls, is not able to compromise the safety of the infrastructure. Therefore, it is possible to conclude that climate effects should not be expected to produce harmful consequences in

the short period, although serviceability problems to the existing manufacts can be encountered because of cumulative displacements over some years.

4 CHAPTER – Numerical modelling of climate effects on slope stability

4.1 Slope-Atmosphere interaction in landslide process

As far as landslide risk assessment is concerned, the main issue is understanding the interaction processes between the most relevant internal and external slopes factors that contribute to the slope stability (COTECCHIA et AL. 2018).

With regard to active landslides, it is well demonstrated that the changes in the displacement rate are strictly connected to the pore-water pressure changes within the slope as a consequence of climate variables (ALONSO et AL. 2003, CALVELLO et AL. 2008, TOMMASI et AL. 2013, VASSALLO et AL. 2015 among many others).

The atmospheric conditions (primarily rainfall) vary with time and, as such, determine a variable boundary condition that causes variations of the pore-water pressure distribution across the whole slope, and, in turn, variations of the available soil strength and slope stability. Seasonal excursions of the piezometric heads of 2–3m have been measured from 30m down to 50m depth in clayey slopes (COTECCHIA et AL. 2014) and shown to be due to the seasonal climatic processes taking place in the very shallow layer of the soil.

Understanding and consequently reproduce this "slope-atmosphere" interaction is not an easy task since several aspects and complex physical processes contribute to its definition. At the ground surface, rainfall R is the main climatic variable to take into account but also temperature, solar radiation, relative humidity and wind speed play an important role. These latter, in combination with the vegetation, contribute in defining the evapotranspiration ET, which represent the loss of water from the soil surface by evaporation and from the crop by transpiration.

Considering the partially saturation is another important aspect to describe properly the state and behaviour of the most surficial soil that, in turn, influence both the ET rate and the runoff RO. This can occur when the soil is saturated to full capacity and rain arrives more quickly than soil can absorb it. The difference R-ET-RO represents the infiltration water flux at ground surface. Therefore, taking into account these processes is important to estimate properly the infiltration development over time.

Evidently, the definition of the internal slope factors such as the stratigraphy of the slope, the presence of discontinuities (e.g. faults and/or shear bands) and the hydro-mechanical

properties of the materials involved is necessary. To achieve this goal, field evidences, in situ and laboratory tests in combination with appropriate monitoring devices are fundamental. It is worth mentioning that, regarding landslide processes, monitoring plays a crucial role since it depicts how the system responds to external factors. Based on monitoring evidences, therefore, it is possible to make a phenomenological interpretation of the ongoing mechanisms in terms of cause-effect.

In this context, the so-called "physically based" numerical approach is the most suitable tool to interpret and/or forecast the landslide mechanism. By means of numerical modelling, in fact, it is possible to reproduce the representative slope geometry and stratigraphy, the hydraulic and mechanical behaviour of the soils and to take into account the physical process relating the pore-water pressure fluctuations to the rainfall regime and their mechanical effects on the slope stability. In this context, the slope can be schematized as a boundary value problem, as shown in **Figure 4-1**.
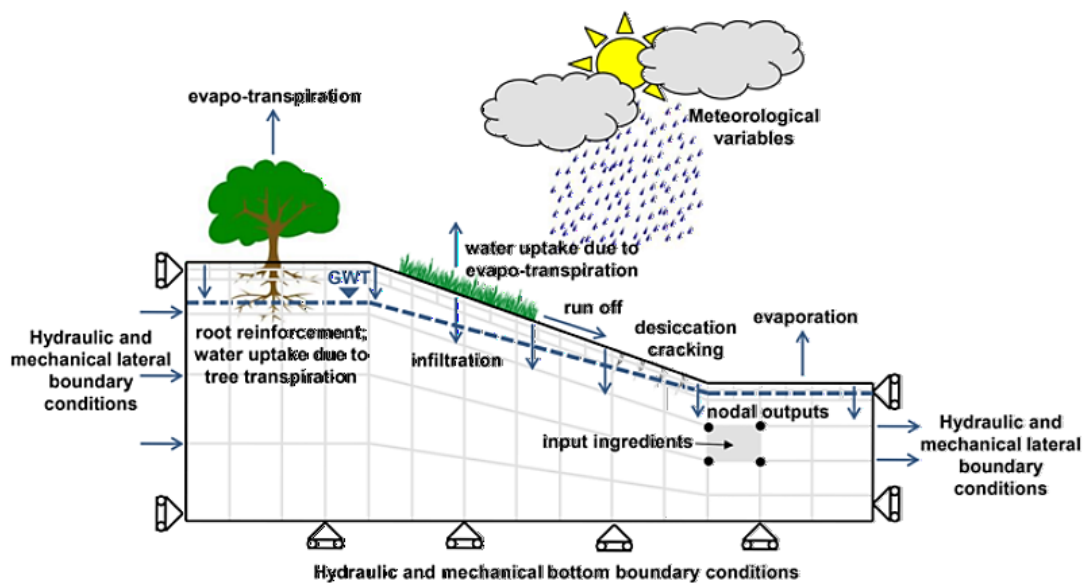
Figure 4-1: Schematic slope model and potential slope-vegetation-atmosphere interaction phenomena (from ELIA et AL. 2017).

Several numerical strategies to model the effects of the slope-atmosphere interaction on the thermal, hydraulic and mechanical state of the slope are discussed in detail by ELIA et AL. (2017). Each strategy is of different level of complexity. This is primary linked to the possibility for each nodal variable and for the corresponding balance equation to account or not for the coupling phenomena. A fully-coupled model, which is the most

complex modelling approach, is the one that accounts for all the hydraulic, thermal and mechanical processes within the soil and for their mutual coupling.

A more easily applicable procedure for modelling the slope-atmosphere interaction is represented by a de-coupled approach. According to this, the hydraulic behaviour can be studied and modelled independently from its mechanical effects on slope stability.

In this case it is possible to simulate the transient seepage in the slope evolving with the atmospheric conditions by accounting solely for the fluid mass-balance equations and disregarding the effects of the variations in temperature within the soil and the deformation of the soil skeleton. Mechanical effects induced by pore-water pressure changes is then evaluated by conducting a limit equilibrium stability analysis.

Despite some limitations of this approach, it is an easy to handle method that is able to take into account the most relevant processes that govern the stability of the slope.

4.2 Methodology adopted

For the case of interest, a de-coupled numerical model has been developed to deepen the salient aspects highlighted by monitoring evidences.

To this aim, hydraulic transient analyses have been carried out by means of finite element method to reproduce the monitored groundwater level fluctuations within the slope as a consequence of rainfall infiltration. In particular, nine years of recorded rainfalls (2010-2018) have been simulated on a daily basis. Following the physically based approach, the evapotranspiration rate, the runoff and the unsaturated behaviour of the soil have been taken into account. Material properties have been assumed according to in situ and laboratory tests results.

The mechanical effects related to the different seepage conditions on the slope stability has been evaluated by limit equilibrium analyses. Even though this method is not able to quantify the displacements exhibited by the landslide, the value and the trend of the safety factor over time can furnish quantitative information regarding the level of stability of the considered landslide.

4.3 Transient hydraulic simulation by means of FEM numerical analysis

The infiltration process within the slope was modelled with the two-dimensional finite element code SEEP/W, a sub-program of GeoStudio software by GEO-SLOPE International Ltd., which is able to simulate seepage processes through both saturated and unsaturated porous media under steady and transient conditions.

The general governing differential equation for 2D seepage under transient conditions can be expressed as:

$$\frac{\partial}{\partial x}\left(k_x \frac{\partial H}{\partial x}\right) + \frac{\partial}{\partial y}\left(k_x \frac{\partial H}{\partial x}\right) + Q = \frac{\partial \theta}{\partial t} \qquad (4\text{-}1)$$

where $H=y+u_w/\gamma_w$ is the total head; k_x and k_y are the hydraulic conductivity in the x and y direction respectively; Q is the applied boundary flux; θ is the volumetric water content; t is the time. Fundamentally, this equation states that the difference between the flow entering and leaving an elemental volume at a point in time is equal to the change in storage of the soil system. Changes in volumetric water content are dependent on changes in the stress state and the properties of the soil. The stress state for both saturated and unsaturated conditions can be described by two state variables (FREDLUND & MORGENSTERN 1976, 1977): *(σ-u_a)* and *(u_a –u_w)*, where σ is the total stress, u_a is the pore-air pressure and u_w is the pore-water pressure.

SEEP/W is formulated for conditions of constant total stress, that is there is no loading or unloading of the soil mass. It also assumes that the pore-air pressure remains constant at the atmospheric pressure during transient processes. This means that *(σ-u_a)* remains constant and has no effect on the change in volumetric water content. Changes in volumetric water content are consequently dependent only on changes in the *(u_a –u_w)* stress state variable, and with u_a remaining constant, the change in volumetric water content is a function only of pore-water pressure changes. As a result, the change in volumetric water content can be related to a change in pore-water pressure by the following equation:

$$\partial \theta = m_w \, \partial u_w \qquad (4\text{-}2)$$

where m_w is slope of the volumetric water content function. If unsaturated behaviour is considered, this function is non-linear when the pore-water pressure is negative. This latter represents the matric suction of the soil, $s=(u_a - u_w)$. In the positive pore-water pressure region, m_w becomes equivalent to m_v, the coefficient of volume compressibility for one-dimensional consolidation.

If the soil is considered only saturated, a linear relationship (with a slope equal to m_v) between the volumetric water content and the pore-water pressure is adopted, in both the positive and negative pore-water pressure regions.

After making some substitutions, the following equation can be written:

$$\frac{\partial}{\partial x}\left(k_x \frac{\partial H}{\partial x}\right) + \frac{\partial}{\partial y}\left(k_x \frac{\partial H}{\partial x}\right) + Q = m_w \gamma_w \frac{\partial H}{\partial t} \qquad (4\text{-}3)$$

This is the most general form of the governing differential equation used in SEEP/W finite element formulation, whose primary unknown is the total head H at each node. Once defined the appropriate boundary conditions (in terms of H at some nodes and/or Q at some other nodes) and the soil properties, the program is able to solve equation (4-3). An incremental time sequence is required for all transient analyses and the appropriate time sequence is problem-dependent and the accuracy of the computed results depends to some extent on the size of the time step.

For the considered case, evaluating the pore-water pressure changes as a consequence of daily rainfalls is the main objective and therefore a calculation time step equal to 1day was considered for all the analyses ($\Delta t_{calculation}=1$day).

After specifying the material model (saturated only or saturated/unsaturated), the program requires the definition of some basic properties that are the saturated hydraulic conductivity (which can be set different along the x and y direction), the volumetric water content at saturation θ_s and m_v. If saturated-unsaturated model is considered, the soil-water characteristic curve SWCC (relation between the volumetric water content and the negative pore-water pressure) and the permeability function (expressing the reduction of the hydraulic conductivity with the increasing of suction) must be also specified.

Boundary conditions, material properties and rainfall time series adopted in the analyses are discussed in the following paragraphs.

4.3.1 Problem geometry, mesh definition and boundary conditions

A 2D representative section of the slope, reported in **Figure 4-2**, was reproduced and discretized with a combination of 4-noded quadrangular and 3-noded triangular elements. As pointed out by TSAPARAS et AL. (2002), when conducting a transient seepage analysis, numerical instabilities can be encountered in the areas located near the ground surface where the pore-water pressures change rapidly during infiltration. This is accentuated when unsaturated behaviour is considered. To overcome such problems a fine mesh is required but cannot be adopted for the whole domain because of the long computation time required for the solution.

Taking into account such aspect, the dimension of the elements was properly set in order to obtain a very fine mesh (1x0.25m quadrangular elements from the surface to a depth of 1m) in the upper part of the slope that progressively becomes coarser moving towards the bottom of the model. Moreover, the mesh was refined along the verticals where the piezometers (S4-26, S4-25, AP2 and S4-9) are located. Adopting this discretization, it has been possible to obtain satisfactory and stable solutions within reasonable time.
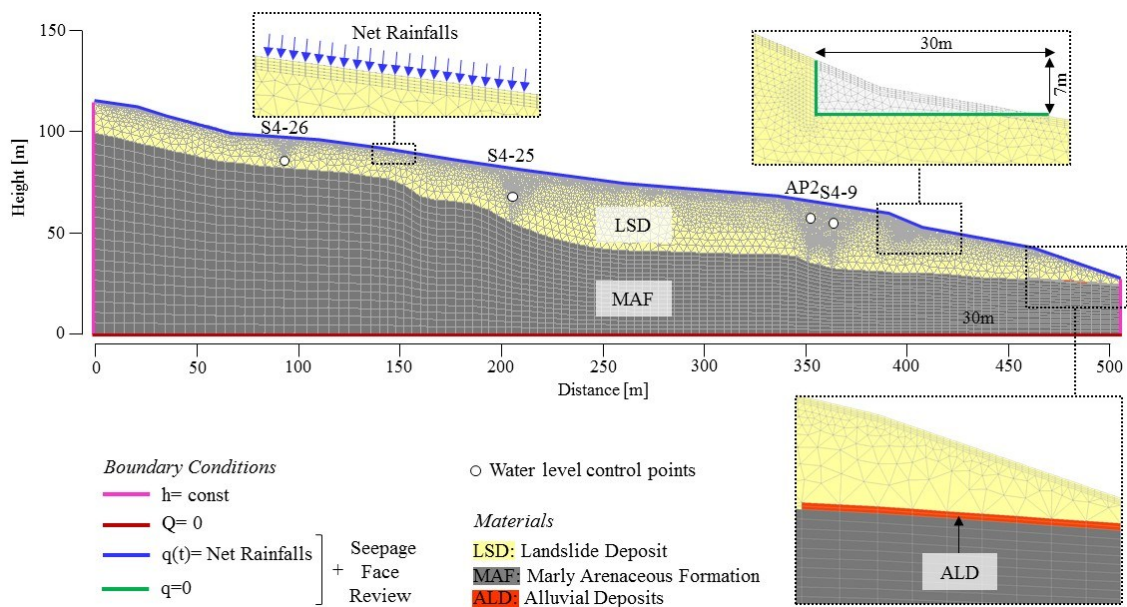
Figure 4-2: 2D FEM model of the slope: mesh and boundary conditions employed in the hydraulic analysis.

The section includes the different materials found in the slope, which are the landslide deposit (LSD), the marly arenaceous base formation (MAF) and the alluvial deposits

(ALD) respectively. For each material, the adopted parameters are discussed in the following paragraph.

Regarding the boundary conditions, the base of the model was considered as impervious and a constant null flux ($Q=0$) was applied at the bottom nodes. At the lateral vertical boundaries, a constant head condition was assigned. In particular, at the right-hand-side a hydraulic head equal to the ground level was assigned owing to the presence of the Chiascio River at that location. At the left-hand-side, instead, a hydraulic head corresponding to 10m below the ground surface was assigned. This has been found to be the condition that best reproduced the groundwater level monitored by the leftmost piezometer (S4-26).

Nine years of net rainfalls (from 2010 to 2018) have been simulated as a unit flow rate "step function" with a daily time resolution ($q(t)=$ Net Rainfalls, $\Delta t_{Rainfalls}=1$day) that was applied at the top surface. The evaluation of the net rainfalls time series is discussed in the following of this chapter. Moreover, the option "seepage face review" was activated in order to avoid the water ponding above the surface and, in turn, to take into account the runoff phenomenon. Basically, at the end of each iteration, the condition along the specified potential seepage face is "reviewed" to check if the condition $u_w<0$ is met. Nodes with computed pressures greater than zero are not allowed, as positive pressure on the surface indicates ponding, which cannot happen along the sloping boundary (the water would run off, not pond!). The specified externally applied influx q_{in} is therefore updated to obtain $u_w=0$. The difference between q_{in} and the water that infiltrates under $u_w=0$ represents the runoff.

Finally, during the 2016-2018 simulation period, the slope geometry has been modified (see **Figure 4-2**) in order to take into account the excavation made for the realization of the infrastructure. To do so, a region approximately corresponding to the excavated soil volume has been removed and a constant unit flow rate equal to zero ($q=0$) was applied to the vertical side with the option seepage face review. This condition has been introduced to simulate the draining effect of the drains located behind the retaining structure. The same condition was also applied along the horizontal side.

4.3.2 Material properties

For all the materials an isotropic hydraulic behaviour has been assumed ($k_x = k_y$). The base formation (MAF) and alluvial deposits (ALD) were considered always saturated. Regarding these materials, no direct measurements of the basic properties (k, θ_s and m_v) were available and therefore typical values for similar soils have been properly assumed. In particular, $k=1x10^{-7}$m/s, $\theta_s=0.2$ and $m_v=2x10^{-5}$kPa^{-1} were assumed for the base formation while $k=1x10^{-4}$m/s, $\theta_s=0.35$ and $m_v=5x10^{-5}$kPa^{-1} were adopted for the alluvial deposits.

Regarding the landslide deposit (LSD), a saturated hydraulic conductivity in the $1-5x10^{-6}$ m/s range was considered according to the results of in situ permeability tests. Results coming from laboratory tests allowed identifying representative values for the saturated volumetric content and the m_v coefficient equal to 0.4 and $1.25x10^{-4}$kPa^{-1}, respectively.

Since for the LSD a saturated-unsaturated model was considered, the SWCC and the permeability function are also required. For the SWCC, the relation proposed by VAN GENUCHTEN (1980) has been adopted and it is defined by the following equation:

$$S_e = \frac{\theta - \theta_r}{\theta_s - \theta_r} = \frac{1}{\left[1+\left(\frac{s}{a}\right)^n\right]^m} \tag{4-4}$$

where
S_e [-] = effective degree of saturation

θ [-] = generic volumetric water content

θ_s [-] = volumetric water content at saturation

θ_r [-] = residual volumetric water content

s [kPa] = soil matric suction

a [kPa], n, m [-]= model parameters (with *m=1-1/n*)

The VG's model parameters depend on the soil type considered and should be calibrated to best-fit experimental data. Unfortunately, specific tests were not carried out and therefore values for similar soils were adopted from literature data. Specifically, reference was made to the data reported by VALENTINO et AL. (2014) and PERANIC et AL. (2018), who carried out several and good quality tests on clayey silt soils of low plasticity.

For more detailed information please refer to the specific publications. Regarding the *n* and *m* parameters, values equal to 1.30 and 0.23 were adopted, while θ_s (representing the water content at high suction values) was set equal to 0.01. Regarding the *a* parameter, instead, values in the 100-200kPa range were found by the Authors. This parameter is correlated to the air entry value AEV (representing the value at which the pores start draining) and, in turn, to the maximum pore-size and pore-size distribution. Since its importance in modelling infiltration processes, as pointed out by TOMMASI et AL. (2013), some sensitivity analyses have been carried out by varying the *a* value in the range reported above. No appreciable differences have been found and therefore a representative value equal to 150kPa was assumed.

From the knowledge of the soil-water retention curve and the saturated hydraulic conductivity (k_s), VAN GENUCHTEN (1980) derived, based on MUALEM (1976) theory, a function to describe the relation between hydraulic conductivity and suction, described by the following:

$$k = k_s \, S_e^{0.5} \left[1 - \left(1 - S_e^{1/m} \right)^m \right]^2 \tag{4-5}$$

Equation (4-4) and (4-5) were adopted for describing the unsaturated behaviour of the LSD and a graphical representation of them is reported in **Figure 4-3**.
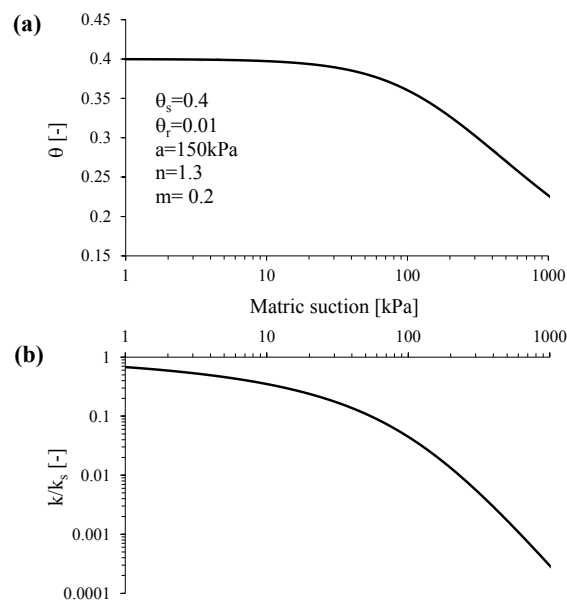
Figure 4-3: (a) SWCC and (b) hydraulic conductivity function (normalized with respect to the saturated hydraulic conductivity) assigned to the LSD material.

4.3.3 Net rainfalls as time-dependent boundary condition

With the aim of taking into account the climate effects, the "reference" evapotranspiration ET_0 (also known as "potential" evapotranspiration) has been considered. This quantity represents the rate, generally expressed in millimetres per unit time, of water lost from a surface fully covered by a grass reference crop with specific characteristics and not short of water (ALLEN et AL. 1998). Under these conditions, ET_0 is a climatic parameter that expresses the evaporating power of the atmosphere at a specific location and time of the year and does not consider the crop characteristics and management practices.
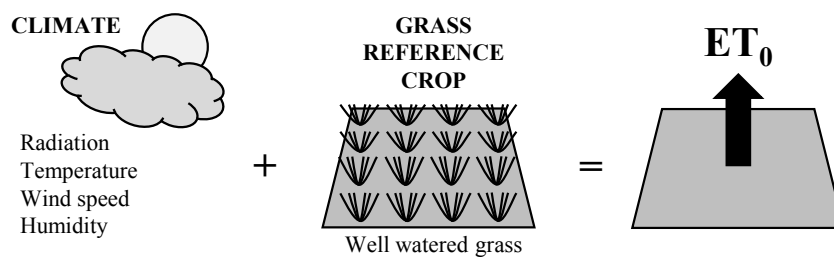
Figure 4-4: Conceptual scheme of the reference evapotranspiration (ET_0).

Although several analytical methods have been developed for evaluating ET_0, the universally recognized method is the one proposed by the United Nation Food and Agriculture Organisation (FAO) based on the Penman-Monteith equation (ALLEN et AL. 1998). This physically based approach has been demonstrated to give the most reliable estimation of the reference evapotranspiration under different climatic conditions and nowadays it is a recommended standard procedure. A major drawback associated with the application of such equation is the relatively high data demand, since the method requires air temperature, wind speed, relative humidity and solar radiation measurements. The number of meteorological stations where all these parameters are observed is limited and the reliability of some data can be affected by a high level of uncertainty.

When solar radiation, relative humidity and wind speed data are missing, the FAO guidelines suggest an alternative equation for ET_0 estimation that is the one proposed by HARHREAVES & SAMANI (1985). This method has been tested using some high quality lysimeter data representing a broad range in climatological conditions and the results have indicated that this equation was nearly as accurate as the Penman-Monteith equation (DROOGERS & ALLEN 2002, HARGREAVES & ALLEN 2003).

The so-called Hargreaves and Samani formula is described by the following equation:

$$ET_0 = 0.0023\ R_a\ (T_m+17.8)\ \Delta T^{0.5} \qquad (4\text{-}6)$$

where

R_a [mm/day] = extraterrestrial solar radiation (in equivalent evaporated water depth)

$T_m = (T_{max} + T_{min})/2$

$\Delta T = T_{max} - T_{min}$

T_{max} [°C] = maximum daily temperature

T_{max} [°C] = minimum daily temperature

This equation, adopted in this work for estimating the reference evapotranspiration on a daily basis, requires only direct measurements of maximum and minimum temperature, while the extraterrestrial solar radiation can be easily computed as a function of the site location and the day of the year (see **Figure 4-5**).
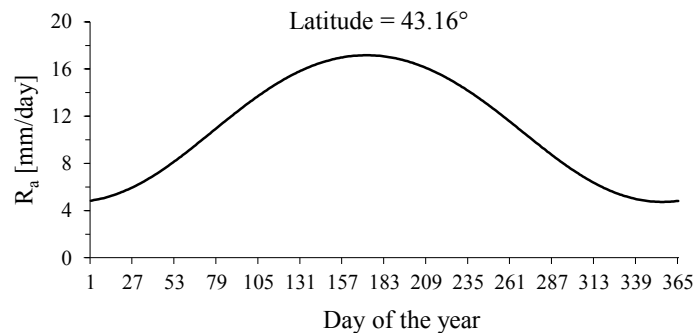
Figure 4-5: Daily extraterrestrial solar radiation for the site of interest.

The obtained *ET₀* has been consequently subtracted to the total rainfall (*R_TOT*) in order to obtain the net rainfalls (*R_NET*) that constitute the time-dependent top boundary condition of the hydraulic model. This latter is reported in **Figure 4-6** with computed reference evapotranspiration, maximum-minimum daily temperatures and total rainfalls (recorded in a meteorological station next to the site).
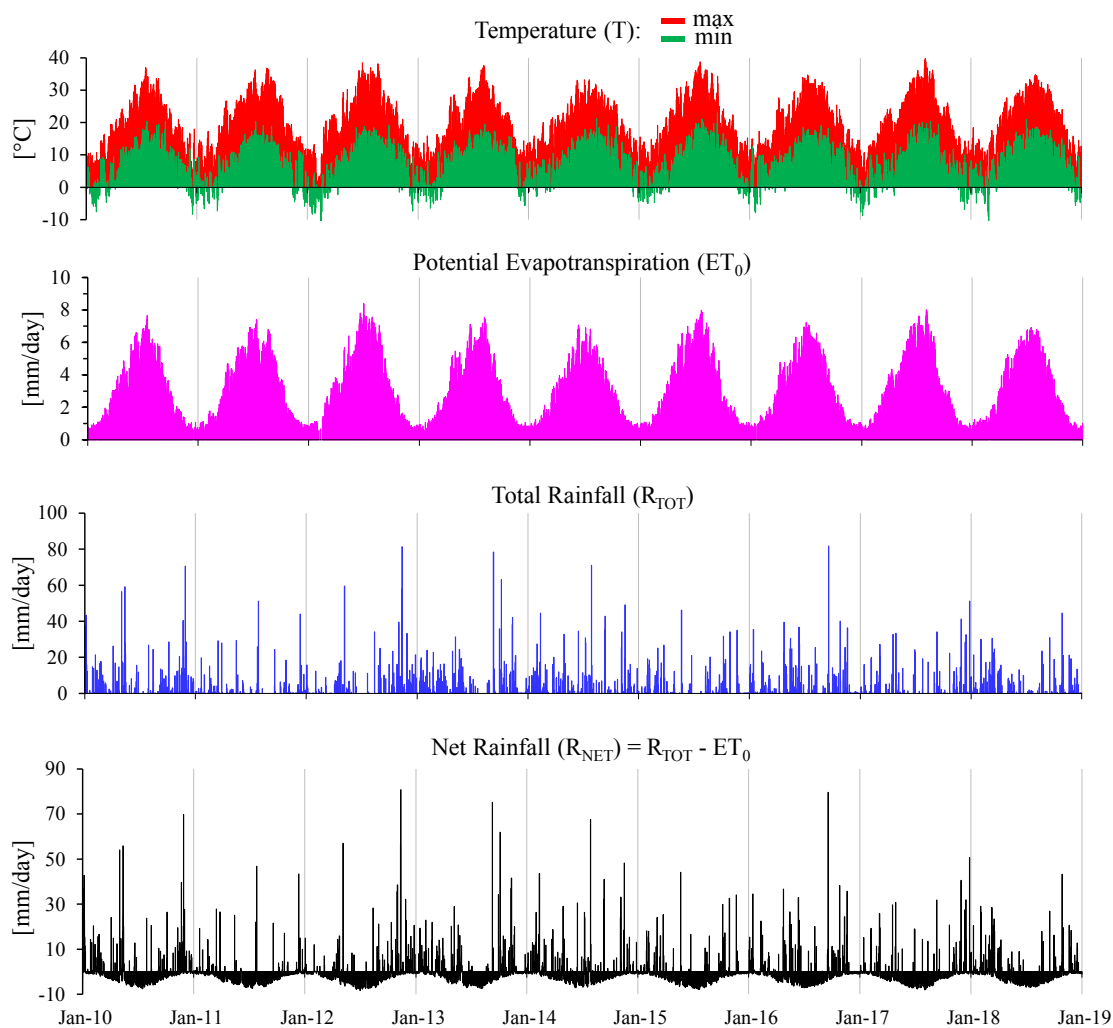
Figure 4-6: 2010-2018 Daily net rainfall series considered in the hydraulic numerical analyses as time-dependent boundary condition. Temperatures, total rainfall and reference evapotranspiration time series are also reported.

As it can be noticed, during non-rainy days and when the ET_0 is bigger than the total rainfall, the net rainfall becomes a negative flow rate acting on the surface of the slope. Some preliminary analyses have been carried out considering both positive and negative values of the net rainfall time series, but the results were not satisfactory since the simulated drawdown of the water level was unrealistically too big and fast, especially during prolonged non-rainy periods. The same evidence was reported by TSAPARAS et AL. (2002). Therefore, only positive values of the series reported in **Figure 4-6** were considered.

Moreover, 2010 net rainfall has been applied cyclically for a certain number of years until a stationary fluctuation of the water level within the slope has been reached. This was done in order to obtain a representative starting condition to evaluate the hydraulic

response induced by the rainfall series occurred in the following years. Regarding the specific case, it has been found that 5 years were more than sufficient to reach the stationary condition mentioned above.

4.4 Stability analysis

2D Limit equilibrium analyses have been conducted by means of the code GeoStudio SLOPE/W (GEO-SLOPE International, Ltd.). The slices method of Morgenstern & Price (1965) was used with a half-sine inter-slice function and considering a total number of slices equal to 100.

Piezometric fluctuations coming the hydraulic analyses were considered and the evolution with time of the factor of safety was determined by running a number of simulations equal to the time steps defined in the transient seepage analysis ($\Delta t_{calculation}$=1day). At each time step, the software considers the pore pressure distribution computed by SEEP/W and calculates the FS for the considered landslide body.

The slip surface was directly introduced using the option "fully specified" and its geometry was reproduced according to inclinometer and morphological evidences, as shown in **Figure 4-7**.
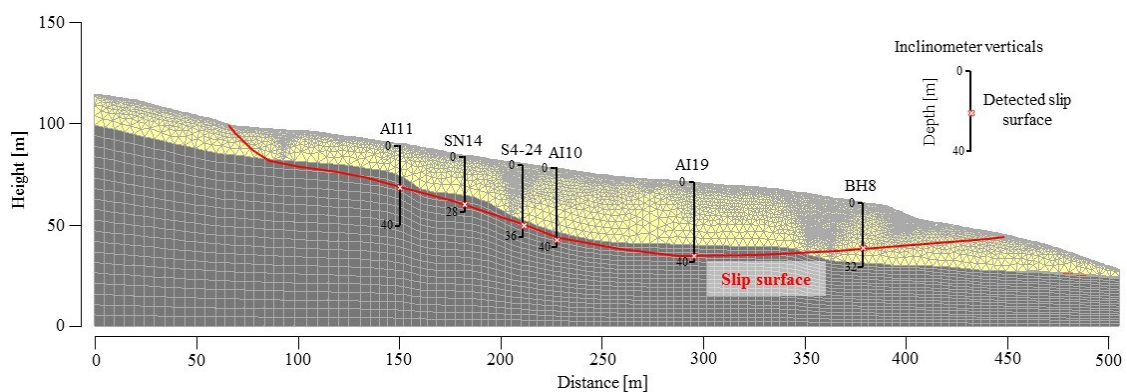
Figure 4-7: Landslide geometry considered in the stability analyses.

Analyses have been carried under effective stress conditions and the Mohr-Coulomb failure envelope has been adopted for all the materials. Congruently with the activity of the landslide that takes place along a pre-existing slip surface, the shear strength at residual was considered. In particular, for both the landslide deposit and the base

formation, a null effective cohesion was assumed, while, regarding the friction angle, values obtained from ring shear tests (14° and 15° respectively) were adopted. Moreover, a saturated unit weight of 20 kN/m^3 has been chosen as a representative value for the materials involved.

The operational shear strength along the slip surface was also back-calculated in order to compare the obtained value with the ones coming from laboratory tests. To do so, the residual friction angle has been varied to obtain a unitary factor of safety during the rainfall event occurred in March 2018 when the AI11 inclinometer recorded the higher displacement rate.

Finally, since the slip surface is always submerged for almost its entire development, the increase of the shear strength due to suction is negligible and thus has not been considered.

4.5   Results

In the following paragraphs, the main results of the hydraulic and stability analyses are reported and critically commented. Limitations regarding the adopted procedure and the assumptions made are also pointed as well as some aspects that, at present, require further insights.

4.5.1   The influence of the unsaturated behaviour on the slope hydraulic response

At first, some simulations were carried out considering the LSD always saturated and hydraulic conductivities obtained by in situ tests were taken into account. Sensitivity analyses on these latter have been made in order to best reproduce the groundwater levels (GWL) measured along the S4-25 vertical (at 13m of depth) during the 2011-2015 period. All the other parameters were set equal to the ones reported in the 4.3.2 Paragraph. Results are shown in **Figure 4-8**.
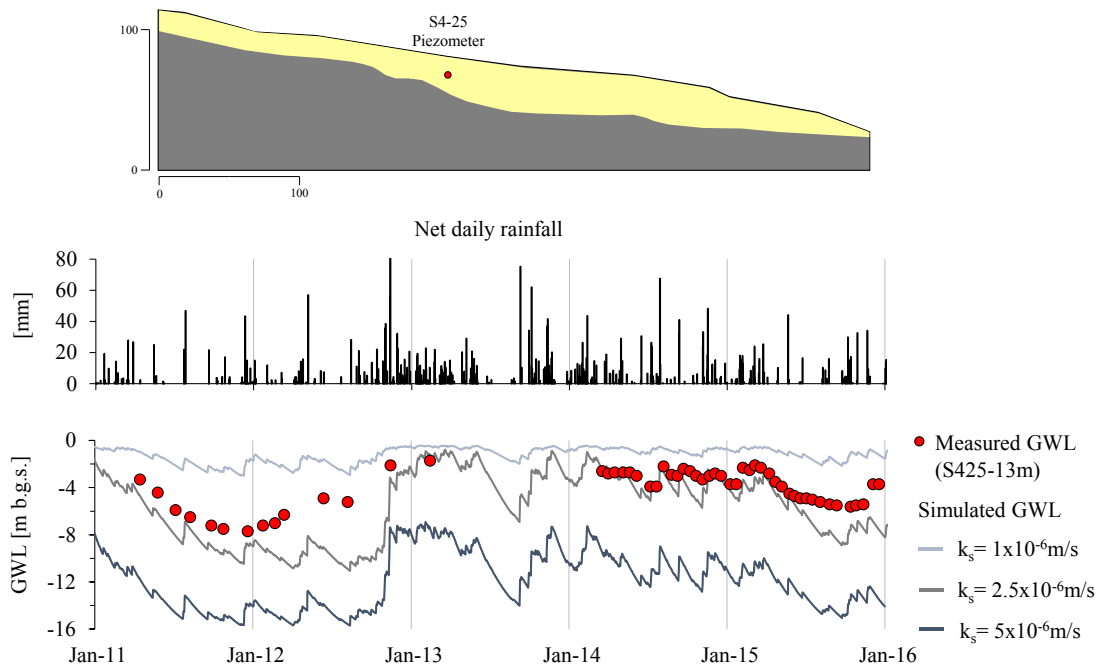
Figure 4-8: Simulated vs. measured GWL (S4-25-13m) as a function of the saturated hydraulic conductivity of the landslide deposit.

Analysing the simulation results, it has been observed that a quite small variation of the permeability coefficient in the $1-5\times10^{-6}$ m/s range strongly influenced the hydraulic response in terms of piezometric levels within the slope. Therefore, good quality measurements of such parameter seems to be necessary for a reliable prediction of the infiltration process.

For the specific case, a general overestimation of measured GWL was found if a permeability equal to 1×10^{-6} m/s is assumed. Simulation results, instead, were found to be well below the measured ones when a permeability equal to 1×10^{-6} m/s is considered. The best fitting has been obtained assigning to the LSD a saturated hydraulic conductivity equal to 2.5×10^{-6} m/s.

Despite this aspect, it can be observed that the lowering of the water level is too fast and the model, thus, still underestimates monitoring data, especially during dry periods.

Considering a partially saturated behaviour of the LSD, a very good agreement between monitored and simulated GWL is achieved instead, as shown in **Figure 4-9**.
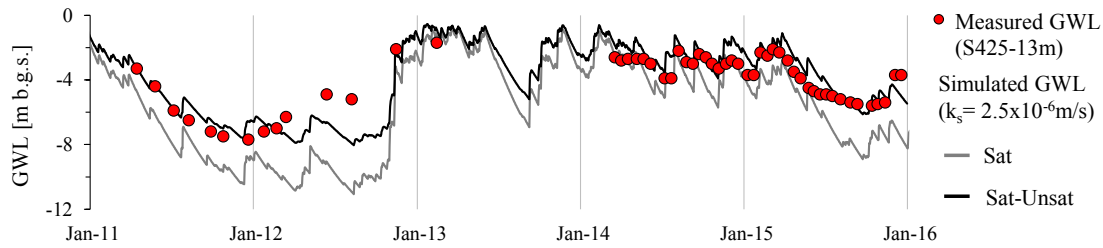
Figure 4-9: Simulated vs. measured GWL (S4-25-13m) considering the partially saturation of the landslide deposit.

To better understand the role played by the partially saturation of the soil and how it influences the infiltration process, the variation with time of the computed effective degree of saturation (S_e) and the relative hydraulic conductivity (k/k_s) are plotted in **Figure 4-10**. Data refer to a point located at a depth of 1m below the surface along the S4-25 vertical.
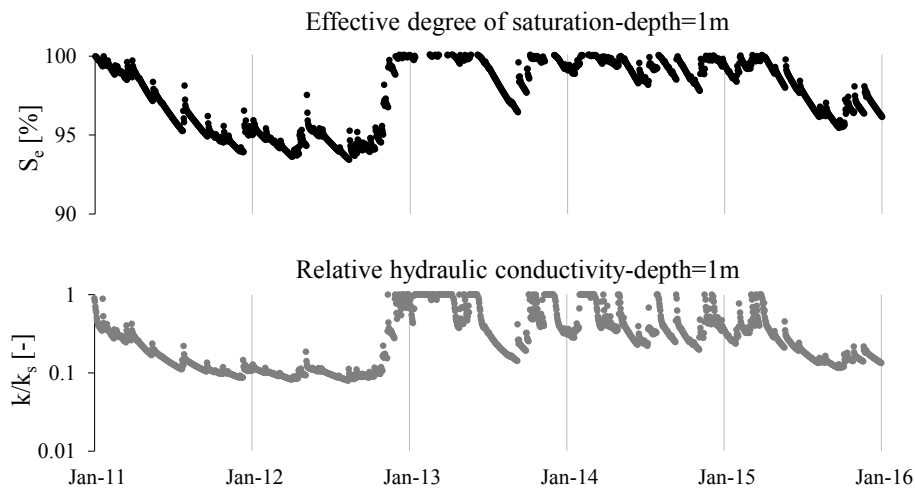
Figure 4-10: Simulated effective degree of saturation and relative hydraulic conductivity along the S4-25 vertical.

It can be noted that the S_e remains definitely elevate through a hydrological year and values below 93% have never been attained over the entire simulation. Despite this aspect, an important reduction of the hydraulic conductivity corresponds to a small decrease of the degree of saturation, attaining values lower than one order of magnitude with respect to its saturated value. This evidence underlines the importance of taking into account the coupling between saturated and unsaturated flow in order to reproduce better the pore-water pressure distribution and its time response to meteorological inputs.

It is therefore appropriate to state that, even though the obtained results are quite satisfactory, specific tests and in situ measurements are necessary to properly describe the unsaturated behaviour of the material considered. Acquiring such data will enable to improve the model and, in case, to validate the simulation results.

4.5.2   Comparison between monitored and simulated GWL at slope scale

In order to evaluate the capability of the model in reproducing the hydraulic regime at slope scale, simulated GWL at the location of the piezometers were compared with monitoring data, as reported in **Figure 4-11**.
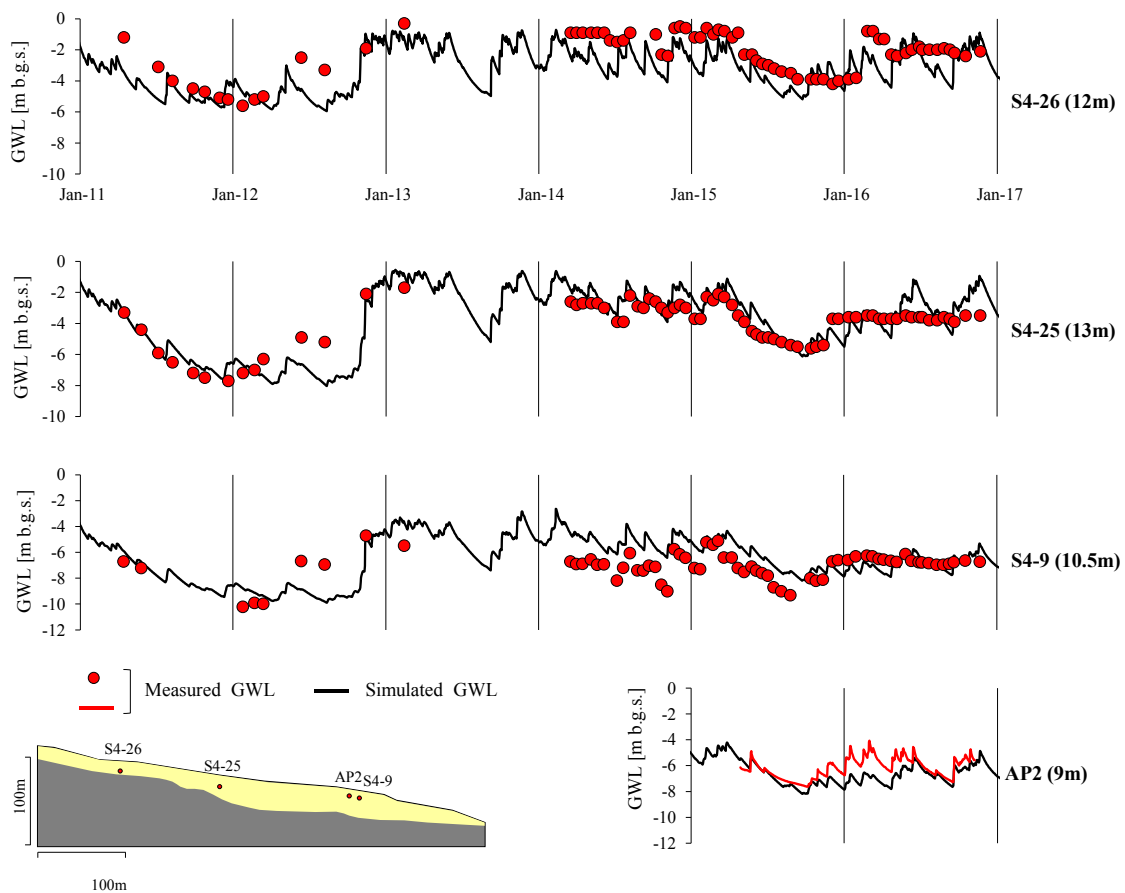
Figure 4-11: Comparison between monitored and simulated groundwater levels.

Results show a good overlapping between simulated and measured data throughout the six years (from 2011 to 2016) during which monitoring measurements are available. Given the complexity of the investigated phenomenon and the assumptions made, the model is able to quantitative reproduce the hydraulic response of the slope as a function

80

of climate inputs. Based on these evidences, it is possible to obtain a reliable estimation of the pore-water pressure changes at any point of interest within the domain. Specifically, the attention has been focused on the estimation of the hydraulic response in correspondence to the slip surface detected by the AI11 inclinometer, for which a detailed displacements records are available. In **Figure 4-12**, computed pore-water pressures along the AI11 vertical (at a depth of 20m) are compared with daily net rainfalls and monitored displacement rate.
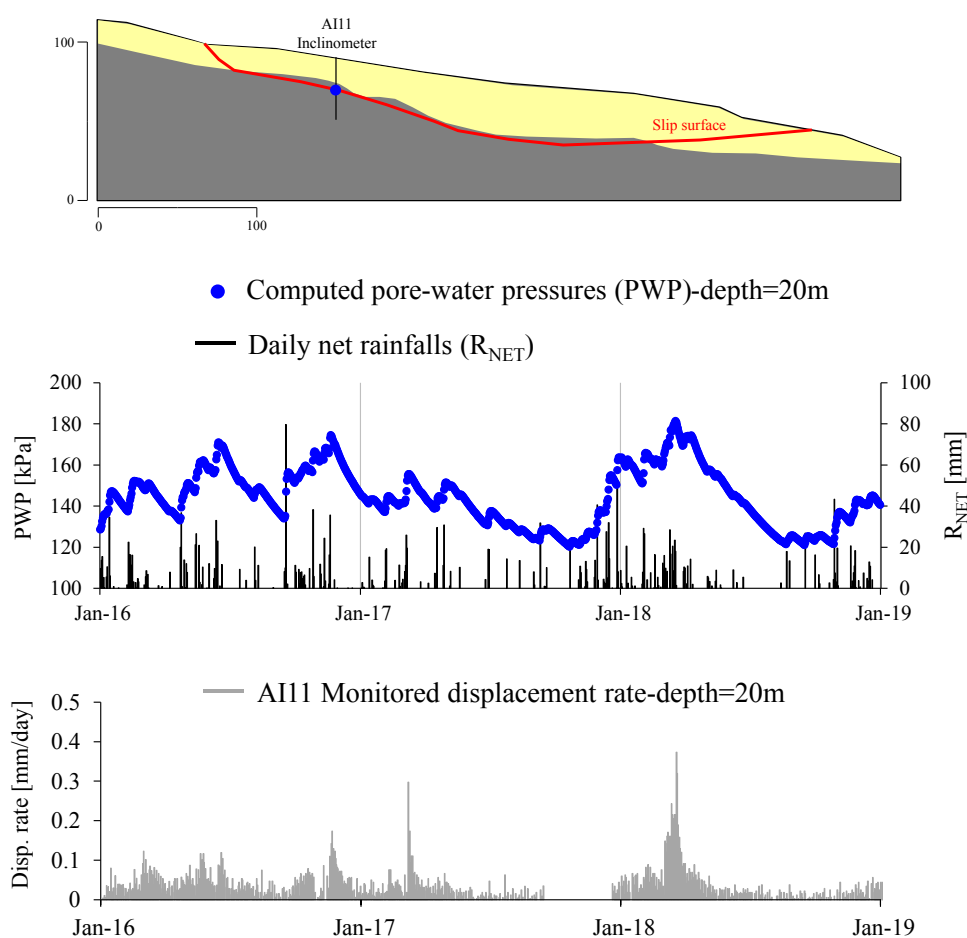
Figure 4-12: Comparison between computed PWP and displacement rate monitored along the AI11 vertical (depth=20m).

It is possible to observe the strictly connection between PWP changes and rainfalls, even on a daily basis. This confirms the fast response of the landslide to rainfall events caused by a rapid infiltration process that leads to a rapid PWP increase in correspondence to the slip surface. The same behaviour has been found at higher depths (up to 35m) along the

slip surface. This evidence allows to state that pore pressure fluctuation due to rainfall is the main aggravating factor not only for shallow landslides but also for deep-seated landslides.

Regarding "La Sorbella" landslide, this aspect becomes clearer if the computed PWP and the monitored displacement rates are compared. In fact, both of them exhibit the same trend and, on average, the higher the PWP the higher the velocity of the landslide.

In this context, the numerical modelling allowed highlighting the salient aspects of the phenomenon and its results seem to be consistent with field evidences.

4.5.3   Transient stability of the landslide

Results of stability analyses are summarised in **Figure 4-13** in terms of safety factor over time as a function of daily net rainfalls and the mobilized shear strength along the slip surface. Congruently with laboratory tests, residual friction angles equal to 15° and 14° have been considered. The back-calculation, carried out by obtaining *FS*=1 during the rainfall event occurred in March 2018, furnished a residual friction angle slightly lower and equal to 13°. For each year, moreover, the maximum and minimum value of the *FS* are reported.
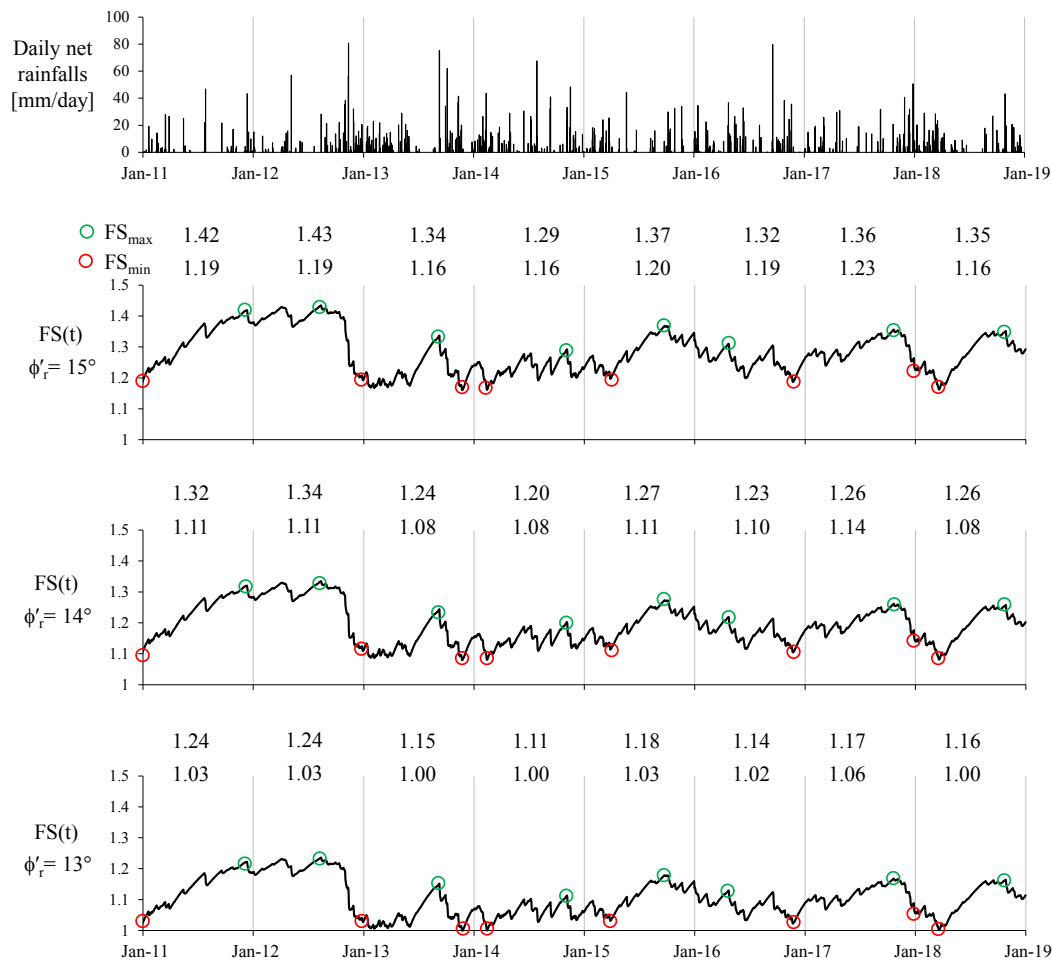
Figure 4-13: Transient stability of the landslide as a function of rainfalls and the mobilized shear strength.

Results indicated that, regardless of the mobilized shear strength considered, during each year the slope *FS* oscillates between a minimum and a maximum value with a relative variation (*FS_max*-*FS_min)/FS_max* in the 8-16% range over the entire simulation period. It is interesting to note that the minimum values are attained between November and March, while the minimum ones are encountered, on average, between August and October. This allows confirming the climate-driven nature of the landslide that exhibits higher displacement rate during the rainiest periods of the year. Despite this aspect, this "background seasonality" in not so pronounced as observed for similar deep-seated landslides in clayey slope (COTECCHIA et AL. 2014), in the sense that the trend of the *FS* is characterized by the occurrence of several drops (even if small) over a hydrological year. This means that the stability of the slope is also influenced by the rainfall regime in the short period, congruently with the fast infiltration process highlighted by the hydraulic modelling. In addition, regardless the friction angle considered, a sensible drop of the

83

safety factor is encountered during March 2018, exactly when the highest displacement rate was recorded.

Even though the shear resistance of the material directly involved in the sliding process requires more insights, the general low values of the *FS* indicate an active unstable behaviour of the slope for which destabilizing forces produce intermittent movements, as highlighted by automatic inclinometer monitoring.

In this sense, it is reasonable to assume that a residual strength is attained, on average, along the slip surface that acts like a ductile discontinuity. Therefore, important accelerations due to a strength reduction of the material can be avoided.

Despite the limitations related to the limit equilibrium method, results of the stability analyses gave a reasonable and quantitative estimate of the landslide level of safety and seem to describe well the mechanics of the observed phenomenon.

5 CHAPTER – Seismic behaviour of an active landslide from field evidences: analysis and interpretation

5.1 Instrumental measurement of coseismic displacements

As described in 3 CHAPTER, the continuous inclinometer monitoring clearly highlighted a kinematic behaviour of the landslide very different from the one related to meteorological inputs. This behaviour is described by the occurrence of three peaks of the displacement rate (see **Figure 5.1**) that took place "instantaneously" and no delayed effects were observed in the following days.
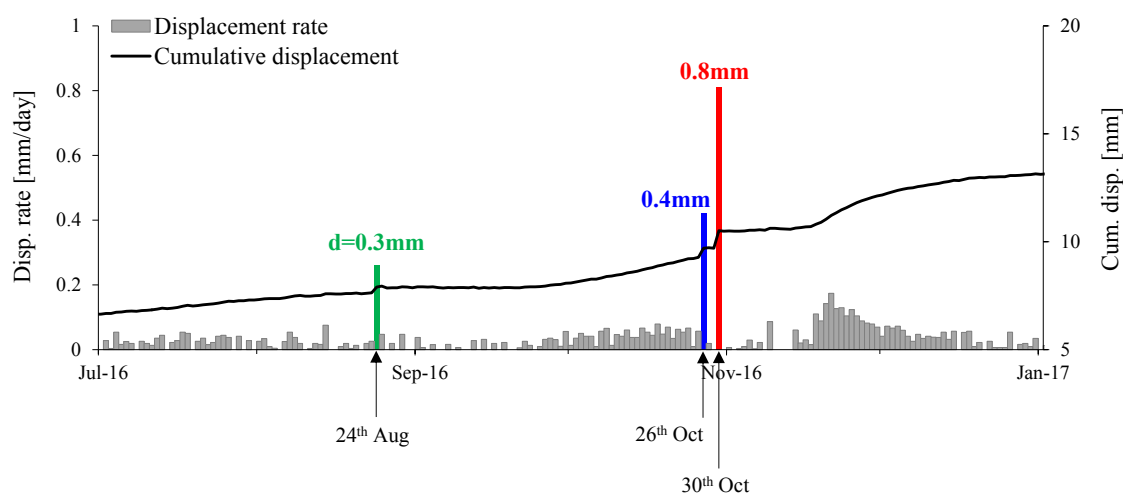
Figure 5-1: Seismic-induced displacements of "La Sorbella" landslide recorded by the AI11 fixed-in-place inclinometer probe (depth=20m) during the 2016 central Italy seismic sequence.

These displacements, moreover, were recorded between August and October 2016, in particular on August 24th, October 26th and 30th respectively, which are the dates of the three mainshocks of the 2016 central Italy seismic sequence.

Their repeated occurrence in those specific dates and their anomalous nature with respect to the ongoing kinematics of the landslide allowed recognizing the seismic-induced origin of such displacements.

At present, similar data, i.e. sub-surface instrumental measurements recorded directly along the slip surface, are not reported in scientific literature. Some Authors (HUTCHINSON & DEL PRETE 1985, KEFEER & MANSON 1998, AL-HOMOUD & TAHTAMONI 2000, PRADEL et AL. 2005) documented post-earthquake landslide

displacements but these were generally estimated or measured by surface field evidences visible to the naked eye (i.e. large displacements).

It is worth noting that the permanent displacements experienced by the landslide are of millimetric order (0.3, 0.4 and 0.8mm respectively) and no evidences of seismic effects were observed on field. This is another relevant aspect since it has been possible to detect the seismic behaviour of a landslide that underwent a deformation level never investigated before.

The small entity of the recorded displacements was not surprising due to the considerable distance (ranging from 50 to 70km) between the landslide and the epicenters of the mainshocks. This fact has been confirmed by the low-energy ground-motions registered by an accelerometric station located nearby the landslide.

The contemporary availability of the actual seismic performance of the landslide (monitored displacements) and the shaking input that produced it (recorded accelerograms) gave a rare opportunity to estimate the critical acceleration (a_y) of the system based on real data.

To do so, the original Newmark's rigid-block method (NEWMARK 1965) has been employed and, in turn, its efficiency in evaluating the seismic response of pre-existing landslides has been tested. Such results have been therefore compared with the ones obtained by a pseudostatic approach.

It is important to underline that the critical acceleration is a crucial parameter for the slope stability assessment under seismic conditions and a reliable estimation of such parameter can contribute to quantitative estimate the associated risk.

Regarding active landslides, as "La Sorbella" landslide is, the definition of the critical acceleration is not immediate since their static level of safety changes seasonally and thus their seismic level of safety changes as well.

5.2 Slope stability assessment under seismic motion

Slope instability related to seismic input is essentially driven by inertial effects, consisting of inertial forces combined with the pre-existing static forces, and/or by a reduction in shear strength. Inertial forces are transient actions that attain their maxima during the earthquake. Conversely, shear strength reduction develops progressively, being mainly

related to the development of excess pore-water pressure and to the cyclic degradation, and tends to be more important after the earthquake, as well documented by LACROIX et AL. (2014).

Therefore, slope instability associated to inertial effects actually consists of displacements that cumulate during earthquake, while instability induced after the end of earthquake resulting in a static failure mechanism. This latter, related to the shear strength reduction, have different characteristics depending on soil behaviour (ductile or brittle) and soil type (coarse or fine-grained).

The transient inertial effects, instead, lead to a more or less progressive accumulation of permanent displacements because of strain diffused over the entire slope and/or strain localisation within a limited failure zone.

After this brief introduction, it should be clear that the slope response to earthquake loading should be evaluated, in principle, using analysis procedures which account for time-dependent seismic action and that allow an evaluation of displacements.

Methods for assessing the stability of slopes during earthquakes have evolved steadily since the early twentieth century to date and can be grouped into three general categories (JIBSON 2011): pseudostatic analysis, stress-deformation analysis and permanent-displacement analysis, each of them has strengths and weaknesses and can be appropriately applied in different situations.

The pseudostatic method, which represents the first effort of considering the effects of earthquakes on slopes and earth structures, is an extension of the conventional static limit equilibrium analysis. In particular, the seismic shaking is modelled by a static body force proportional to the weight of the soil mass through the so-called "seismic coefficient" or "pseudostatic coefficient" $k=a/g$, where a is the ground acceleration and g is the acceleration due to gravity. Normally, only the horizontal component of the ground acceleration is considered since the vertical one is often of small entity and the effects of vertical forces tend to average out to near zero.

The most useful aspect of this method is the possibility of estimating in a simple manner the critical acceleration of the system, obtained by conducting a limit equilibrium analysis using different values of k until FS is equal to one. The resulting pseudostatic coefficient is called the "yield coefficient" k_y, and the associate acceleration value, $k_y \times g$, is the "yield" or "critical acceleration". In this framework, the pseudostatic method is able to

evaluate the minimum acceleration that a certain earthquake should possess to cause failure and in turn to produce permanent displacements, but no information about the amount of such displacements can be obtained. Moreover, the main features of an earthquake input, such as its duration, its frequency content and the variability of the amplitude of the acceleration are not contemplated.

Stress-deformation analysis, instead, is the most advanced tool for assessing the stability of slopes and earth structures under seismic conditions (SEED et AL. 1973, SERFF et AL. 1976, KRAMER 1996,). This method involved much more complex modelling of slopes using a mesh in which the internal stresses and strains within elements are coupled based on the applied external loads, including gravity and seismic loads. The advantage of stress-deformation modelling is that it gives the most accurate picture of what actually happens in the slope during an earthquake. Despite this aspect, this analysis method has several drawbacks. In fact, it is computationally intensive and it requires a high-quality soil-property data as well as an accurate model of the soil behaviour (non-linear, stress-dependent, cyclic model). Most procedures, moreover, model only distributed deformation and the amount of deformation is limited. A very fine mesh is required to capture local deformation for landslides that move along a discrete basal failure surface. This is why such approach is generally reserved for critical projects for which the needed data are available and the time and effort involved in the modelling procedure are justified.

The permanent-displacement approach lies in between the two methods previously mentioned and it is the most used. This method, in fact, is able to take into account the main features of an earthquake motion and to quantify the slope performance in terms of permanent displacement cumulated at the end of the shaking. The original Newmark's method (NEMARK 1965) and later modifications are discussed in detail in the following paragraphs.

5.2.1 Newmark's method for the evaluation of coseismic displacements

NEWMARK (1965) introduced a method to assess the performance of slopes and earth structures that bridges the gap between overly simplistic pseudostatic analysis and overly complex stress-deformation analysis. In developing his deformation-based procedure, Newmark analogized an earth mass sliding over a shear surface to a rigid block sliding

over a plane. This procedure assumes that permanent displacement initiates when earthquake-induced inertial forces acting on a potential sliding mass exceed the yield resistance of the slip surface. The yield or critical acceleration is generally estimated by conducting a pseudostatic analysis. Displacement continues until the inertial forces fall below the yield resistance, and the velocities of the sliding mass and the underlying ground coincide. The permanent displacement of the sliding mass may be calculated by integrating the relative velocity during slippage as a function of time. A scheme of the method is reported in **Figure 5-2**.
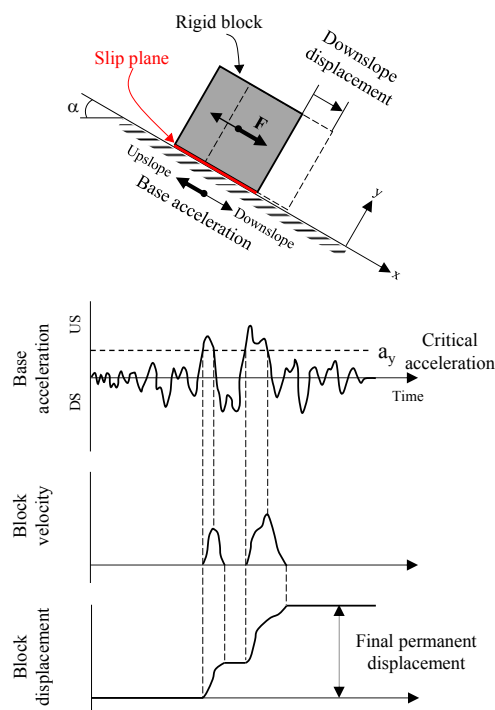
Figure 5-2: Scheme of the Newmark's rigid-block method.

A key assumption of Newmark's method is that it treats a landslide as a rigid-plastic body: the mass does not deform internally, experiences no permanent displacement at accelerations below the yield level and deforms plastically along a discrete basal shear surface when the critical acceleration is exceeded. Moreover, the soil does not undergo strength loss (e.g. no cyclic degradation of the material is accounted for) as a result of shaking and the effects of dynamic pore-water pressure are neglected. As a result, the critical acceleration remains constant throughout the analysis. In addition, the upslope

resistance to sliding is taken to be infinitely large such that upslope displacement is prohibited and vertical accelerations are ignored.

In order to overcome some of these assumptions, a number of modifications have been proposed since its original formulation. SARMA (1975) developed a procedure that accounts for the generation of pore pressure along the shear surface. TIKA-VASSILIKOS et AL. (1993) suggested approaches to account for shear-rate effects when conducting a Newmark analysis. MATASOVIC et AL. (1997) accounted for strain softening soils and geosynthetic interfaces. JIBSON & JIBSON (2003) allowed specifying strain-dependent critical acceleration as well as bi-lateral displacement. YAN et AL. (1996) modified the original Newmark procedure to account for vertical accelerations.

It is worth noting that for "coherent" landslides (KEFEER 1984) that move (or have already moved in the past) along one or more shear surfaces, many of the assumptions listed above can be considered valid. Regarding such instability phenomena, in fact, coseismic displacements are the result of shear strains developed along a limited shear band as a consequence of temporary mobilisation of the available shear strength. Little internal deformations may occur inside the soil mass, but, in general, their entity is negligible respect to the block-type displacement the soil mass undergoes. This is particularly true when the sliding mass is composed of stiff material. For such phenomena, moreover, the effects related to a strength reduction, both in terms of cyclic degradation of the material and the generation of excess pore-water pressure, can be avoided. This can be explained by the fact that for pre-existing landslides the shear strength along the sliding surface is at residual (the lowest possible resistance the material can offer) and the sliding mechanism is essentially a constant volume process, thus the development of excess pore- water pressure is unlikely to occur.

5.2.2 On the rigid behaviour of the sliding mass

The assumption of a rigid behaviour of the mass, instead, should be evaluated carefully with respect to the nature of the landslide. "Rigid" means that the sliding mass is assumed to accelerate with the ground (i.e. the sliding mass has a natural period equal to zero) and that the motion within the slope is uniform. Because of the coupled dynamic response and sliding of earth masses, actual deformations in these systems can vary significantly

from those computed in a rigid-block analysis (WARTMAN et AL. 2003, RAMPELLO et AL. 2010). This is due to the fact that the rigid-block procedure neglects the dynamic response of the sliding mass. This latter depends essentially on the stratigraphy of the deposit, on the deformability of the materials, on the landslide body geometry and it can be quantified by the natural or fundamental site frequency $F_s=1/T_s$, where T_s is the natural or fundamental site period. In one-dimensional conditions, this can be set equal to $4H/V_s$, where H is the maximum vertical distance between the ground surface and the slip surface, and V_s is the shear-wave velocity of the material above the slip surface.

In brief, the landslide body can experience a shaking motion higher or lower than the input motion depending on the frequency content of the mass with respect to the one of the considered input (quantified by $F_{in}=1/T_{in}$). Therefore, in order to evaluate the reliability of the rigid-block assumption in estimating the permanent displacement, a comparison between the frequency content of the input and the one of the landslide are required (RATHJE & BRAY 1999, 2000, WARTMAN 2003, JIBSON 2011).

A more realistic description of the seismic performance of slopes can be obtained by taking into account the deformability of the sliding mass during ground motion, for instance using a de-coupled approach (MAKDISI & SEED 1978). According to this, a seismic response analysis is first carried out to define an equivalent acceleration time history, e.g. the horizontal equivalent acceleration HEA (BRAY & RATHJE, 1998), which accounts for soil deformability. This equivalent history is then used to compute the displacements with a rigid-block sliding analysis. The seismic response analyses can be performed in one-dimensional (1D) or two-dimensional (2D) conditions and the non-linear soil behaviour can be described through the equivalent linear approximation. This latter is known to yield a reasonable estimate of soil response at moderate levels of seismic intensity.

In literature, fully coupled methods based on the permanent-displacement approach are also proposed (RATHJE & BRAY 1999, 2000, BRAY & TRAVASAROU 2007). In this case, the dynamic response of mass and the permanent displacement associated to the sliding process are modelled together. Coupled analysis is the most sophisticated form of sliding-block analysis and also the most computationally intensive. In addition to the critical acceleration, other required inputs include the shear-wave velocities of the materials above and below the slip surface, the thickness of the potential landslide, the

models to describe the stiffness and the damping of the soils. Moreover, an impediment to the application of coupled analysis is the lack of published software packages (JIBSON 2011).

5.3   2016 Central Italy seismic sequence

From August to December 2016, an extended region of central Italy has experienced a long-lasting seismic sequence (CHIARALUCE et AL. 2017) characterized by three mainshocks of moderate-to-large intensity (M_w=5.9-6.5) and hundreds of aftershocks. Without any conventional foreshocks beforehand, the sequence started with an M_w 6.0 mainshock occurred on 24 August close to the town of Accumoli. Two months later, on 26 October, another mainshock with M_w 5.9 occurred 25km to the north near the town of Visso. Then, four days later, on 30 October, the largest shock of the sequence with M_w 6.5 hit the area in between the two previous events near the town of Norcia. This latter was the strongest Italian seismic event since the 1980 M_w 6.9 Irpinia earthquake. The seismic sequence resulted in almost 300 casualties and left more 20,000 homeless. The historical towns of Amatrice, Arquata del Tronto, Accumoli and Pescara del Tronto were completely destroyed and other local towns and villages experienced severe damages.

These surficial earthquakes have been caused by normal faulting, the prevalent style of faulting in the area, all of them having NW-SE or NNW-SSE strike and dip towards SW. This is consistent with the tectonic activity of the area located across the northern and central Apennines of Italy that is currently undergoing postorogenic extension. As a result, seismic sequences characterized by the occurrence of multiple shocks are quite common for this sector of the Apenninic chain. The 2016 sequence, in fact, occurred in a gap between two earlier seismic events, the 1997 M_w 6.0 Umbria-Marche earthquake to the north-west and the 2009 M_w 6.1 L'Aquila earthquake to the south-east.

In **Table 5-1** are summarized the main features of the 2016 mainshocks (named "Accumoli", "Visso" and "Norcia" respectively).

Mainshocks	Lat-Lon [DD]	Date/hh:mm:ss (UTC)	M_W	Depth [km]	Fault type
"Accumoli"	42.70-13.23	2016-08-24/01:36:32	6.0	8.1	Normal
"Visso"	42.91-13.13	2016-10-26/19:18:05	5.9	7.5	Normal
"Norcia"	42.83-13.11	2016-10-30/06:40:17	6.5	9.2	Normal

Table 5-1: Main features of the 2016 seismic sequence mainshocks (data taken from www. http://itaca.mi.ingv.it).

Beyond the direct damages to several buildings, many coseismic surface effects have been also recognized and documented.

LANZO et AL. (2018) provided a very detailed report of the ground-related damage effects of the earthquakes based on field observations. Among other aspects, a large number of landslides, which are the main coseismic effects related to ground shaking, have been detected after the mainshocks. In particular, mainly rock falls and rock slides occurred in the epicentral area. More detailed information about landslides caused by the seismic sequence and their impact on transportation routes can be found in MARTINO et AL. (2019). The most significant phenomenon was the rock avalanche that dammed the Nera River and interrupted a regional road.

Data of large-scale coherent landslides are scarce so far, especially concerning phenomena occurred far away from the epicentral area. In this context "La Sorbella" landslide represents an important evidence of a far-field landslide that experienced the effects of the 2016 seismic sequence. In fact, as shown in **Figure 5-3**, the investigated landslide was located at a distance of tens of kilometres (in the range of 50-70km) from the epicenters of the mainshocks. These considerable distances partly justify the small entity of monitored displacements that would never have been possible to detect without a good quality monitoring system.
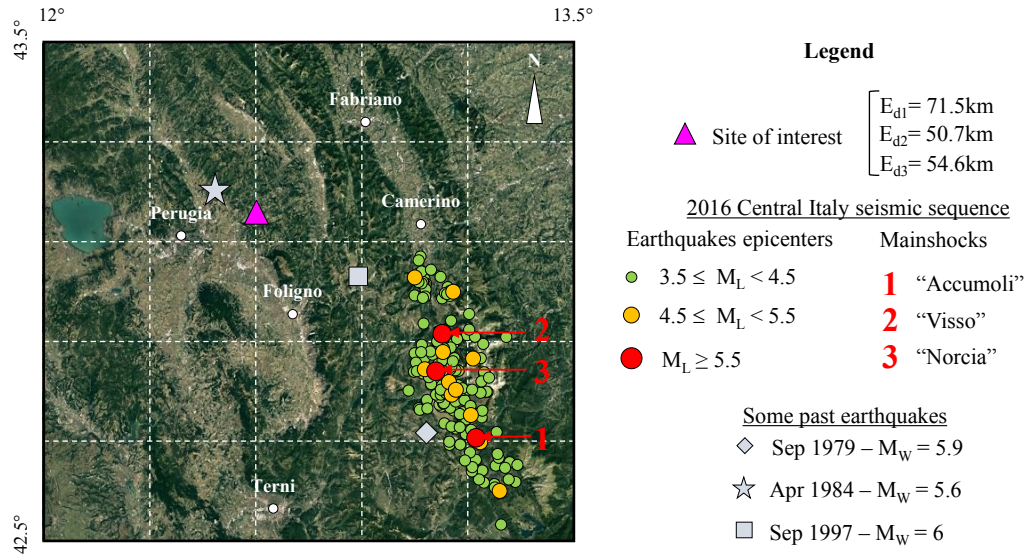
Figure 5-3: Location of the site of interest respect to the 2016 central Italy seismic sequence. Epicenters of some past relevant earthquakes are also reported.

In **Figure 5-3** are also reported the locations of the mainshocks of past seismic sequences occurred in the area: the 1979 M_w 5.9 Valnerina earthquake (grey rhombus), the 1984 M_w 5.6 Gubbio earthquake (grey star) and the 1997 M_w 6.0 Umbria-Marche earthquake (grey square). This underlines the high seismic hazard of the area where events of moderate intensity have already occurred, even closer to "La Sorbella" landslide.

5.4 Ground motions recorded in the site of interest

Thanks to the presence of a seismic station located in the close proximity of "La Sorbella" landslide (less than 1km), it has been possible to know the shaking motions the area experienced as a consequence of the three mainshocks. The station owns to the Italian Accelerometric Network (RAN), managed by the Department of Civil Protection (DPC), and data (in terms of general information and acceleration time histories) are open source and can be consulted and downloaded from the www.ran.protezionecivile.it website. For the Valfabbrica (VAL) seismic station, all the three components of the motion (E-W, N-S and U-D respectively) are available. In **Figure 5-4** the position of the station with respect to the landslide is reported together with the main information of the installation site.
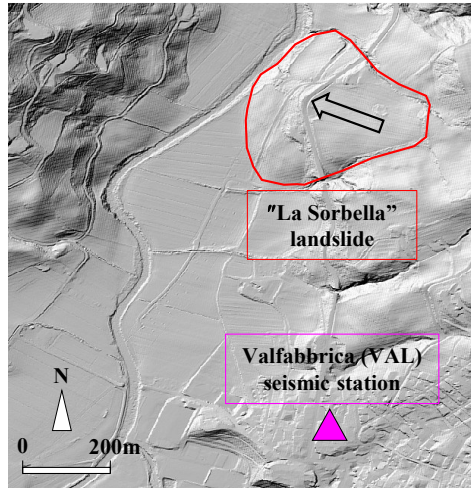
Valfabbrica (VAL) seismic station

- Lat-Lon: 43.16°-12.60°
- Height: 348 m a.s.l.
- Ground type[(1),(2)]:   B
- Topographic category[(3)]:   T1
- Housing: Building basement

Note
(1) $V_{s,30}$= 360-800 m/s according to Eurocode 8
(2) Not direct measured but assumed from geological evidences
(3) Average slope ≤ 15° according to Italian Building Code (NTC08)

Figure 5-4: Location of Valfabbrica (VAL) seismic station with respect to "La Sorbella" landslide.

Peak ground accelerations (PGA) recorded at VAL station are summarized in **Table 5-3** regarding the "Accumoli", "Visso" and "Norcia" mainshocks (EQ1, EQ2 and EQ3 respectively).

Mainshocks	E_d [km][*]	Peak Ground Accelerations [g]					
		East	West	North	South	Up	Down
EQ1	71.5	0.04	0.06	0.03	0.04	0.01	0.01
EQ2	50.7	0.04	0.04	0.04	0.04	0.03	0.03
EQ3	54.6	0.07	0.07	0.07	0.06	0.03	0.03

[*] Epicentral distance

Table 5-2: Peak Ground Accelerations recorded at VAL station.

Horizontal PGA in the 0.03-0.07g range have been recorded. These values are of low intensity, especially with respect to the ones recorded in the epicentral area (>0.5g), and consistent with the considerable distances between the site of interest and the mainshocks epicenters. This is an important aspect since it allows to state that the landslide is very sensitive to shaking motions, even of low intensity. This is not surprising since "La Sorbella" landslide is an active instability phenomenon and thus characterized by a low level of safety under static conditions.

In order to estimate properly the shaking conditions experienced by the landslide body, a deconvolution of the VAL seismic signals should be carried out first. The obtained accelerograms, then, can be used as inputs for a 1D or 2D seismic site response analysis

that accounts for the main characteristics of the landslide. At the current level of knowledge, unfortunately, this methodology cannot be adopted since the lack of specific field and laboratory investigations.

Despite this aspect, it is worth mentioning that the distance between the VAL station and "La Sorbella" landslide is small and both sites are characterized by similar topographic conditions and outcropping lithotypes.

As a first approximation, therefore, the recorded signals at VAL station have been assumed representative of the shaking conditions the landslide experienced and were considered in the analyses.

5.5   Definition of the acceleration time histories used for the analyses

For each event, the E-W and the N-S accelerograms were combined and subsequently projected along the movement direction of the landslide. This has been done in order to evaluate the directivity of the seismic motion and to estimate in a more realistic manner the shaking condition experienced by the landslide. Results are shown in **Figure 5-5**.
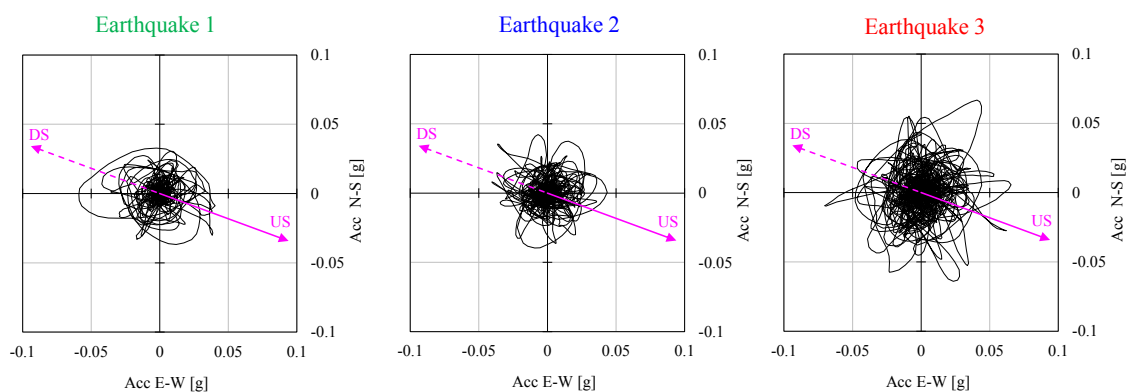
Figure 5-5: Composition of the E-W and N-S acceleration time histories recorded at VAL station for the three mainshocks considered. The upslope (UP) and downslope (DW) direction of the landslide are also reported.

The "oriented" accelerograms are reported in **Figure 5-6**. In particular, the half-accelerogram referring to the upslope direction has been considered in the displacement-based analysis. This is due to the fact that destabilizing inertial forces acting downslope are opposite to the upslope accelerations. The three upslope-accelerograms are characterized by PGA equal to 0.046g, 0.041g and 0.068g, respectively.

Some synthetic parameters of the acceleration time histories are also reported: Arias intensity (I_a), significant duration (D_{5-95}), predominant period (T_p), predominant frequency (F_p) and mean period (T_m) (RATHJE et AL. 1998).
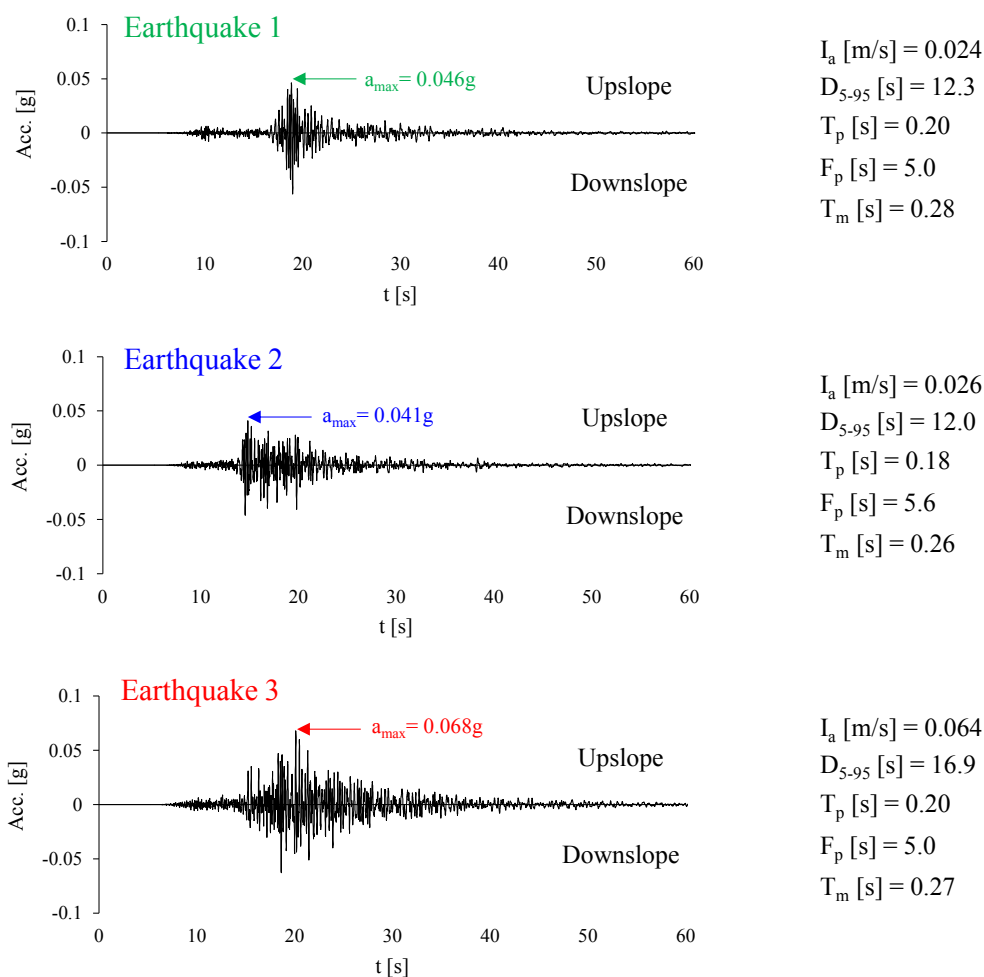
Figure 5-6: Composed accelerograms employed in the analysis and their main characteristics.

5.6 Estimation of the critical acceleration of "La Sorbella" landslide

For the present case study the availability of accurate measures of the displacement exhibited by the soil mass caused by three different earthquakes as well as the knowledge of the corresponding seismic signals, offers a unique opportunity to estimate the actual critical acceleration of the landslide. To do so, the Newmark's rigid-block method has been used as a back-calculation instrument and the acceleration time histories recorded at VAL station have been considered. Regarding "La Sorbella" landslide, the most limiting aspect of the adopted procedure is the assumption of the rigid behaviour of the sliding

mass. Under this assumption, in fact, the input accelerations are considered constant within the whole mass and possible asynchronous motions are not contemplate. In brief, phenomena (e.g. resonance effect) related to the interaction between the frequency content of the inputs and the one of the landslide are neglected.

Aware of this assumption, at present the original Newmark's method seems to be a reasonable tool to interpret the observed phenomenon and to obtain a first estimate of the critical acceleration.

Pseudostatic approach has been also employed to assess in a different manner the critical acceleration of the system and, in turn, to test the consistency of the values coming from the displacement-based analysis.

5.6.1 Newmark's rigid-block method

For each event considered (EQ1, EQ2 and EQ3 respectively), the half-accelerogram referring to the upslope direction has been double integrated using the software NEWMARK-TRPX (TROPEANO 2010). Such procedure were repeated by fixing several values of the critical acceleration (a_y) and the corresponding permanent displacement (d) has been consequently calculated. In this way, it was possible to define the correlation a_y-d represented by the curves reported in **Figure 5-7**. Once defined this correlation, it has been possible to estimate directly the critical accelerations associate to the monitored displacements. These values result equal to 0.035g, 0.024g and 0.041g for the EQ1, EQ2 and EQ3 respectively. Such values update the ones formerly obtained by FERRETTI et AL. (2019).
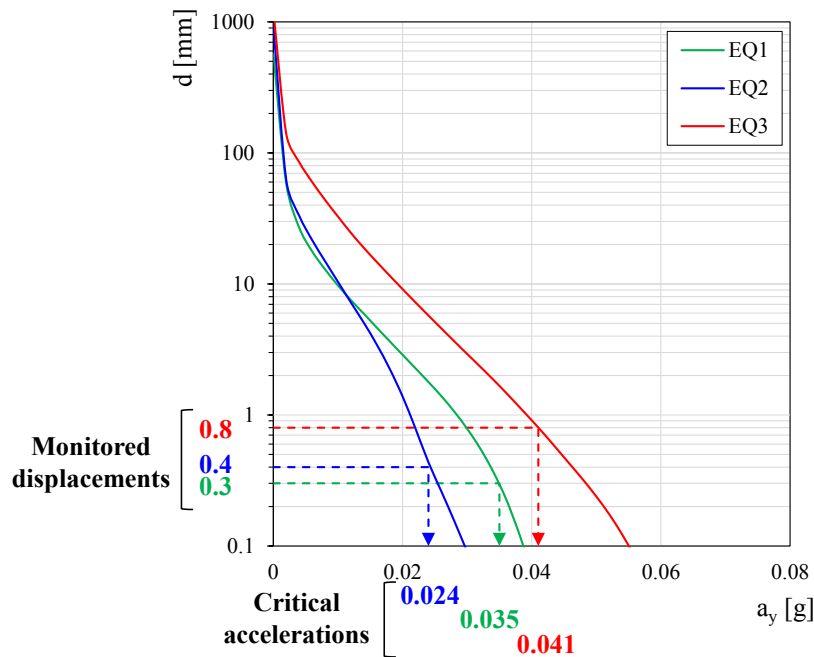
Figure 5-7: Critical accelerations values obtained using the Newmark's rigid-block method.

The low entity of the critical acceleration values reflects the metastable condition of the landslide under static conditions, which undergoes seasonal reactivations as a consequence of the rainfall regime.

Such results have been compared with available literature data regarding similar case studies.

CRESPELLANI et AL. (1996) estimated a critical acceleration ranging between 0.017-0.045g for the Calitri landslide (HUTCHINSON & DEL PRETE 1985), a pre-existing and large-scale landslide in southern Italy activated by the Irpinia earthquake in November 1980. This landslide took place in stiff clayey soils and surface displacements of metric order were observed.

PRADEL et AL. (2005) estimated a critical acceleration in the 0.026-0.052g range for a deep landslide activated by the Northridge (California) earthquake in January 1994. The sliding surface involved a Miocene formation made of sandstone and siltstone and an average displacement equal to 5cm was assessed.

The range of the critical acceleration found for "La Sorbella" landslide (i.e. 0.024-0.041g) is in good agreement with the ones reported above. This evidence can be considered a first confirmation about the representativeness of the results obtained.

5.6.2 Pseudostatic method

The pseudostatic approach has also been employed to evaluate the critical acceleration as a function of the real geometry of the landslide, the seasonal fluctuations of the groundwater level and the average shear resistance mobilized. In fact, all these features influence the static level of safety of the landslide, quantified by its factor of safety, and in turn its seismic level of safety, quantified by the critical acceleration. On the contrary, the displacement-based procedure adopted is not able to take into account such aspects explicitly and how they influence the critical acceleration value. In this context, the pseudostatic method seems to be a useful tool to estimate the critical accelerations of the system to compare with the ones coming from the Newmark's method.

Regarding the 2016, results of the hydraulic and stability analyses described in the 4 CHAPTER have been considered. The FS, in particular, have been computed considering a residual friction angle in the 13°-15° range and, at each stability analysis, a horizontal seismic coefficient (k) has been added. This latter has been made to vary iteratively until *FS*=1 in order to evaluate the yield coefficient (k_y) and thus the critical acceleration ($k_y \times g$). Results are illustrated in **Figure 5-8** in terms of the variation with time of the critical acceleration as a function of the *FS*. Over the entire period, the maximum and minimum *FS* and the corresponding max and min a_y are pointed out. Daily net rainfalls and critical accelerations estimated by Newmark's method are also reported.
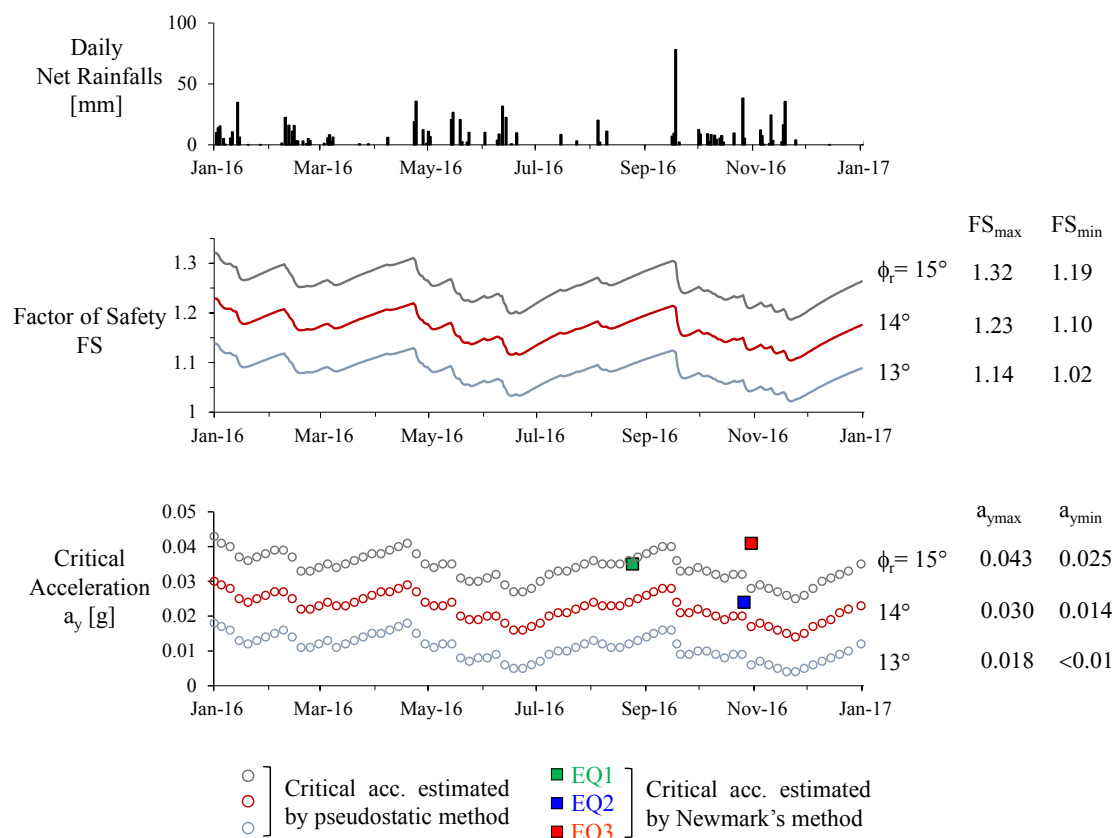
Figure 5-8: Critical acceleration values obtained by pseudostatic method as a function of the transient stability of the landslide.

Taking into account the groundwater level fluctuations and the average shear strength mobilized along the slip surface, the values of the critical acceleration obtained by the pseudostatic method embrace the ones estimated by displacement-based method.

It is worth mentioning that both methods are affected by some uncertainties, related essentially to the hydraulic modelling, the effective shear resistance of the material and the shaking motion experienced by the landslide. Despite these aspects, results are consistent and thus a critical acceleration in the 0.02-0.04g range can be considered a reliable estimation for "La Sorbella" landslide. This fact allows to confirm the representativeness of the observed phenomenon and to underline the high seismic hazard of the landslide, being very susceptible to ground motions (even of low intensity!).

It is interesting to underline that the variability of the critical acceleration is connected to the transient stability of the landslide. For the specific case, it has been found that a small relative variation of the factor of safety, about 10% over the year considered, leads to an important relative variation of the critical acceleration $(a_{ymax}-a_{ymin})/a_{ymax}$, up to 50%. PRADEL ET AL. (2005) have already pointed out this evidence.

As far as active landslides are concerned, this is an important attitude and it should be taken into account in the evaluation of the seismic performance of the slope. In line with this thinking, the same seismic event could theoretically lead to different scenarios, in terms of permanent displacement, depending on the period it occurs. Specifically, more severe seismic-induced effects should be expected in the rainy periods of the year, during which the stability of the slope is already affected by meteorological factors.

5.7 On the representativeness of the observed phenomenon and open issues

Since seismic induced landslides are typically observed close to the epicenters, it is not immediate to correlate the monitoring evidences of "La Sorbella" landslide with the occurrence of earthquakes that took place several tens of kilometres far from the site.

In order to confirm the representativeness of the observed phenomenon, current data have been compared with available literature data regarding the far field occurrence of seismically induced landslides.

In a pioneering study, KEFEER (1984) presented a set of upper bound curves for the maximum distance of seismically induced landslides as a function of event magnitude, which was based on a dataset of 40 worldwide earthquakes. He grouped the types of landslides into three simple categories: disrupted slides and falls, coherent slides, lateral spreads and flows. "La Sorbella" landslide can be grouped into the second category, i.e. coherent slides. Later studies carried out by other Authors have updated the dataset through the years. The most recent worldwide database is the one proposed by DELGADO et AL. (2011). The Authors pointed out that the proposed upper bounds by KEFEER (1984) are appropriate in most cases, although a number of "outliers" was observed. The term "outliers" stands for those landslides that occur at much further distances than maximum expected distances. The Authors focused on these cases and analysed their main features in terms of both materials involved and the most likely triggering factors.

In particular, they found that far field coherent landslides were more frequent on marly-clayey soils slopes, which is precisely the condition of "La Sorbella" landslide. Moreover, they highlighted a set of possible causes that may act alone or in combination to explain the occurrence of seismically induced landslides at long distances from the seismic focus.

This set includes the occurrence of repeated seismic events, environmental factors (e.g. rainfall) and site effects. Among these latter, the Authors individuated the so-called "self-exiting process" (BOZZANO et AL. 2008, BOZZANO et AL. 2010), not necessarily of topographical type. In this case, a pre-existing (active or dormant) landslide is excited by the earthquake and the amplification of ground motion induced by the landslide mass may generate a self-triggering process that reactivates the landslide.

In **Figure 5-9**, data referring to "La Sorbella" landslide are compared with the ones summarised by DELGADO et AL. (2011) regarding far field coherent landslides.
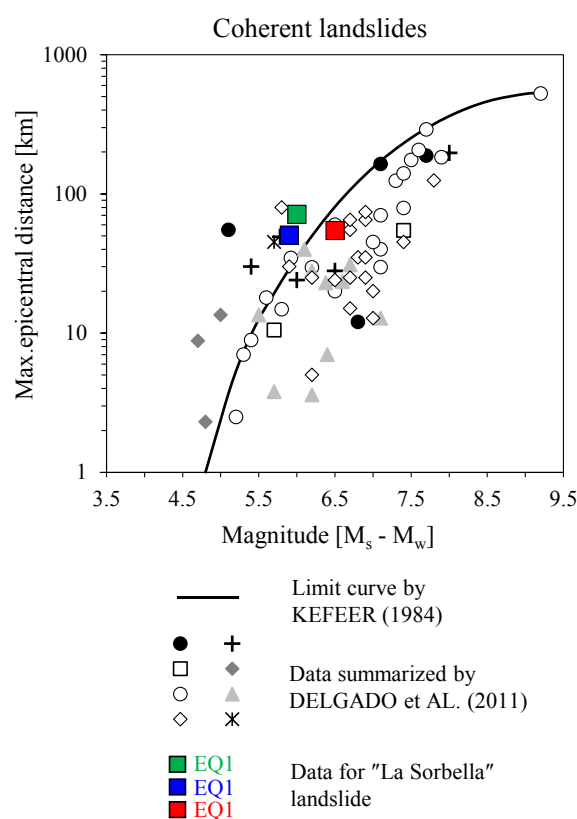
Figure 5-9: Distribution of maximum distances for seismic-induced coherent landslides as a function of earthquake magnitude: current data versus literature data (modified from DELGADO et AL.)

As it can be seen, data observed for "La Sorbella" landslide fall close to the limit curve proposed by Kefeer for coherent landslides and, in two cases, slight above it. This very little scatter between the limit curve and the current data can be justified by the very little monitored displacements if compared with those implicitly assumed by an inventory built on case studies for which large displacements were observed. In this context, evidences coming from the case of interest are in good agreement with literature data and the two

events that lies above the limit do not seem to be "outliers" related to the occurrence of a self-exciting process. This aspect can be demonstrated by referring to practical recommendations reported by WARTMAN et AL. (2003). The Authors, based on results of shaking table physical modelling, indicated that the rigid-block assumption is reliable or even overconservative if the "tuning ratio", that is the ratio between the predominant frequency of the input motion and the natural frequency of the landslide, is larger than 1.3. Regarding "La Sorbella" landslide, a first approximation of the natural frequency can be given by $V_s/4H$: for a representative value of the shear wave velocity equal to 360m/s and a maximum height of the sliding mass equal to 35m, the natural frequency of the slope is 2.6Hz. Since the predominant frequencies of the recorded seismic motions are in the 5-5.6Hz range, the resultant tuning ratio ranges between 1.9 and 2.1. So, at first glance, the effects related to the self-exciting phenomenon can be excluded or, however, they do not influence significantly the results obtained by the displacement-based method. Because of the is latter aspect in combination with the active nature of the landslide, which moves along a well-defined basal surface where the residual strength is already attained and the generation of excess pore–water pressure is unlikely to occur , the Newmark's rigid-block method is a valid tool in estimating the critical acceleration of the landslide . Such estimate, moreover, is in good agreement with one coming from the pseudostatic method, which highlighted that the general level of safety of the landslide is low enough to experience permanent displacement as a consequence of low-intensity ground shakings. These considerations allow confirming the representativeness of the observed phenomenon, i.e. monitored displacements are effectively related to seismic effects and their entity is consistent with the acceleration time histories recorded in the area.

Consequently, the critical acceleration in the 0.02-0.04g range can be considered a quantitative and reliable estimate of the seismic "vulnerability" of slope. In this specific case, since the low values attained, such vulnerability is high and the occurrence of a moderate to strong earthquake next to the landslide could lead to severe consequences.

6 CHAPTER – Concluding remarks

Within the framework of landslide risk assessment, this study addressed the analysis of the main slope processes that govern the stability of natural slopes. For this purpose, a diagnosis methodology that accounts for monitoring evidences and numerical analyses have been developed with regard to a real case study.

"La Sorbella" landslide, well representative of a widespread type of instability phenomena, is a large-scale slow moving landslide that affects a gentle slope in Umbria region (central Italy). Since the presence of a national road located at its toe, it has been intensively monitored to keep its evolution under control.

Thanks to a continuous displacement monitoring, it has been possible to obtain a detailed description of the landslide kinematics. In particular, an intermittent attitude has been highlighted by the occurrence of evident displacement rate peaks, indicating a pronounced mobility of the sliding mass during certain periods. A careful analysis of such events allowed recognizing the rainfall regime and the seismic motions as the main causes affecting the stability of the slope. The possibility to distinguish the difference between seismic and rainfall induced displacements underlines the potential of the continuous monitoring in the diagnosis of the mechanisms governing such complex natural systems. A comparison between daily rainfalls and daily displacements gave a first confirmation of the climate driven nature of the landslide. The most evident accelerations, in fact, took place during the rainiest periods of the year while no appreciable movements were recorded after prolonged dry periods. In this case, therefore, viscous-type phenomena were not encountered and the intermittent kinematics was recognised to be strictly connected to the rainfall regime. Despite the considerable depth of the sliding surface, it was observed a very small time lag between the rainfall peaks and the corresponding peaks of the displacement rate, indicating a fast infiltration process that causes a rapid increase of pore pressures along the slip surface. Moreover, it was observed that similar rainfall events occurred in differ periods (dry vs. wet periods) did not affect the stability of the slope in the same manner. In this sense, the evapotranspiration rate, antecedent rainfalls over longer periods and rainfall patterns seem to be important aspects that should be considered in order to understand properly the hydraulic processes occurring within the slope and how they affect the stability.

To this aim, a numerical modelling have been employed in order to deepen and confirm the phenomenological interpretation based on monitoring evidences. In particular, the transient nature of the infiltration process has been simulated by means of finite element numerical analyses. A 2D representative section of the slope were reproduced and all the materials found in the slope were considered. Several years of historical rain series were simulated on a daily basis and the reference evapotranspiration, the runoff and the partial saturation of the soil were taken into account in order to best reproduce the physics of the system. Results of such analyses were found satisfactory and a good fitting between computed and monitored groundwater levels were obtained. Such numerical approach, therefore, turned out to be a valid interpretative tool, able to reproduce quantitatively the hydraulic response of the slope as a function of climate inputs. The mechanical effect produced by the different seepage conditions have been evaluated by means of limit equilibrium analyses. It was observed that the variation of the safety factor reflects the seasonal pore water pressure fluctuations and, thus, confirms the close dependency of the slope stability on the rainfall regime. This latter, therefore, seems to be the main aggravating factor not only for shallow landslides but also for deep-seated ones. By considering friction angles coming from both laboratory tests and back calculation, the values of the factory of safety are generally low and oscillate next to one. This aspect allows confirming that the landslide is a pre-existing and actively unstable phenomenon, coherently with the intermittent kinematics depicted by continuous inclinometer monitoring. In addition, it is reasonable to assume that a residual strength is attained, on average, along the slip surface that acts like a ductile discontinuity. Therefore, important accelerations due a strength reduction of the material involved in the shearing process can be avoided. This aspect, in combination with the fact that the landslide exhibited accelerations of small entity (even after periods of particular intense rainfalls), allows to state that climate effects should not be expected to produce harmful consequences in the short period. Nevertheless, serviceability problems to existing manufacts can be encountered because of cumulative displacements over long time periods.

Taking into account some limitations of the adopted method (de-coupled hydro-mechanical approach) and some uncertainties related to the characterization of the materials involved, the procedure permitted to reproduce the most relevant processes that govern the slope stability under climatic inputs.

An enhancement of the actual monitoring system and the acquisition of more data in combination with specific investigations seem to be necessary not only to a more rational knowledge of the ongoing phenomenon but also to improve the reliability of the numerical model. Under these conditions, the simulation could became not only a valid interpretative tool but also a reliable predictive instrument for safety purposes. In this context, a coupled hydro-mechanical modelling can contribute to reach this goal.

As mentioned before, the continuous monitoring system clearly detected the effects induced by the 2016 central Italy seismic sequence on "La Sorbella" landslide, represented by sudden increases of the daily displacement rate. Their repeated occurrence in the dates of the sequence mainshocks and their "anomalous" nature with respect to the ongoing kinematics of the landslide allowed recognizing the seismic-induced origin of these displacements. Such precious in-situ measurements gave the opportunity to evaluate the slope level of safety under earthquake motions. In fact, the contemporary availability of permanent displacements exhibited by the slope (i.e. monitored displacements) and the shaking inputs that produced them (i.e. recorded accelerograms nearby the site) gave a rare opportunity to estimate the critical acceleration of the system on real data. To do so, the Newmark's rigid-block method was used as a back-calculation tool. Obtained values were found to be consistent with literature data concerning similar instability phenomena. It is appropriate to state that, regarding pre-existing landslides, most of the Newmark's method assumptions can be considered valid and, if dynamic interaction phenomena can be excluded, this method seems to be a valid instrument in evaluating the seismic performance of these type of landslides.

Moreover, another estimate of the critical acceleration was made by the pseudostatic approach with the aim of taking into account the influence of the groundwater fluctuation and the mobilized shear strength along the slip surface. It is worth noting that both methods furnished the same range of the critical acceleration values. Such evidence confirmed the representativeness of the observed phenomena and a critical acceleration in the 0.02-0.04g seems to be a reliable estimate for the case of interest. Such small values look to be congruent with the active nature of the landslide, characterized by a general low level of safety under static conditions, and highlights the high seismic vulnerability of the slope: the occurrence of a moderate to strong earthquake next to the landslide could lead to severe consequences.

Finally, following a displacement-based approach, the defined critical accelerations can be employed for assessing the slope performance as a function of different seismic scenarios. Such procedure should take into account the frequency content of the selected input with respect to the one of the landslide.

At the current level of knowledge, specific tests and investigations are necessary to widen the seismic behaviour of the landslide and, thus, reliable forecasts cannot be made.

REFERENCES

A.G.I. (1977): *Raccomandazioni sulla programmazione ed esecuzione delle indagini geotecniche.* Associazione Geotecnica Italiana.

AL-HOMOUD A.S. & TAHTAMONI W. (2000): *Comparison between predictions using different simplified Newmark's block-on-plane models and field values of earthquake induced displacements.* Soil Dynamics and Earthquake Engineering, 19:73-90.

ALLEN R.G., PEREIRA L.S., RAES D., SMITH M. (1998): *Crop evapotranspiration-Guidelines for computing crop water requirements.* FAO Irrigation and Drainage, Paper 56.

ALONSO E.E., GENS A., DELAHAYE C.H. (2003): *Influence of rainfall on the deformation and stability of a slope in overconsolidated clays: a case study.* Hydrogeology Journal, 11(1):174-192.

ASSEFA S., GRAZIANI A., LEMBO-FAZIO A. (2015): *A deep-seated movement in a marly-arenaceous formation: analysis of slope deformation and pore pressure influence.* IOP Conf. Series: Earth and Environmental Science 26. Proceedings of the International Symposium on Geohazards and Geomechanics, Warwick, United Kingdom, September 10-11.

ASSEFA S., GRAZIANI A., LEMBO-FAZIO A. (2017): *A slope movement in a complex rock formation: Deformation measurements and DEM modelling.* Engineering Geology, 219: 74-91.

BOTTINO G., CHINGHINI S., LANCELLOTTA R., MUSSO G., ROMERO E., VIGNA B. (2011): *Plane slope failures in the Langhe region of Italy.* Geotechnique, 61 (10): 845-859.

BOZZANO F., LENTI L., MARTINO S., PACIELLO A., SCARASCIA MUGNOZZA G. (2008): *Self-excitation process due to local amplification responsible for the reactivation of the Salcito landslide (Italy) on 31 October 2002.* Journal of Geophysical Research, 113 B10312.

BOZZANO F., LENTI L., MARTINO S., PACIELLO A., SCARASCIA MUGNOZZA G. (2010): *Evidences of landslide earthquake triggering due to self-excitation process.* International Journal of Earth Sciences, 100 (4):861-879.

BRAY J.D. & RATHJE E.M. (1998): *Earthquake-induced displacements of solid-waste landfills.* Journal of Geotechnical and Geoenvironmental Engineering, 124: 242–253.

BRAY J.D. & TRAVASAROU T. (2007): *Simplified procedure for estimating earthquake-induced deviatoric slope displacements.* Journal of Geotechnical and Geoenvironmental Engineering, 133: 381–392.

BROZZETTI F. & LAVECCHIA G. (1994): *Seismicity and related extensional stress field: the case of the Norcia Seismic Zone (Central Italy).* Annales Tectonicae, 3 (1): 36-57.

CALÒ F., ARDIZZONE F., CASTALDO R., LOLLINO P., TIZZANI P., GUZZETTI F., LANARI R., ANGELI M-G., PONTONI F., MANUNTA M. (2014): *Enhanced landslide investigations through advanced DInSAR techniques: The Ivancich case study, Assisi, Italy.* Remote Sensing of Environment, 142: 69-82.

CALVELLO M., CASCINI L., SORBINO G. (2008): *A numerical procedure for predicting rainfall-induced movements of active landslides along pre-existing slip surfaces.* International Journal for Numerical and Analytical Methods in Geomechanics, 32: 327-351.

CALVELLO M., CASCINI L., SORBINO G. (2008): *A numerical procedure for predicting rainfall-induced movements of active landslides along pre-existing sip surface.* International Journal for Numerical and Analytical Methods in Geomechanics, 32:327-351.

CASCINI L., CALVELLO M., GRIMALDI G.M. (2014): *Displacement trends of slow-moving landslides: classification and forecasting.* Journal of Materials Science, 11 (3): 592-606.

CHIARALUCE et AL. (2017): *The 2016 Central Italy seismic sequence: a first look at the mainshocks, aftershocks and source models.* Seismological Research Letters, 88 (3): 757-771.

COMEGNA L., PICARELLI L. (2008): *Anisotropy of a shear zone*. Geotechnique, 58 (9): 737-742.

COROMINAS J., MOYA J., LEDESMA A., LLORET A., GILI J.A. (2005): *Prediction of ground displacements and velocities from groundwater level changes at the Vallcebre landslide (Eastern Pyrenees, Spain).* Landslides, 2: 83-96.

COTECCHIA F., PEDONE G., BOTTIGLIERI O., SANTALOIA F., VITONE C. (2014): *Slope-atmosphere interaction in a tectonized clayey slope: a case study.* Rivista Italiana di Geotecnica, 1: 34-61.

COTECCHIA F., SANTALOIA F., TAGARELLI V. (2018): *Geo-hydro-mechanics for quantitative landslide hazard assessment (QHA).* Proceedings of the XVI Danube-

European Conference on Geotechnical Engineering, Skopje, Republic of Macedonia, June 7-9, Volume 2: 55-82.

CRESPELLANI T., MADIAI C., MAUGERI M. (1996): *Analisi di stabilità di un pendio in condizioni sismiche e post-sismiche*. Rivista Italiana di Geotecnica, 1: 50-61.

CROIZER M.J. (1988): *Landslides: Causes, Consequences and Environment.* Croom Helm, pp. 252.

CROIZER M.J. & GLADE T. (2005): *Landslide Hazard and Risk: Issues, Concepts and Approaches*. Landslide Hazard and Risk, chapter 1, Glade T., Anderson M.G. and Croizer M.J. Eds., Wiley.

CRUDEN D.M., VARNES D.J. (1996): *Landslides types and processes.* In Landslides: investigation and mitigation. Transportation research board, US National Research Council, Sepcial report 247, Whashington DC, Chapter 3: 36-75.

D'ELIA B., PICARELLI L., LEROUEIL S., VAUNAT J. (1998): *Geotechnical characterization of slope movements in structurally complex clay soils and stiff jointed clays.* Rivista Italiana di Geotecnica, 3: 5-32.

DELGADO J., GARRIDO J., LOPEZ-CASADO C., MARTINO S., PELAEZ J.A. (2011): *On far field occurrence of seismically induced landslides*. Engineering Geology, 123: 204-213.

DI MAIO C., SCARINGI G., VASSALLO R. (2014): *Residual strength and creep behaviour on the slip surface of specimens of a landslide in marine origin clay shales: influence of pore fluid composition.* Landslides, 12 (4): 657–667.

DI MAIO C., VASSALLO R., VALLARIO M., PASCALE S., SDAO F. (2010): *Structure and kinematics of a landslide in a complex clayey formation of the Italian Southern Apennines.* Engineering Geology, 116: 311-322.

DROOGERS P., ALLEN R.G. (2002): *Estimating reference evapotranspiration under inaccurate data conditions*. Irrigation and Drainage Systems, 16: 33-45.

ELIA G. et AL. (2017): *Numerical modelling of slope-vegetation-atmosphere interaction: an overview.* Quarterly Journal of Engineering Geology and Hydrogeology, 50: 249-270.

ESU F. (1977): *Behaviour of slopes in structurally complex formations.* Proceedings of the International Symposium of The Geotechnics of Structurally Complex Formations, Capri, Italy, vol. II: 292-304.

FARALLI L., MELELLI L., VENANTI L.D. (2004): *The large Acqualoreto landslide (Terni, Umbria, central Italy): mass movements analysis and risk evaluation.* Italian Journal of Technical and Environmental Geology, 3: 15-33.

FERRETTI A., FRUZZETTI V.M.E., RUGGERI P., SCARPELLI G. (2019): *Seismic induced displacements of "La Sorbella" landslide (Italy).* Proceedings of the VII International Conference on Earthquake Geotechnical Engineering, Earthquake Geotechnical Engineering for Protection and Development of Environment and Constructions, Silvestri & Moraci eds., Rome, Italy, June 17-20, pp. 2373-2380.

FLAGEOLLET J.C. (1996): *The time dimension in the study of mass movements.* Geomorphology, 15: 185-190.

FREDLUND D.G. & MORGENSTERN N.R. (1976): *Constitutive relations for volume change in unsaturated soils.* Canadian Geotechnical Journal, 13 (3): 261-276.

FREDLUND D.G. & MORGENSTERN N.R. (1977): *Stress state variables for unsaturated soils.* American Society of Civil Engineers, 103 (5): 447-466.

GLASTONBURY J., FELL R. (2008): *Geotechnical characteristics of large slow, very slow and extremely slow landslides*. Canadian Geotechnical Journal, 45: 984-1005.

GRANA V., TOMMASI P. (2014): *A deep-seated slow movement controlled by structural setting in marly formations of Central Italy.* Landslides, 11: 195-212.

GRIMALDI G.M. (2008): *Modelling the displacements of slow moving landslides.* PhD thesis, Università degli Studi di Salerno, Italia.

GUERRERA F., MARTIN-MARTIN M., RAFFAELLI G., TRAMONTANA M. (2015): *The Early Miocene "Bisciaro volcaniclastic event" (northern Apennines, Italy): a key study for the geodynamic evolution of the central-western Mediterranean.* International Journal of Earth Sciences, 104 (4): 1083–1106

GUERRERA F., TRAMONTANA M., DONATELLI U. (2012): *Space/time tectono-sedimentary evolution of the Umbria -Romagna-Marche Miocene Basin (North Apennines, Italy).* Swiss Journal of Geosciences, 105 (3): 325-341.

GUZZETTI F., CARRARA A., CARDINALI M., REICHENBACH P. (1999): *Landslide hazard evaluation: a review of current techniques and their application in a multi-scale study, Central Italy*. Geomorphology, 31: 181-216.

HARGREAVES G.H. & ALLEN R.G. (2003): *History and Evaluation of Hargreaves Evapotranspiration Equation.* Journal of Irrigation and Drainage Engineering, 129: 53-63.

HARGREAVES G.H. & SAMANI Z.A. (1985): *Reference Crop Evapotranspiration from Temperature.* Applied Engineering in Agriculture, 1: 96-99.

HAWKINS A.B. & McDONALD C. (1992): *Decalcification and residual shear strength reduction in Fuller's Earth Clay.* Geotechnique, 42 (3): 453-464.

HERRERA G. et AL. (2018): *Landslides databases in the Geological Surveys of Europe.* Landslides, 15: 359-379.
HUNGR O., LEROUEIL S., PICARELLI L. (2014): *The Varnes classification of landslide types, an update.* Landslides, 11: 167-194.

HUTCHINSON J.N. (1988): *General report: morphological and geotechnical parameters of landslides in relation to geology and hydrogeology.* In Proceedings of the 5th International Symposium on Landslides, Lausanne, vol. I: 3-35.

HUTHCINSON J.N. & DEL PRETE M. (1985): *Landslide at Calitri, southern Apennines, reactivated by the earthquake of the 23rd November 1980.* Geologia Applicata e Idrogeologia, 20 (1): 9-38.

JENG C.J., YO Y.Y., ZHONG K.L. (2017): *Interpretation of slope displacement obtained from inclinometers and simulation of calibration tests.* Natural Hazards, 87 (2): 623-657.

JIBSON R.W. & JIBSON M.W. (2003): *Java programs for using Newmark's method and simplified decoupled analysis to model slope performance during earthquakes.* US Geological Survey Open-File Report 03-005, version 1.1.

JIBSON R.W. (2011): *Methods for assessing the stability of slopes during earthquakes-A retrospective.* Engineering Geology, 122: 43-50.

KEFEER D.K. & MANSON M.W. (1998): *Regional distribution and characteristics of landslides generated by the earthquake.* Kefeer D.K. Ed., The Loma Prieta, California, Earthquake of October 17, 1989-Landslides, U.S. Geological Survey Professional Paper 1551-C: 7-32.

KEFEER D.K. (1984): *Landslides caused by earthquakes.* Geological Society of America Bulletin, 95: 406-421.

KRAMER S.L. (1996): *Geotechnical Earthquake Engineering.* Prentice Hall, Upper Saddle River, NJ.

LACROIX P., PERFETTINI H., TAIPE E., GUILLIER B. (2014): *Coseismic and postseismic motion of a landslide: Observations, modeling and analogy with tectonic faults.* Geophysical Research Letters, 41 (19): 6676-6680.

LANZO et AL. (2018): *Reconnaissance of geotechnical aspects of the 2016 Central Italy earthquakes*. Bulletin of Earthquake Engineering, 17 (10): 5495-5532.

LEROUEIL S. (2001): *Natural slopes and cuts: movement and failure mechanisms.* Geotechnique, 15 (1): 197-243.

LEROUEIL S., VAUNAT J., PICARELLI L., LOCAT J., LEE H., FAURE R. (1996): *Geotechnical characterization of slope movements.* Proceedings of the 7th International Symposium on Landslides, Trondheim, vol. I

LOLLINO G., ARATTANO M., ALLASIA P., GIORDAN D. (2006): *Time response of a landslide to meteorological events.* Natural Hazards and Earth System Sciences, 6: 179-184.

MAKDISI F.I. & SEED H.B. (1978): *Simplified procedure for estimating dam and embankment earthquake-induced deformations.* ASCE Journal of the Geotechnical Engineering Division, 104:849–867.

MANFREDINI M., BERTINI T., CUGUSI F., GRISOILA M., ROSSI DORIA M. (1985): *Geological outline of Italy: bearing of the geological features on the geotechnical characterization on the example of some typical formations.* Geotechnical Engineering in Italy-An overview, Associazione Geotecnica Italiana, 159-184.

MANSOUR M.F., MORGENSTERN N.R., MARTIN C.D. (2011): *Expected damage from displacement of slow-moving slides*. Landslides, 8: 117-131.

MANTOVANI E., VITI M., CENNI N., BABBUCCI D., TAMBURELLI C. (2015): *Present Velocity Field in the Italian Region by GPS Data: Geodynamic/Tectonic Implications.* International Journal of Geosciences, 6: 1285-1316.

MARINOS & HOEK (2001): *Estimating the geotechnical properties of heterogeneous rock masses such as flysch.* Bulletin of Engineering Geology and the Environment, 60 (2): 85-92.

MARTINO et AL. (2019): *Impact of landslides on transportation routes during the 2016–2017 Central Italy seismic sequence.* Landslides, 16 (6): 1221-1241.

MATASOVIC N., KAVAZANJIAN E., YAN L. (1997): *Newmark deformation analysis with degrading yield acceleration.* Proceedings of Geosynthetics '97, Long Beach, California, vol. II: 989- 1000.

MORGENSTERN N.R. & CRUDEN D.M. (1977): *Description and classification of geotechnical complexities.* Proceedings of the International Symposium of The Geotechnics of Structurally Complex Formations, Capri, Italy, vol. II: 195-204.

MORGENSTERN N.R. & TCHALENKO J.S. (1967): *Microscopic Structures in Kaolin Subjected to Direct Shear.* Geotechnique, 17 (4): 309-328.

MUALEM Y. (1976): *A new model for predicting the hydraulic conductivity of unsaturated porous media.* Water Resource Research, 30: 1153-1171.

NEWMARK N.M. (1965): *Effects of earthquakes on dams and embankments.* Geotechnique, 15 (2): 139-160.
OBERTI G., BAVESTRELLO F., ROSSI P.P., FLAMIGNI F. (1986): *Rock mechanics investigations, design and construction of the Ridracoli dam.* Rock Mechanics and Rock Engineering, 19: 113-142.

PARDESHI S.D., AUTADE S.E., PARDESHI S.S. (2013): *Landslide hazard assessment: recent trends and techniques.* SpringerPlus 2 (523).

PERANIC J., ARBANAS Z., CUOMO S., MACEK M. (2018): *Soil-water characteristic curve of residual soil from a flysch rock mass.* Geofluids 2018, article ID 6297819.

PETLEY D. (2012): *Global patterns of loss of life from landslides.* Geology, 40 (10): 927-930.

PICARELLI L. (2007): *Considerations about the mechanics of slow active landslides in clay.* Progress in Landslide Science, Sassa K., Fukuoka H., Wang F., Wang G. eds. Springer, Berlin, Heidelberg.

PICARELLI L. & DI MAIO C. (2010): *Deterioration processes of hard clays and clay shales.* Geological Society, London, Engineering Geology Special Publications, 23: 15-32.

PICARELLI L. (2011): *Discussion to the paper "Expected damage from displacement of slow-moving slides" by M.F. MANSOUR, N.R. MORGENSTERN and C.D. MARTIN.* Landslides, 8: 553-555.

PICARELLI L., URCIOLI G., RUSSO C. (2004): *Effect of groundwater regime on the behaviour of clayey slopes.* Canadian Geotechnical Journal, 41 (3): 467-484.

POPESCU M.E. (2002): *Landslide Causal Factors and Landslide Remedial Options.* Proceedings of the 3rd International Conference on Landslides, Slope Stability and Safety of Infrastructures, Singapore, pp. 61-81.

PRADEL D., SMITH P.M., STEWART J.P., RAAD G. (2005): *Case history of landslide movement during the Northridge earthquake.* Journal of Geotechnical and Geoenvironmental Engineering, 131 (11): 1360-1369.

RAJANI B., ROBERTSON P.K., MORGENSTERN N.R. (1995): *Simplified methods for pipelines subjected to transverse and longitudinal soil movements.* Canadian Geotechnical Journal, 32 (2): 309-323.

RAMPELLO S., CALLISTO L., FARGNOLI P. (2010): *Evaluation of slope performance under loading conditions.* Rivista Italiana di Geotecnica, 4: 29-41.

RATHJE E.M. & BRAY J.D. (1999): *An examination of simplified earthquake-induced displacement procedures for earth structures.* Canadian Geotechnical Journal, 36 (1): 72-87.

RATHJE E.M. & BRAY J.D. (2000): *Nonlinear coupled seismic sliding analysis of earth structures.* Journal of Geotechnical and Geoenvironmental Engineering, 126: 1002-1014.
RATHJE E.M., ABRAHAMSON N.A. & BRAY J.D. (1998): *Simplified frequency content estimates of earthquake ground motions.* Journal of Geotechnical and Geoenvironmental Engineering, 124 (2): 150-159.

RICCI LUCCHI F. (1986): *The foreland basin system of the Northern Apennines and related clastic wedges: a preliminary outline*. Giornale di Geologia, 48 (1-2): 165-185.

RUGGERI P., SEGAO D., VITA A., PATERNESI A., SCARPELLI G. (2016): *Deep-seated landslide triggered by tunnel excavation.* Proceedings of the 12th International Symposium on Landslides, Napoli, Italy, June 12-19.

SHARPE C.F.S. (1938): *Landslides and related phenomena: a study of mass movement of soil and rock.* Columbia University Press, New York.

SARMA S.K. (1975): *Seismic stability of earth dams and embankments*. Geotechnique, 25 (4): 743-761.

SEED H.B., LEE K.L., IDRISS I.M., MAKDISI R. (1973): *Analysis of the slides in the San Fernando dams during the earthquake of Feb. 9, 1971.* Report No. EERC 73-2. Earthquake Engineering Research Center, University of California, Berkeley.

SERFF N., SEED H.B., MAKDISI F.I., CHANG C.Y. (1976): *Earthquake-induced deformations of earth dams.* Report No. EERC 76-4. Earthquake Engineering Research Center, University of California, Berkeley.

SKEMPTON A.W. & PETLEY D.J. (1967): *The strength along structural discontinuities of stiff clays.* Proceedings of the Geotechnical Conference, Oslo, vol. II: 55-69.

SKEMPTON A.W., HUTCHINSON J.N (1969): *Stability of natural slopes and embankment foundations.* Proceedings of the 7th International Conference of Soil Mechanics and Foundation Engineering, Mexico, State of Art volume, 291-340.

STARK T.D., JAFARI N.H., LEOPOLD A.L., BRANDON T.L. (2015): *Soil Compressibility in Transient Unsaturated Seepage Analyses*. Canadian Geotechnical Journal, 51 (8): 858-868.

TAGARELLI V. & COTECCHIA F. (2018): *Shallow to deep climate-induced instabilities in clayey slopes: numerical modelling for early warning*. Incontro Annuale dei Ricercatori di Geotecnica, Genova, Italia, 4-6 Luglio.

TERZAGHI K. (1950): *Mechanisms of Landslides*. Geotechnical Society of America, Berkeley, 1950, pp. 83-125.

TIKA-VASSILIKOS T.E, SARMA S.K., AMBRASEYS N.N. (1993): *Seismic displacement on shear surfaces in cohesive soils*. Earthquake Engineering and Structural Dynamics, 22: 709-721.

TINTERRI R. & MUZZI MAGALHAES P. (2011): *Synsedimetary structural control on foredeep turbidites: an example from Miocene Marnoso-Arenacea formation, Northern Apennines, Italy*. Hubbard B.W. et al. eds., The stratigraphic evolution of deep-water architecture: Marine and Petroleum Geology, 28 (3): 629-657.

TOMMASI P., BOLDINI D., CALDARINI G., COLI N. (2013): *Influence of infiltration on the periodic re-activation in an overconsolidated clay slope*. Canadian Geotechnical Journal, 50: 54-67.

TOMMASI P., PELLEGRINI P., BOLDINI D., RIBACCHI R. (2006): *Influence of rainfall regime on hydraulic conditions and movement rates in the overconsolidated clayey slope of the Orvieto hill (central Italy)*. Canadian Geotechnical Journal, 43: 70-86.

TOMMASI P., RIBACCHI R., SCIOTTI M. (1997): *Slow movements along the slip surface of the 1900 Porta Cassia landslide in the clayey slope of the Orvieto Hill*. Rivista Italiana di Geotecnica, 2: 49-58.

TROPEANO G. (2010): *Previsione di spostamenti di pendii in condizioni sismiche*. PhD thesis, Università della Calabria, Italia.

TSAPARAS I., RAHARDJO H., TOLL D.G., LEONG E.C. (2002): *Controlling parameters for rainfall-induced landslides*. Computers and Geotechnics, 29: 1-27.

URCIOLI G. & PICARELLI L. (2008): *Interaction between landslides and man-made works*. Landslides and Engineered Slopes, vol. 2: 1301-1308. Chen et al. eds., Taylor & Francis Group, London.

URCIOLI G., PICARELLI L., LEROUEIL S. (2007): *Local soil failure before general slope failure*. Geotechnical and Geological Engineering, 25: 103-122.

VALENTINO R., MEISINA C., BORDONI M., ZIZIOLI D., BITTELLI M. (2014): *Processi di interazione suolo-atmosfera su un pendio soggetto a frane superficiali: un caso studio nell'Oltrepò Pavese*. Incontro Annuale dei Ricercatori di Geotecnica, Chieti, Italia, 14-16 Giugno.

VAN GENUCHTEN M.T. (1980): *A closed form equation for predicting the hydraulic conductivity of unsaturated soils.* Soil Science Society of America Journal, 44 (5): 892-898.

VARNES D.J. (1978): *Slope movement types and processes.* Landslides: analysis and control, special report 176: Transportantion research board, National Academy of Sciences, Washington DC, 11-33.

VARNES D.J. (1984): *Landslide hazard zonation: a review of principles and practice.* Natural Hazard Series, vol. 3, UNESCO, Paris.

VASSALLO R., GRIMALDI G.M., DI MAIO C. (2015): *Pore water pressures induced by historical rain series in a clayey landslide: 3D modelling.* Landslides, 12: 731-744.

VASSALLO R., PAGLIUCA R., DI MAIO C. (2013): *Monitoring of the movements of a deep, slow, clayey landslide and 3D interpretation.* Italian Journal of Engineering Geology and Environment, 6: 359-367.

VAUNAT J., LEROUEIL S. (2002): *Analysis of post-failure slope movements within the framework of hazard and risk analysis.* Natural Hazards, 26 (1): 83-109.

VAUNAT J., LEROUEIL S., FAURE R.M. (1994): *Slope movements: a geotechnical perspective.* Proceedings of the VII International Congress of the International Association of Engineering Geology, Lisbon, Portugal, September 5-9, vol. III: 1637-1646.

VAUNAT J., LEROUEIL S., TAVENAS F. (1992): *Hazard and risk analysis of slope instability.* Proceedings of the I Canadian Symposium on Geotechnique and Natural Hazards, Vancouver, Canada, May 6-9, pp. 397-404.

WARTMAN J., BRAY J.D., SEED R.B. (2003): *Inclined plane studies of the Newmark sliding block procedure.* Journal of Geotechnical and Geoenvironmental Engineering, 129: 673-684.

YAN L., MATASOVIC N., KAVAZANJIAN E. (1996) *Seismic response of rigid block on inclined plane to vertical and horizontal ground motions acting simultaneously.* Proceedings of the 11th ASCE Engineering Conference, Fort Lauderdale, Florida, vol. II: 1110-1113.